UCLouvain

École polytechnique de Louvain

Review and evaluation of the bond wrench test

Assessment of its characteristics, applications and limitations

Author: **Olivier KESTEMONT**
Supervisors: **João SARAIVA ESTEVES PACHECO DE ALMEIDA, Michele GODIO**
Readers: **Igor BOUCKAERT, Jean-François Rondeaux, Pierre LATTEUR**
Academic year 2022-2023
Master [120] in Civil Engineering

Abstract

The present study focuses on evaluating the flexural bond strength of masonry using the bond wrench test (BWT). The research begins by reviewing the existing literature on the BWT, with a specific emphasis on the test's applications and limitations. Subsequently, the study explores the influence of variations in the BWT configuration through experimental investigation to understand their impact on test results. For this purpose, a total of 60 bonds from masonry prisms made of clay bricks and cement mortar were tested. The main conclusion of this study is that joint precompression is the sole parameter influencing BWT results, which contrasts with the existing literature. This divergence from previous research is attributed to the inherent weakness of the bonds tested in the present study. This weakness was highlighted by the fact that 30% of the joints tested failed during BWT installation process, prior to the start of the test. These results encourage further research to extend the generalisation of the findings to stronger masonry bonds and various material combinations.

Acknowledgements

The realisation of this master thesis would not have been possible without the help and support of numerous individuals.

First of all, I would like to express my deep gratitude to João Saraiva Esteves Pacheco de Almeida and Michele Godio, my supervisors, as well as Igor Bouckaert for their availability, invaluable assistance in the research, and their ever-present positivity and kindness.

I would also like to express my appreciation to the members of the LEMSC for enabling the experimental part of this work. Special thanks to Christophe Bayart and Pierre Mertens for their precious advice and help with the experimental setup, and to Justin Toussaint and Raphael Ollevier for manufacturing the bond wrench apparatus.

A special note of gratitude is owed to Jean-Marc Dujeux and Florent Tasseroul from JMD Construction for the fabrication of the prisms.

Many thanks also to my family and friends, especially Esther, Philippe, and Pierre, for their proofreading and valuable advice.

Lastly, but certainly not least, special thanks to my parents and Julie for their constant support and encouragement in this project, as well as in all past and future ones.

Disclaimer: In the process of improving the quality of the English text in this thesis, OpenAI's GPT-3 was employed to assist in refining and enhancing the clarity and coherence of the written content.

Contents

Abstract **i**

Acknowledgments **iii**

List of Figures **xi**

List of Tables **xiii**

Introduction **1**
Motivation and objectives 1
Organisation of the document 2

1 Masonry flexural bond strength **5**
1.1 Importance of the flexural bond strength 5
1.2 Tensile and flexural behaviour of masonry bond 6
1.2.1 Softening behavior of the bond interface 6
1.2.2 Tensile versus flexural bond strength 7
1.3 Factors affecting the flexural bond strength 9
1.3.1 Brick properties 9
1.3.2 Mortar properties 10
1.3.3 Quality of masonry work 11
1.3.4 Construction conditions 11
1.3.5 Curing conditions 12
1.4 Summary of the chapter 12

2 Review of the bond wrench test **13**
2.1 Flexural bond strength tests 13
2.1.1 The beam test 13
2.1.2 The Bond wrench test 15
2.2 Application in standards 17
2.2.1 ASTM C1072-13 (America) 18
2.2.2 AS 3700 :2017 - Appendix D (Australia) 20

2.2.3 EN 1052-5:2005 (Europe) . . . 23
2.2.4 Comparison between the 3 standards . . . 27
2.2.5 Application of the standards in practice . . . 28
2.3 Evaluation . . . 29
2.3.1 Comparison with flexural strength test . . . 29
2.3.2 Influence of the apparatus on the stress distribution . . . 31
2.3.3 Bias between standards . . . 32
2.3.4 Influence of the test set-up and the specimen type . . . 34
2.4 Variants of the traditional bond wrench test . . . 37
2.4.1 Modified bond wrench test . . . 37
2.4.2 Pure couple bond wrench test . . . 38
2.4.3 In-situ bond wrench test . . . 39
2.4.4 CMOD controlled bond wrench test . . . 40
2.5 Summary of the chapter . . . 41

3 Experimental setup and methodology 43
3.1 Initial objectives of the experimental phase . . . 43
3.2 Masonry material and construction . . . 45
3.2.1 Bricks . . . 45
3.2.2 Mortar . . . 47
3.2.3 Construction and curing conditions . . . 51
3.3 Construction of a bond wrench test apparatus . . . 52
3.4 Instrumentation . . . 56
3.4.1 Loading devices . . . 56
3.4.2 Deformation measurement . . . 57
3.5 Test procedure . . . 58
3.6 First set of test . . . 60
3.7 Final objectives of the experimental phase . . . 61
3.8 Summary of the chapter . . . 61

4 Experimental results and discussion 63
4.1 Test battery description . . . 63
4.2 Influence of lever arm length and loading rate . . . 64
4.3 Influence of joint precompression . . . 68
4.4 Failure modes . . . 71
4.5 LVDt's measurement . . . 74
4.6 General comments . . . 76
4.7 Summary of the chapter . . . 76

Conclusion and future developments 78

Bibliography **86**

Appendix **86**

Extended results 87

Bond wrench shop drawings 90

Pure couple bond wrench apparatus 97

Technical sheets of the materials 100

List of Figures

1 Illustration of the bond wrench test [3]. 2

1.1 Composition of masonry structures [7]. 5
1.2 Illustration of bond behavior in a deformation-controlled tensile test [12]. . . . 6
1.3 Direct tensile tests: a) Test with adhesive plate [16], b) Test with drilled holes in the units [17]. 8
1.4 (a) Load-deflection diagram for masonry under flexure, (b) successive stress distributions in the fracturing joint. The positive sign represents tensile stress, the negative sign represents compressive stress [18]. 9
1.5 Tensile bond surface characteristics [20]: (a) Representative net bond surface observed in tensile specimens featuring solid clay units; (b) Extension of the net bond surface from specimens to the entire wall. 9

2.1 Beam test execution [3]. 14
2.2 Schematic diagram of the beam test [29]. 14
2.3 Bond wrench test procedure. Left: The prism is clamped to the retaining frame. Middle: The cantilever arm is clamped to the top brick and loaded. Right: Failure of the tested joint [3]. 16
2.4 Schematic diagram of the bond wrench test. 17
2.5 Schematic diagram of the ASTM C1072 apparatus. 19
2.6 Schematic diagram of the AS 3700 bond wrench apparatus. 21
2.7 Schematic diagram of the EN 1052-5 [41] bond wrench apparatus. 24
2.8 Failure modes which provide a valid bond strength results. 1 = tension face, 2 = compression face. 25
2.9 Practical implementations of the bond wrench test: a) American-inspired with displacement control [42], b) American-inspired using a manual jack [3], c) Long lever arm loaded with a hand-filled container [14], d-e) Australian-inspired with physical exertion [43, 44]. 28
2.10 Flexural strength test on masonry wallette. a) Loading parallel to the bed joints. b) Loading perpendicular to the bed joints.[41] 29
2.11 Relationship between bond wrench test and flexural parallel strength test [45] 30
2.12 Calibration device.[4]. 31

2.13 On the left: the ASTM C1072 apparatus loaded with a bucket. On the rigth: The AS 3700 apparatus after the failure of a joint. [6] 33
2.14 a) Force-controlled and b) CMOD-controlled set-up for laboratory tests on couplets. Set-up for in-situ tests on c) couplets and d) wallets[9] 35
2.15 a) stack-bonded couplets, b) running-bonded couplets and c) running-bonded wallets [9]. 35
2.16 Variation of flexural bond strength of stack-bonded couplets with varying bond wrench test configurations in function of hardening time [9]. 36
2.17 Relationship between flexural bond strength and pre-compression for: a) CS masonry, and b) clay masonry [9]. 37
2.18 Modified bond wrench test [8]. 38
2.19 Pure couple bond wrench test apparatus [49]. 39
2.20 In-situ bond wrench testing [50, 51]. 40
2.21 Illustration of recorded data using the CMOD-controlled bond wrench test setup: a) Applied force plotted against CMOD, and b) Vertical displacement of the hydraulic jack [9]. 41

3.1 Bricks utilized for the present study. 46
3.2 Flow Table Test Apparatus: (a) Flow Table, (b) Conical Mold. Components: 1. Base, 2. Flow Table, 3. Mortar Cone, 4. Tappet [53, 54]. 48
3.3 Illustration of the mortar flexural and compressive testing [15]. 49
3.4 Mortar sample of the present study. 50
3.5 Masonry prisms of the present study prepared for the curing process. 51
3.6 Bond wrench frame holding a prism. Components: 1. Adjustable support, 2. Clamping mechanism for prism restraint, 3. Profiles guiding and preventing torsional movement of the lever arm. 52
3.7 Adjustable support: a) General view. b) Side view. 53
3.8 Clamping mechanism for prism restraint: a) General view, b) and c) Side views. 54
3.9 Prism secured within the frame and lever arm affixed to its upper brick. P is the applied load. 55
3.10 Lever arm: a) General view, b) Side view. 55
3.11 Loading equipment. Components: 1. Lever arm, 2. Ball joint, 3. Load cell, 4. Hydraulic jack. 56
3.12 Placement of LVDT, targeting the area of maximum tensile strain. 57
3.13 Test procedure: a) Clamping the second uppermost brick of the prism to the apparatus, b) Clamping the lever arm to the top brick of the prism, c) Running the test, d) Bond failure. 58
3.14 Schematic diagram of the bond wrench test. 59
3.15 Lever arm in contact with the apparatus frame during testing. 61

4.1 Flexural bond strength by test type. 65

4.2 Flexural bond strength as a function of angular loading rate. 66
4.3 Flexural strength as a function of lever arm length. 67
4.4 Flexural bond strength as a function of the position of the joint in the prism (excluding setup failures). 69
4.5 Flexural bond strength as a function of the position of the joint in the prism (including setup failures). 70
4.6 Percentage of occurrence of the various failure modes in the present study. Black percentage indicates valid results only. Blue percentage accounts for failure during set-up. 72
4.7 Failure modes observed during the study. Mode 1 on the left, mode 2 on the right. 72
4.8 Flexural bond strength as a function of the failure mode, considering only valid results. 73
4.9 LVDT measurement: Joints G3 and I3. 74
4.10 LVDT measurement: Joints K3 and K4. 75
4.11 LVDT measurement: Joints K5 and L5. 75
4.12 Pure couple bond wrench apparatus: Side view [49]. 97
4.13 Pure couple bond wrench apparatus: Front view [49]. 97
4.14 Pure couple bond wrench apparatus: General view [49]. 98
4.15 Pure couple bond wrench apparatus: Top view [49]. 98
4.16 Pure couple bond wrench apparatus: Load cell [49]. 99

List of Tables

2.1 Comparison of the application of the bond wrench test in American, Australian, and European Standards. 27
2.2 Comparison of flexural bond strength results: Australian vs. American bond wrench test [6]. 33

3.1 Initial Rate of Absorption (IRA) of the bricks used in the present study. . . . 47
3.2 Mortar classification based on flow value [55]. 48
3.3 Flexural and compressive strength of the mortar of the present study. 50

4.1 Experimental campaign overview. 64
4.2 Student t-Test results. 65
4.3 Results based on the angular loading rate. Considering only valid results. . . . 66
4.4 Results based on the lever arm length. Considering only valid results. 67
4.5 Results based on the joint position in the prism. Considering only valid results. 68
4.6 Results based on joint position in the prism. Accounting for set-up failure with a value of 0. 70
4.7 Summary of the results based on the failure mode considering only valid results. 73

Introduction

Motivation and objectives

Unreinforced masonry stands as one of the oldest construction materials in the world, having been employed in the creation of various architectural wonders such as Greek temples, the Colosseum, and medieval cathedrals. Even in the current global real estate landscape, this construction method remains prevalent. The Belgian building stock adheres to this trend, with a significant portion being composed of masonry constructions, especially in the case of historical buildings.

Comprising units of stones, bricks, or concrete blocks that are interconnected through mortar joints, unreinforced masonry exhibits a diverse array of strength characteristics within a single structure. The wide spectrum of unit and mortar compositions, geometric arrangements, curing procedures, moisture presence, and the craftsmanship quality contribute to its varied properties. Nevertheless, the common features are that masonry has a heterogeneous and brittle behaviour with a strong resistance in compression and a low resistance in flexural tension. This weakness is mainly caused by the bond interface between the unit and the mortar, whose tensile strength is almost always lower than that of the latter two [1]. As a result, the bond interface significantly impacts crack resistance and the transmission and support of lateral loads, such as those induced by wind and seismic activity [2].

Hence, the flexural bond strength at the brick-mortar interface assumes a pivotal role in evaluating the out-of-plane critical capacity of masonry walls, essential for designing appropriate structures and assessing as well as renovating existing masonry edifices.

Within this framework, the bond wrench test operates as a method for assessing the flexural bond strength of masonry. The bond wrench test finds application in several national and international standards, including European, Australian and American standards, among others. It consists of a simple test setup in which a stack-bonded masonry prism, composed of several bricks in height, is positioned within an apparatus. This apparatus fixes the penultimate brick of the prism (i.e., the one below the top) and applies a bending moment to the top brick through the use of a lever arm. The test is repeated until all the joints of the prism

have been tested. An illustration of the test is depicted in Figure 1.

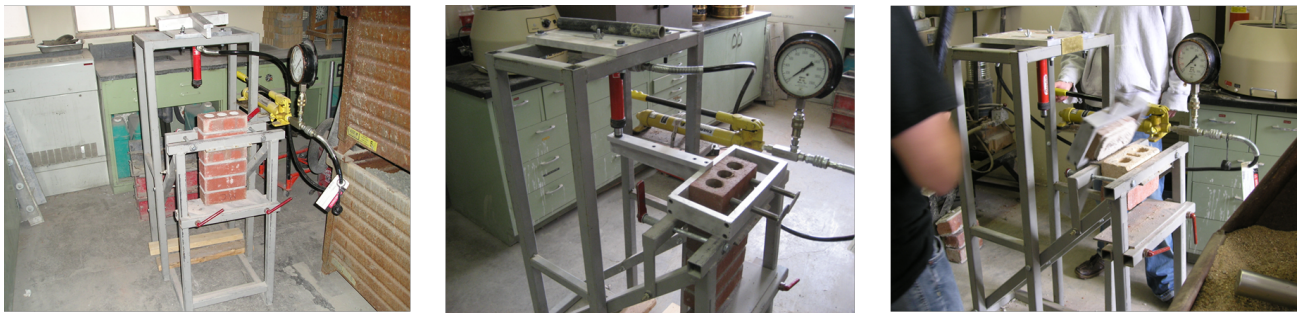

Figure 1: Illustration of the bond wrench test [3].

The first aim of the present study is to conduct a literature review into the applications of the bond wrench test across the various international standards and within the research context. This assessment involves identifying the test's advantages, limitations, and deficiencies. In this review, it appears that while the fundamental principles of the test remain uniform across international standards, distinct criteria exist for diverse parameters (the lever arm's length, the characteristics of the clamping mechanisms of the lever arm, and the rate at which load is applied).

Furthermore, existing studies suggest that the aforementioned parameters may influence the outcomes of the test [4–6]. Consequently, the second part of this work focuses on conducting an experimental evaluation of the bond wrench test's sensitivity to variations of the diverse parameters mentioned above.

Finally, this study aims at enhancing the comprehension and characterization of the behavior exhibited by the brick-mortar interface during the test.

Document organisation

This study comprises five sections:

Chapter 1 provides an overview of the masonry flexural bond strength. It highlights the significance of this parameter in characterising masonry, followed by a description of the bond interface behavior under both tensile and flexural loading. Lastly, it investigates diverse factors influencing the bond strength.

Chapter 2 conducts an examination of the bond wrench test. It starts with a general introduction to the test and its counterpart, the beam test, both used to determine flexural

bond strength of masonry joints. The chapter explores the test's implementation in different standards and research contexts, followed by an evaluation. Finally, the chapter ends with a presentation of several variants of the test.

Chapter 3 sets out the initial objectives of the experimental phase based on the insights derived from the review of the bond wrench test conducted in Chapter 2. It introduces the materials employed for carrying out the experiments and outlines the development of a bond wrench apparatus within the LEMSC (Laboratoire Essais Mécaniques, Structures et Génie Civil) at UCLouvain. The chapter subsequently focuses on the devices utilized for executing the experiments, followed by an exploration of the test procedure applied during the experimental phase. The observations and outcomes of an initial set of tests are also discussed. Ultimately, the chapter concludes by refining the objectives of the experimental phase, based on the various observations and constraints arising from the initial test phase.

Chapter 4 starts with general comments and observations regarding the outcomes of the experimental phase. It investigates the impact of several parameters within the bond wrench test setup on the flexural bond strength of masonry joints. Results are compared with findings from other studies.

The concluding chapter provides a summary of the work conducted in this master's thesis. It deliberates on the findings, acknowledges the study's limitations, and explores various possibilities for future developments.

Chapter 1

Masonry flexural bond strength

This chapter investigates the parameter assessed by the bond wrench test: the masonry flexural bond strength. It begins by highlighting the importance of this element in the characterisation of masonry. Subsequently, the behavior of the bond interface in both tensile and flexural loading is described. Finally, it examines the diverse factors that influence the bond strength.

1.1 Importance of the flexural bond strength

Unreinforced masonry is composed of units of stones, bricks or concrete blocks that are usually bonded by mortar joints (see Figure 1.1). Due to the wide variety of unit and mortar types, geometric configurations, curing process, presence of moisture and quality of masonry work, a wide range of strength characteristics can be obtained, even in the same structure.

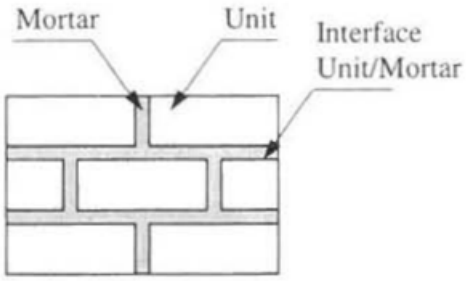

Figure 1.1: Composition of masonry structures [7].

However, the common features are that masonry has a heterogeneous and brittle behaviour with a strong resistance in compression and a low resistance in flexural tension. This weakness is mainly caused by the bond interface between the unit and the mortar, whose tensile strength is almost always lower than that of the latter two [1]. Accurately quantifying the flexural bond

strength of masonry joints proves challenging due to its dependence on a multitude of factors (refer to Section 1.3). However, to provide a general perspective on the anticipated range, standard clay bricks combined with mortar made of cement and/or lime generally manifest mean flexural bond strengths spanning approximately 0.05 MPa to 1 MPa [1, 8–12]. These values offer a magnitude estimate, and it's noteworthy that more robust bonds exist [13, 14].

Given its weakness, the bond interface, exerts considerable influence on the resistance to cracking and on the transfer and support of lateral loads, such as wind and earthquakes, which cause flexural tensile stresses [2]. Furthermore, it has been demonstrated that an increase in bond strength has a positive impact on the masonry compressive strength [8].

1.2 Tensile and flexural behaviour of masonry bond

Sections 1.2.1 and 1.2.2 discuss the non-linear response characterising the tensile behavior of the bond interface, as well as the differentiation between the tensile and flexural strength of masonry bonds.

1.2.1 Softening behavior of the bond interface

The non-linear response of masonry under tensile is mainly caused by a softening phenomenon which characterise quasi-brittle material such as concrete, bricks and mortars. This softening behavior is represented in Figure 1.2.

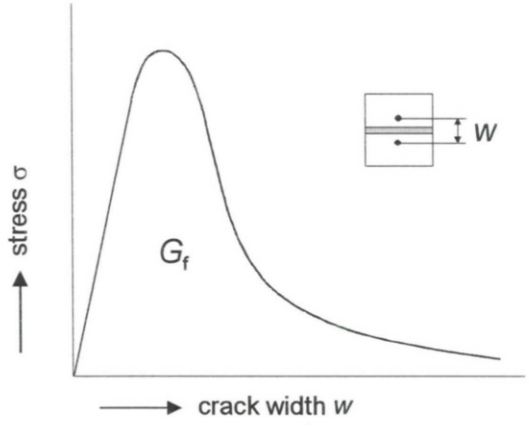

Figure 1.2: Illustration of bond behavior in a deformation-controlled tensile test [12].

Three successive parts of the stress/crack width curve represented in Figure 1.2 can be identified [12, 15]:

1. At the beginning, the behaviour is linear elastic and the stiffness is maximum.

2. Then the strength continues to increase, but the stiffness starts to decrease. This is due to the appearance of micro-cracks.

3. After reaching the stress peak, micro-cracks merge together to form a macroscopic crack. This crack then propagates through the material and results in a decrease in stiffness and stress as deformations increase, until complete fracture occurs.

The area under the diagram of Figure 1.2 represents the fracture energy, denoted as G_f. Fracture energy is the energy per unit area required to initiate a crack where no further tensile stresses can be transmitted [12].

Quantifying the tensile bond fracture energy is important for characterising the quasi-brittle behaviour of masonry or for predicting the progression of cracking and masonry failure using non-linear analysis. Even a slight alteration in the tensile bond fracture energy can lead to differences in evaluating aspects such as the out-of-plane capacity and in-plane capacity of masonry walls. Moreover, variations in the fracture energy can impact assessments of crack width and the extent of damage in masonry structures [9].

1.2.2 Tensile versus flexural bond strength

There are two methods to determine the tensile bond strength of masonry:

1. Direct tensile tests: Figure 1.3.a illustrates a direct tensile test, where the tensile load is applied using metal plates affixed to the units with adhesive [16]. In Figure 1.3.b, loading is applied using rods passing through the bricks, via holes drilled in the units [17]. It should be noted that the two mentioned direct tensile tests are not an exhaustive list.

2. Indirect tensile tests (i.e, flexural tests): These include methods like the bond wrench test and the beam test (described in Section 2.1).

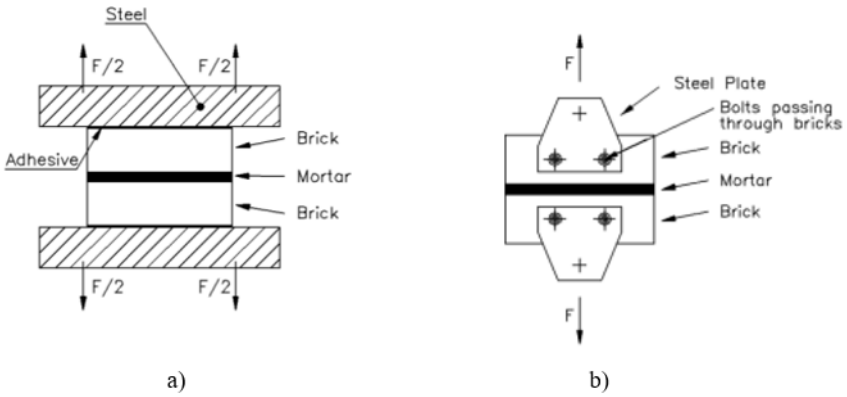

Figure 1.3: Direct tensile tests: a) Test with adhesive plate [16], b) Test with drilled holes in the units [17].

However, the two aforementioned test methods for characterizing tensile bond strength do not give the same results [15].

A first reason for this difference is that tensile and flexural strength of masonry bond are related but different properties [12]. The difference lies in the tensile softening behavior which can causes stress redistribution under flexural loading [18]. This phenomenon is depicted in Figure 1.4. When the extreme fibers reach the tensile bond strength, a crack forms as the bending moment continues to increase. However, unlike a perfectly brittle material, the stress at the level of the extreme fibers does not immediately drop to zero; instead, it gradually decreases by following the downward part of the curve represented in Figure 1.2. As the crack propagates, the bending moment reaches a maximum value. If this maximum moment is maintained or increased, failure suddenly occurs as the crack continues to propagate [19]. Usually, the flexural strength is defined as the ultimate bending moment divided by the elastic section modulus. Therefore, a fictitious linear stress distribution is assumed. As a result, the calculated value needs to be corrected by a factor to deduce the actual tensile bond strength. This corrective factor is commonly taken to be 1.5. However, it is important to note that this constitutes a rough approximation [16].

Another factor contributing to the difference in results between direct and indirect tensile tests is the fact that the various methods initiate failure at distinct locations within the joint. Typically, in the bond wrench test, failure starts from one edge, which may not necessarily reflect the entirety of the adhesive surface of the mortar with the unit (see Figure 1.5) [15].

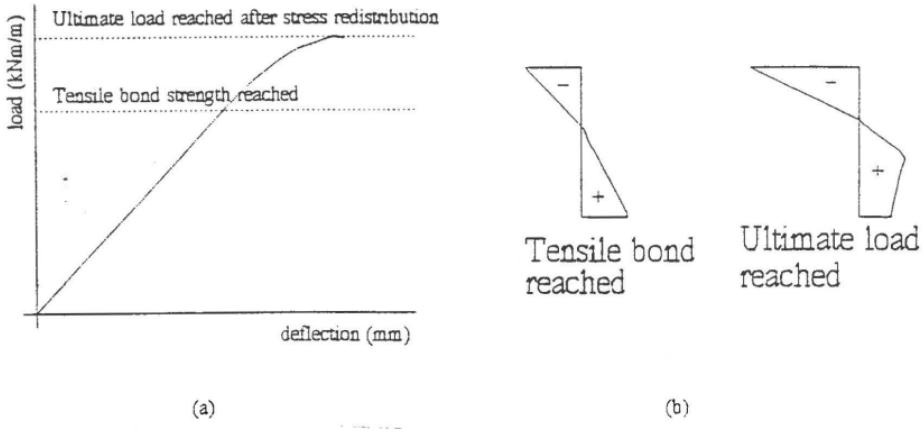

Figure 1.4: (a) Load-deflection diagram for masonry under flexure, (b) successive stress distributions in the fracturing joint. The positive sign represents tensile stress, the negative sign represents compressive stress [18].

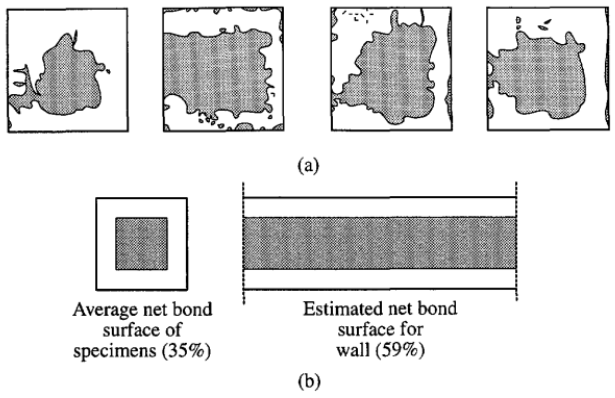

Figure 1.5: Tensile bond surface characteristics [20]: (a) Representative net bond surface observed in tensile specimens featuring solid clay units; (b) Extension of the net bond surface from specimens to the entire wall.

1.3 Factors affecting the flexural bond strength

The masonry bond strength is affected by a multitude of factors, including the properties of the units and mortars, the quality of workmanship and the construction and curing conditions. These elements collectively contribute to the observed variability in bond strength, which can exhibit significant fluctuations even within the same structure. This section examines the influence of the aforementioned factors on the bond strength.

1.3.1 Brick properties

The primary brick properties that impact bond strength are its surface texture and suction. Surfaces featuring a rough texture and pores exhibit enhanced receptivity to wet mortar, pro-

moting increased adhesion as the mortar fills voids and establishes a mechanical attachment. Conversely, smooth or coated surfaces tend to diminish bond strength [1, 21].

Regarding suction, an increase in the brick's suction leads to a reduction in bond strength, caused by the swift loss of water from the mortar. The brick's initial rate of absorption (IRA) serves as an indicator of its suction capacity. A high IRA implies swift moisture transfer from the mortar to the brick, resulting in a weakened bond. Conversely, a low IRA prevents the brick's ability to absorb sufficient moisture for optimal bond development [1, 21].

1.3.2 Mortar properties

Most mortars are a mixture of cement, lime, sand and water to which may be added various admixtures including workability enhancers, set accelerators, and retarders. Mortar properties that influence bond strength include compressive strength, workability, composition, and water retention.

In general, flexural strength increases as the compressive strength of the mortar increases, regardless of the type of masonry unit [22]. This is reflected in Eurocode 6 [23], which classifies the flexural strength of masonry according to the type of unit and the compressive strength of the mortar, with higher mortar strength implying higher flexural strength.

The workability of mortar also significantly affects bond strength. Achieving complete contact between mortar and brick is important for bond development, and the ease of mortar spreading is determined by its workability [1]. Lime, plasticizers, or air-entraining agents can be incorporated into the mix to enhance the workability [2].

The composition of mortars is also important. Lean mortars, exhibit notably lower flexural bond strength compared to richer cement mortars [22]. The incorporation of elements such as lime, plasticizers, or air-entraining agents to enhance mortar workability can lead to a slight reduction in bond strength, provided that recommended limits by manufacturers and standards are followed [24, 25]. However, an excessive use of these additives can significantly reduce the contact layer of cementitious material along the brick/mortar interface, leading to a decrease in bond strength [24]. On the contrary, the inclusion of hydrated lime has been shown to enhance bond strength by improving workability and moisture retention [24].

Pavia *et al.* [1] give the following indications on the influence of mortar's water retention on the bond strength of masonry joints: Mortars experience water loss through evaporation and trough suction when in contact with absorbent bricks. Effective water retention allows the mortar maintaining adequate moisture levels for proper curing and bonding. It also ensures that the mortar retains plasticity, allowing for the positioning of bricks without leading

to bond failure. In situations involving low-absorption bricks, mortars with low water retention tend to release excess moisture, resulting in the accumulation of water at the interface. This excess moisture can cause the brick to essentially "float," thereby diminishing the bond strength. However the bond strength is more adversely impacted when mortars are overly dry as opposed to being too wet. Mortars that are too wet to be easily worked still exhibit favorable bond strength, whereas dry mixtures show a considerable decline in bond strength.

1.3.3 Quality of masonry work

Workmanship is an element directly impacting the masonry bond strength.

Defects in the construction process that can have a negative impact on bond strength include [1, 2]:

- Incorrect dosing and mixing of mortar or a lack of consistency in batching mix constituents leading to variations in mortar composition within the same structure (and therefore variations in bond strength).
- Inadequate or incomplete application of mortar onto the surfaces of the units, as illustrated in Figure 1.5.
- Inadequate curing conditions.
- Disturbance of masonry units or joints before proper curing.

1.3.4 Construction conditions

Insights into the impact of hot and cold weather on masonry construction are provided by the Brick Industry Association (America) [26]:

- Elevated temperatures during construction can have detrimental effects on the quality of masonry work. Particularly in hot weather, rapid evaporation and water absorption from the mortar may be of significant concerns. Swift water loss due to evaporation reduces the available water for proper hydration, thereby reducing mortar strength development. This also results in decreased workability of the mortar, necessitating retempering to maintain a workable state. Retempering the mortar to replace water lost through evaporation is a recommended practice, if necessary. While the compressive strength might experience a minor decrease, bond strength may be weakened if water is not added [21]. However, research has indicated that retempering can lead to a decrease bond strength when done an excessive time after the mixing of the mortar [27]. Consequently, the ASTM C270 (American norm) [25] requires that mortar should not be used beyond two and a half hours after mixing, as the setting process begins. However, this timeframe might be shortened in hot weather conditions [26].

- Effective cement hydration occurs when material temperatures are elevated to 4.4 °C or higher. Successful curing of mortar relies on the hydration of cement. This chemical process produces a certain amount of heat, enabling the maintenance of material temperatures above 4.4 °C even when surrounding ambient temperatures are moderately lower. Nonetheless, with further decreases in ambient temperatures, this chemical reaction may decelerate or stop entirely unless sufficient heat is preserved within the mortar. In situations where cement hydration remains incomplete, the outcome could be a soft and friable mortar with compromised durability.

1.3.5 Curing conditions

The post-construction application of moist curing practices is aimed at optimizing cement hydration, resulting in an improved bond, particularly in the case of high suction bricks [2]. Consequently, masonry specimens that undergo air curing demonstrate diminished flexural bond strength in comparison to the results achieved when employing methods like wrapping the specimens with polyethylene sheeting or wetting them after fabrication [28].

1.4 Summary of the chapter

This chapter, initiated by highlighting the importance of the flexural bond strength in the response of masonry under lateral loads such as wind and earthquakes. Subsequently, it investigated the quasi-brittle behavior of the bond interface under tensile and its implication into the disparity between the flexural and tensile strength of the bond interface. Moreover, the discussion extended to various factors influencing the flexural bond strength. These included brick and mortar properties, workmanship quality, and construction and curing conditions. Brick properties discussed were the surface texture and suction. Rough surfaces enhance adhesion, while high brick suction weakens the bond due to rapid moisture loss. Mortar properties encompass compressive strength, workability, composition, and water retention. Higher compressive strength enhances bond strength, workability affects mortar spreadability, and proper water retention supports curing and bonding. Quality of masonry work influences bond strength through proper application of mortar, curing, and prevention of disturbances. Construction conditions, such as hot and cold weather, can affect cement hydration, potentially leading to reduced bond strength. The post-construction application of moist curing practices, such as wrapping the specimens with polyethylene sheeting, can optimise cement hydration, resulting in an improved bond.

Chapter 2

Review of the bond wrench test

This second chapter reviews the existing literature related to the bond wrench test. This test method is used to determine the masonry flexural bond strength, an essential parameter investigated in Chapter 1. The chapter begins with a general description of the test and its alternative, the beam test. Then the applications of the bond wrench test in American, Australian and European standards is described and compared. Subsequently, the existing literature evaluating the test is explored. Finally, variants of the test setup are presented.

2.1 Flexural bond strength tests

Two main tests are currently used to determine the masonry flexural bond strength: the beam test and the bond wrench test. The subsequent sections provide an overview of these tests, focusing on their implementation according to American, Australian, and European standards.

2.1.1 The beam test

This test method is included in the American and Australian standards. The corresponding documents are respectively:

- The ASTM E518: Standard Test Methods for Flexural Bond Strength of Masonry [29].
- The AS 3700, Appendix D: Method of test for flexural strength [30].

It is not included in European standard. The test is composed of a masonry prism with several joints. The specimen is placed horizontally on its supports as a simply supported beam. Two points loads are then applied such as illustrated in Figure 2.2. The distance between each support and the adjacent point load is one-third of the span length. The load is applied at a uniform rate of travel of the moving head in the ASTM E518 procedure. In the AS 3700 procedure, the load is increased steadily and without shock until failure occurs. The maximal

Figure 2.1: Beam test execution [3].

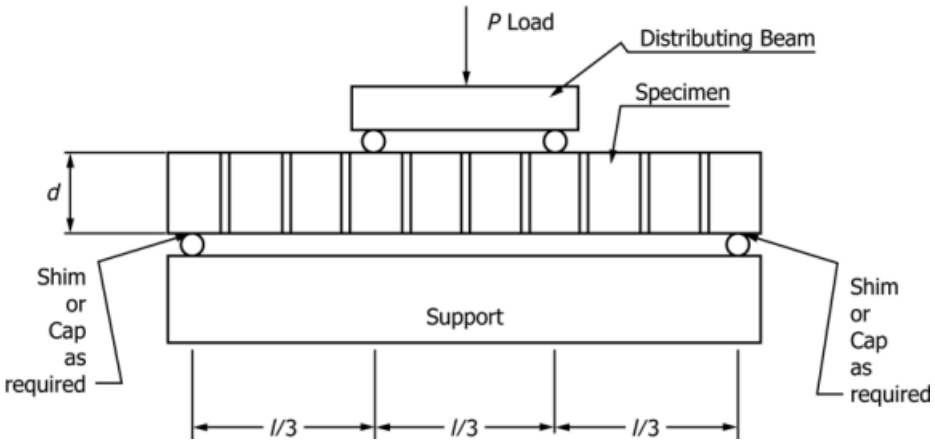

Figure 2.2: Schematic diagram of the beam test [29].

load is then recorded.

The flexural bond strength f_m [Pa] is calculated based on a linear stress distribution hypothesis:

$$f_m = \frac{M}{Z} \tag{2.1}$$

With M [Nm] the bending moment value located at mid-span of the specimen and Z [m^3] the section modulus of the cross-section of the specimen. The self weight of the prism should be taken into account when calculating the bending moment at mid-span of the prism. In the Australian standard, the flexural bond strength f_m is corrected by a masonry pier strength factor k_{sp} which value is function of the number of courses in the specimen: it is equal to 1.00 for a 4-high pier, 1.20 for a 7-high pier and 1.25 for a 9-high pier.
The reason for this strength factor is not indicated in the standard. It can be assumed that it is used to take into account a statistical consideration on the number of joints under maximum bending stress: The higher the number of joints under maximum stress, the higher the

probability of having a weak joint that will break first [12, 31].

Failure should occur inside the middle third of the beam. If this does not occur, the result for the specimen is not considered.

This general description of the test corresponds to that indicated in the American and Australian standards. The main differences that can be highlighted are:

- The alternative possibility of applying a uniformly distributed load instead of two point loads in the American standard.
- The application of the load in a displacement-controlled protocol in the American standard versus in a force-controlled protocol in the Australian standard.
- The significance and use of the test: The American standard limits the use of this test "to provide simplified and economical means for gathering comparative research data on the flexural bond strength developed with different types of masonry units and mortar or for the purpose of checking job quality control (materials and workmanship)" [29]. The Australian standard extends the use of the beam test to the determination of the flexural strength.

Some drawbacks of the beam test can be highlighted. Firstly, although there are several joints in each specimen, only one result is obtained per prism. Secondly, for very weak bonds, the self-weight of the prism may cause the specimen to break before the test is performed. In addition, several joints may open, making the behaviour of the beam non-linear before reaching the peak. Finally, as mentioned before, test results may vary depending on the number of joints subjected to maximum bending stress.

2.1.2 The Bond wrench test

The bond wrench test is also included in the American and Australian standards as an alternative to the beam test. In addition, it is part of the test methods for masonry included in the Eurocode 6 [23]. The corresponding documents for the American, Australian and European standards are respectively:

- The ASTM C1072: Standard test methods for measurement of masonry flexural bond strength [32].
- The AS 3700, Appendix D: Method of test for flexural strength [30].
- The EN 1052-5: Methods of test for masonry - Part 5: Determination of bond strength by the bond wrench method [33].

The implementation of the test in each standard is detailed in Section 2.2. Here, a general presentation of the test is made.

The bond wrench test was developed in 1980 in Australia. It is more recent than the beam test which was already included in the American standard (ASTM) since 1974. There are variations in the execution of the test between the different standards, but the general principle remains the same. The test is carried out on a small masonry prism composed of several joints. The second unit, starting from the top, is clamped to a retaining frame. A cantilever arm is affixed to the top brick, and the load applied at its end is incrementally increased until the top brick detaches from the rest of the assembly. Throughout the test, the bending moment generated by the load applied at the lever arm's end induces tensile stresses in one half of the mortar joint and compressive stresses in the other half. However, the load causes additional uniform compressive stresses inside the joint.

After the top brick has detached from the prism, the cantilever arm is attached to the new top brick and the test can be carried out again. Therefore, a prism composed of, for example, 6-bricks allows to test 5 mortar joints in total. Figure 2.3 shows the different steps to perform the test.

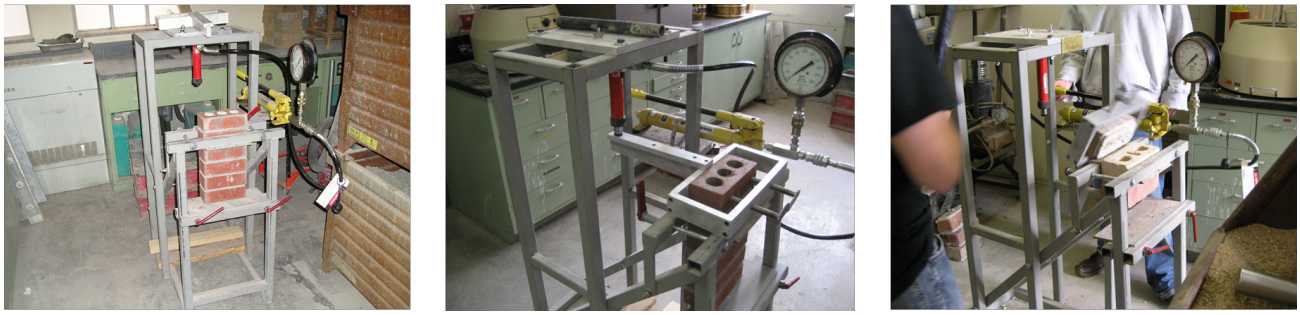

Figure 2.3: Bond wrench test procedure. Left: The prism is clamped to the retaining frame. Middle: The cantilever arm is clamped to the top brick and loaded. Right: Failure of the tested joint [3].

Assuming a linear stress distribution, the flexural tensile bond strength f_m is calculated with the following formula (see Figure 2.4):

$$f_m = \frac{P_1.L_1 + P_2.L_2}{Z} - \frac{P_2 + P_1}{A} \tag{2.2}$$

With Z $[m^3]$ the section modulus of the cross-section of the specimen, P_1 $[N]$ the weight of the loading arm, P_2 $[N]$ the maximal applied load, $L_1[m]$ the distance from the centre of gravity of the lever arm to the centre of the prism, L_2 $[m]$ the length of the cantilever arm, A $[m^2]$ the area of the cross-section of the specimen.

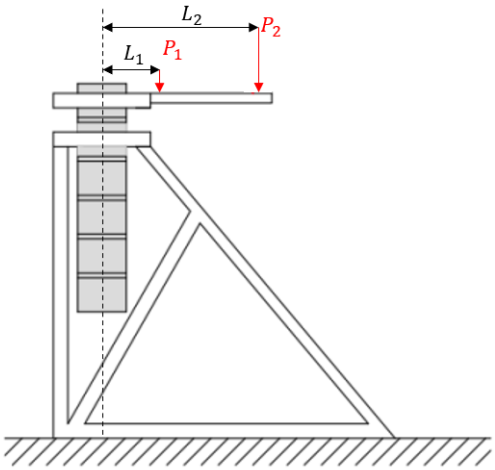

Figure 2.4: Schematic diagram of the bond wrench test.

The advantages of the bond wrench test rely in the simplicity of the test set-up equipment and the possibility to test each joint of the prism (unlike the beam test who gives only one result per prism). This makes it a very simple and cost-effective test.
Similar to the beam test, a disadvantage is that for very weak bonds, the self weight of the lever arm could lead to the tested joint to fail before running the test. Another drawback is that the test may be sensitive to variations in its configuration. This is discussed in section 2.3. Furthermore, bond wrench tests often exhibit notable coefficients of variation, typically ranging from 15% to 50%, even under well-controlled laboratory conditions [9]. This variability is particularly pronounced in cases involving masonry that exhibits weak bonding, such as historical masonry and masonry that is deteriorating.

2.2 Application in standards

In the following sections, the implementation of the bond wrench test in the American [32], Australian [30] and European [33] standards is detailed and compared. The main parameters studied in the different standards are:

- The scope of the test.
- The evaluation of the units and mortars.
- The preparation of the specimens and the curing conditions.
- The test apparatus.
- The test procedure.

- The measurements and observations.

2.2.1 ASTM C1072-13 (America)

Scope of the test

The scope of the test is to evaluate the flexural bond strength, normal to the bed joints, of masonry built of manufactured masonry units. Three different methods are specified for three different uses:

1. A method to test laboratory prepared specimens. Its purpose is to compare the bond strengths of masonry mortars. It uses very specific standard concrete masonry units.
2. A method to test field prepared specimens for preconstruction evaluation of materials or for quality control purposes during construction works.
3. A method to test prisms removed from existing masonry walls.

The following lines describe the method to test field prepared specimens.

It is specified that "the flexural bond strength determined by this test method shall not be interpreted as the flexural bond strength of a wall constructed of the same material, nor shall it be interpreted as an indication of extent of bond for purposes of water permeability evaluation. However, if effects of construction conditions, specimen size, workmanship, and curing conditions are taken into account, the results may be used to estimate the flexural strength of a wall" [32]. However, no practical information is given on how to perform this estimate based on the effects cited.

Evaluation of the units and mortars

The mortar is sampled and tested to determine initial consistency by cone penetrometer or flow table and air content. Clay units are sampled and tested to determine initial rate of absorption. Procedures are provided in ASTM C780 [34] and ASTM C67 [35].

Preparation of the specimens and curing conditions

An appropriate number of stack-bonded prisms, with a maximum of 5 joints in each, shall be fabricated. A total number of at least 15 mortar joints shall be tested. In addition, all prism specimens must be constructed in no more than 30 minutes. Care should be taken to handle the prisms as little as possible and in such a way that the joints are not subjected to detrimental tensile stress.
After construction, the prisms must be sealed in moisture-proof bags. The specimens should cure for 28 days after which they are tested unless otherwise specified.

Apparatus

Detailed technical drawings containing all the dimensions and elements of the test apparatus are provided in the standard. Schematic diagrams are provided in Figure 2.5. A notable dimension is the length of the lever arm: 0.515 m. The upper clamping bracket is connected to the unit by means of clamping bolts that adjust the position of a bearing plate.

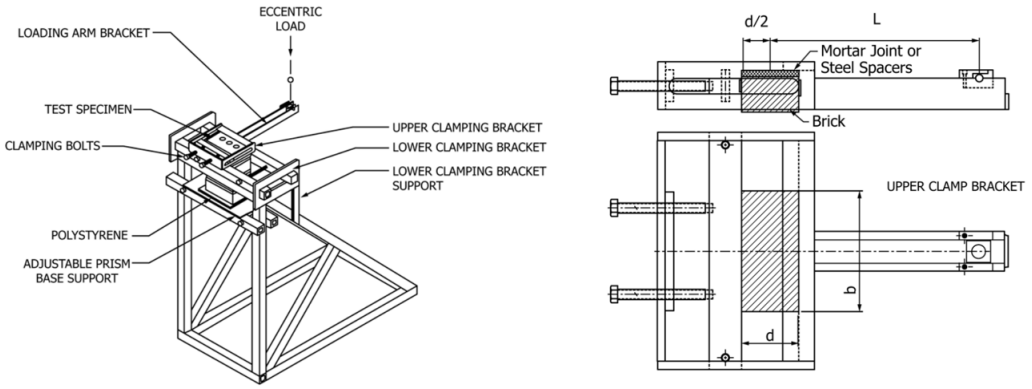

Figure 2.5: Schematic diagram of the ASTM C1072 apparatus.

The mass of the upper clamping bracket including the loading arm, is determined with an accuracy of ±25 g. The equilibrium point is found using a trial-and-error process by varying the position of the frame upon a knife edge balance.

Test procedure

- The prism is placed vertically in the support frame and clamped firmly into a locked position using the lower clamping bracket at the level of the second unit starting from top.

- Then, the upper clamping bracket is attached to the top. Each clamping bolt is tightened with a maximum torque of 5.7 Nm. The lower base support is moved away from the bottom of the prism so that no contact is made during the test.

- The load is applied at a uniform rate in such a way that the total load is reached between 1 min and 3 min. **It shall be measured with an accuracy of ±2% with maximum error of 22 N**. It can be applied by any means, such as a testing machine, hydraulic jack, dead weights, etc. but must be within ±3° of vertical. If the dead weights of the lever arm and the upper unit that is pulled out are neglected, an error of ±2% in the calculation of F_1 leads to an error of ±2% in the evaluation of f_m.

Measurement

Load may be measured using the testing machine indicator, proving ring, load cell, or any device capable of the prescribed precision. **"Special attention must be given to non-recording load measuring devices. Since failure of the specimen is sudden, the device must be continuously monitored or the failure load will be lost."[32]**

Calculation of the results

The calculation of the results (flexural bond strength f_m) is based on formula 3.4. The exact formulation in the standard is the following:

$$f_m = \frac{6.(P.L + P_1.L_1)}{bd^2} - \frac{(P + P_1)}{bd} \tag{2.3}$$

With P [N] the maximum applied load, P_1 [N] the weight of the loading arm (this includes the weight of the top unit who is pulled out), L [mm] the distance from center of prism to loading point, L_1 [mm] the distance from center of prism to centroid of loading arm, b [mm] the cross-sectional width of the mortar-bedded area and d [mm] the cross-sectional depth of the mortar-bedded area.

2.2.2 AS 3700 :2017 - Appendix D (Australia)

Scope of the test

The scope of the test is to determine the flexural strength of masonry. This makes an important difference with the American and European standards who limit the use of the test to evaluate the flexural *bond* strength.

Evaluation of the units and mortars

No specific guidelines.

Preparation of the specimens and curing conditions

Stack-bonded prisms, with a number of joints between two and seven, shall be manufactured. A total number of at least six bonds shall be tested.
For curing, the piers forming the sample shall be fully wrapped in a single vapour-proof sheet and left undisturbed. Testing of the prisms shall be carried out 7 days after construction for plain masonry and 28 days after filling the cores with grout for grouted masonry.

Apparatus

Schematic diagrams of Figure 2.6 represent the apparatus. Only certain requirements for the gripping blocks are provided, which allows for a wide flexibility in the design of the device compared to ASTM C1072 [32].

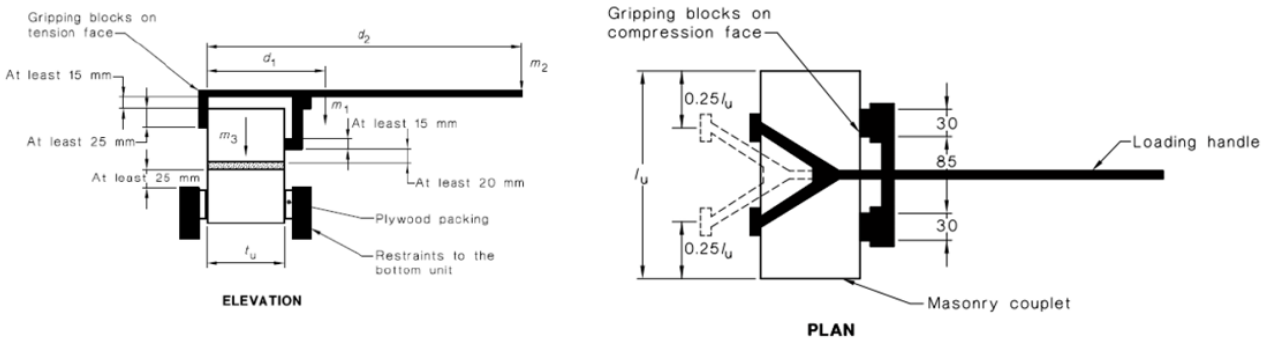

Figure 2.6: Schematic diagram of the AS 3700 bond wrench apparatus.

The gripping blocks are subject to the following requirements:

- Their length shall be 30 mm.
- Those that are perpendicular to the face of the masonry unit shall be at least 20 mm thick.
- The height of the gripping blocks in contact with the masonry unit on the tension side shall be at least 25 mm.
- The height of the gripping blocks on the tension side shall be such that a gap of at least 15 mm is maintained between the top surface of the top unit and the loading arm. The purpose is to ensure that only the gripping blocks come into contact with the specimen during the test.
- The gripping blocks shall be located as far away as possible from the top interface of the joint under test. A minimum distance of 20 mm is required.

Test procedure

As a general rule, the means by which the load is applied and measured shall be capable to determine the flexural stress at failure to an accuracy within 0.01 MPa.

The steps in the procedure are as follows:

- The lower part of the specimen is securely held by a suitable frame. The stability of the entire apparatus must be maintained when fully loaded.

- Then, the top masonry unit of the prism is clamped to the bond wrench in a suitable manner (Figure 2.6) to prevent the unit from being crushed. The wrench is adjusted so that its arm is horizontal.

- From there, two methods are possible for applying the load:

  – The suspended container method: An empty container is hung at the point of load application. The bottom of the container should not be more than 100 mm above the ground or other level of support. The container is loaded at a steady rate of between $10\,\mathrm{kg\,min^{-1}}$ ($1.65\,\mathrm{N\,s^{-1}}$) and $15\,\mathrm{kg\,min^{-1}}$ ($2.45\,\mathrm{N\,s^{-1}}$) until the top portion of the specimen separates from the restrained lower portion. Loading can be done using dry sand or other suitable material.

  – The Testing machine method: If it has the required accuracy, a load-measuring machine may be substituted for the suspended container for the determination of m_2 (Figure 2.6).

Measurement

To perform the calculation, the following parameters shall be measured:

- The mass of the container and contents together m_2 to within ±100 g. This is substitute by a load-measuring machine with adequate accuracy if using the testing machine method.

- The mass of the top masonry element of the prism and any mortar adhering to it m_3, to within ±100 g.

- The width t_u of the top masonry unit, to within ±2 mm.

Calculation of the results The calculation of the results (flexural bond strength f_m) is based on formula 3.4. The exact formulation in the standard is the following:

$$f_m = \frac{M}{Z} - \frac{F}{A} \tag{2.4}$$

With M [N mm] the bending moment about the centroid of the bedded area of the test joint at failure, Z [$\mathrm{mm^3}$] the section modulus of the design cross-sectional area, F [N] the total compressive force on the bedded area of the tested joint, and A [$\mathrm{mm^2}$] the design cross-sectional area of the member.

The calculation of M and F are given by the following formulas:

$$M = 9.81\, m_2 \left(d_2 - \frac{t_u}{2}\right) + 9.81\, m_1 \left(d_1 - \frac{t_u}{2}\right) \tag{2.5}$$

$$F = 9.81\,(m_1 + m_2 + m_3) \tag{2.6}$$

With m_1, m_2, m_3 [kg] the masses of components used in flexural strength testing, d_1 [mm] the distance from the inside edge of the tension gripping block to the centre of gravity, d_2 [mm] the distance from the inside edge of the tension gripping block to the loading handle and t_u [mm] the width of the masonry unit.

2.2.3 EN 1052-5:2005 (Europe)

Scope of the test

The scope of the test is to determine the flexural bond strength of masonry.

Evaluation of the units and mortars

The moisture content of the units shall be measured, in accordance with EN 772-10 [36]. A sample of the units is submitted to a compression test following the EN 772-1 [37].

The fresh mortar is subjected to a test for the determination of its consistence (EN1015-3 [38]) and a test to determine its air content (EN1015-7 [39]). At time of testing the bond strength, a test to determine the mean compressive strength of the mortar is conducted following the EN 1015-11 [40].

Preparation of the specimens and curing conditions

No indications are given on the number of joints that should contain the prisms. The only requirement is to build enough specimens such that at least 10 valid results are available (failure modes providing valid results are presented in Figure 2.8).

Specimens should be constructed within 30 minutes of completion of the conditioning of the units. The mortar used should not be mixed for more than one hour before application unless it is designed for longer use.

The prims are pre-compressed using a uniformly distributed mass to create a vertical stress between $2 \times 10^{-3}\,\mathrm{N\,mm^{-2}}$ and $5 \times 10^{-3}\,\mathrm{N\,mm^{-2}}$. The prisms are then maintained pre-compressed and undisturbed in polyethylene sheets during a curing period of 28 days. Test of the specimens are performed at an age of $28 + 1$ days.

Apparatus

Schematic diagrams of the apparatus are represented in Figure 2.7. The only requirements in the design of the device are the following:

- The height of the gripping blocks in contact with the masonry unit on the tension side shall be at least 10 mm.
- The length of the lever arm of the wrench (e_1) should be at least of 1 m.
- The tensile stress applied to a specimen caused by the weight of the lever arm and clamping devices shall not exceed 0.05 N mm^{-2}.
- Care shall be taken to ensure that the specimen is not subjected to torsional stress.

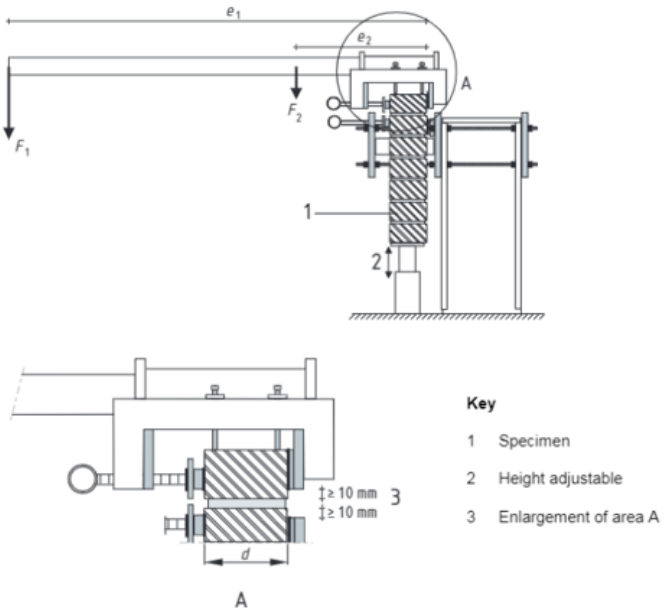

Figure 2.7: Schematic diagram of the EN 1052-5 [41] bond wrench apparatus.

Test procedure

- Clamping the prism in such a way that the second unit starting from the top is restrained from rotation and the joint under test is 10 to 15 mm away from the clamping device. Thin layers of material (such as plywood) may face the clamp to ensure an even grip. Clamping device should be stable throughout the loading period.
- Carefully clamping the top unit with plywood or other material to ensure an even grip if necessary. The loading arm is adjusted to be horizontal.

- Applying smoothly the load such that failure occurs in 2 to 5 minutes. No method for applying the load is proposed, there are only requirements on the accuracy of the load measurement.

Measurement

The following measurement are required to perform the calculations:

- The weight of the top unit and any adherent mortar (W) with an accuracy of ±1% .
- The applied load (F_1) with an accuracy of ±1%. If the dead weights of the lever arm and the upper unit that is pulled out are neglected, an error of ±1% in the calculation of F_1 leads to an error of ±1% in the evaluation of f_m.
- The dimension of the specimen with an accuracy of ± 1 mm.

The failures modes providing valid results are represented in Figure 2.8. These indicate whether the weakest part of the test specimen is the unit, the mortar or the interface between the two.

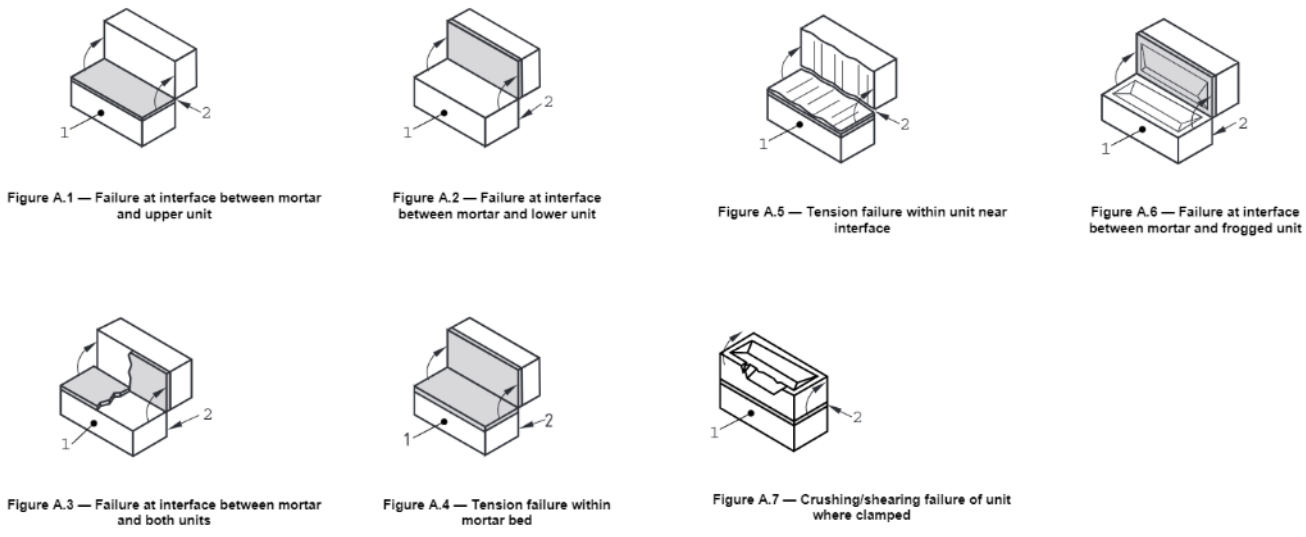

Figure 2.8: Failure modes which provide a valid bond strength results. 1 = tension face, 2 = compression face.

Calculation of the results

The calculation of the results (flexural bond strength f_m) is based on formula 3.4. The exact formulation in the standard is the following:

$$f_m = \frac{F_1.e_1 + F_2.e_2 - \frac{2}{3}d(F_1 + F_2 + W/4)}{\frac{b.d^2}{6}} \tag{2.7}$$

With b [mm] the mean width of the bed joint tested, d [mm] the mean depth of the specimen, e_1 [mm] the distance from the applied load to the tension face of the specimen, e_2 [mm] the distance from the center of gravity of the lower and upper clamp from the tension face, F_1 [N] the applied load, F_2 [N] the weight of the bond wrench and W [N] the weight of the masonry unit pulled off the specimen and any adherent mortar.

2.2.4 Comparison between the 3 standards

Table 2.1 summarises and compares the key parameters for the application of the bond wrench test in the different standards. In addition to Table 2.1, a comparison of the loading rates

	American	Australian	European
Scope	- Flexural bond strength.	- Flexural strength.	- Flexural bond strength.
Evaluation of units	- Initial rate of absorption.	- No requirements	- Moisture content. - Compression test
Evaluation of mortars	- Consistency of fresh mortar. - Air content of fresh mortar	- No requirements	- Consistency of fresh mortar. - Air content of fresh mortar. - Mean compressive strength at the time of testing.
Curing	- 28 days, sealed in moisture-proof bags.	- 7 days for plain masonry, sealed in moisture-proof bags. - 28 days for grouted masonry, sealed in moisture-proof bags.	- 28 days, sealed in moisture-proof bags.
Apparatus	- Complete technical drawings provided. - Length of the lever arm: 0.515 m. - Clamping mechanism: Continuous bearing plate - No requirements about the distance between gripping blocks and the joint.	- Only schematic diagrams. - Length of the lever arm: No requirements. - Clamping mechanism: Separate bearing pads - Requirements about the distance between gripping blocks and the joint.	- Only schematic diagrams. - Length of the lever arm: at least 1 m. - Clamping mechanism: Not specified - Requirements about the distance between gripping blocks and the joint.
Test procedure and measurement	- The load is applied at a uniform rate. The total load is reached between 1 min and 3 min. - Load is applied and measured by any means but a certain level of accuracy is required.	- The load is applied at a uniform rate between $1.65\,\mathrm{N\,s^{-1}}$ and $2.45\,\mathrm{N\,s^{-1}}$. - Load is applied and measured by any means but a certain level of accuracy is required.	- The load is applied at a uniform rate. The total load is reached between 2 min and 5 min. - Load is applied and measured by any means but a certain level of accuracy is required.

Table 2.1: Comparison of the application of the bond wrench test in American, Australian, and European Standards.

between the European and American standards in terms of applied bending moment M can be made:

- The European standard suggests a lever arm of 1 m and a loading period of 2-5 minutes. This means that to reach, for example, a 100 N force, one would have $M = 100$ Nm to be applied in 5 minutes: $0.33\,\mathrm{N\,m\,s^{-1}}$.
- The American standard requires a lever arm of 0.5 m, which yields (still for a 100 N force) a moment of 50 Nm in 3 minutes: $0.28\,\mathrm{N\,m\,s^{-1}}$.

It can be seen that these two results are very similar.

2.2.5 Application of the standards in practice

The preceding sections have presented the implementation of the bond wrench test in the three most referenced standards in scientific articles: the American, Australian, and European standards. However, it is worth noting that these standards are not always strictly followed in practice. They are used as references, but their specific requirements are not always met due to limited resources or practical challenges in compliance.

As a result, there exists a wide variety of implementations of the bond wrench test in practice. Often, few details are provided regarding the test setup, and the standards are merely cited. Figure 2.9 provides some non-exhaustive examples. The lever arms have distinct clamping mechanisms, different lengths (typically ranging from 300 mm to 900 mm, although occasionally shorter or longer), and varying methods of applying the load (such as through a controlled hydraulic jack, manually operated jack, hand-filled container, or physical exertion).

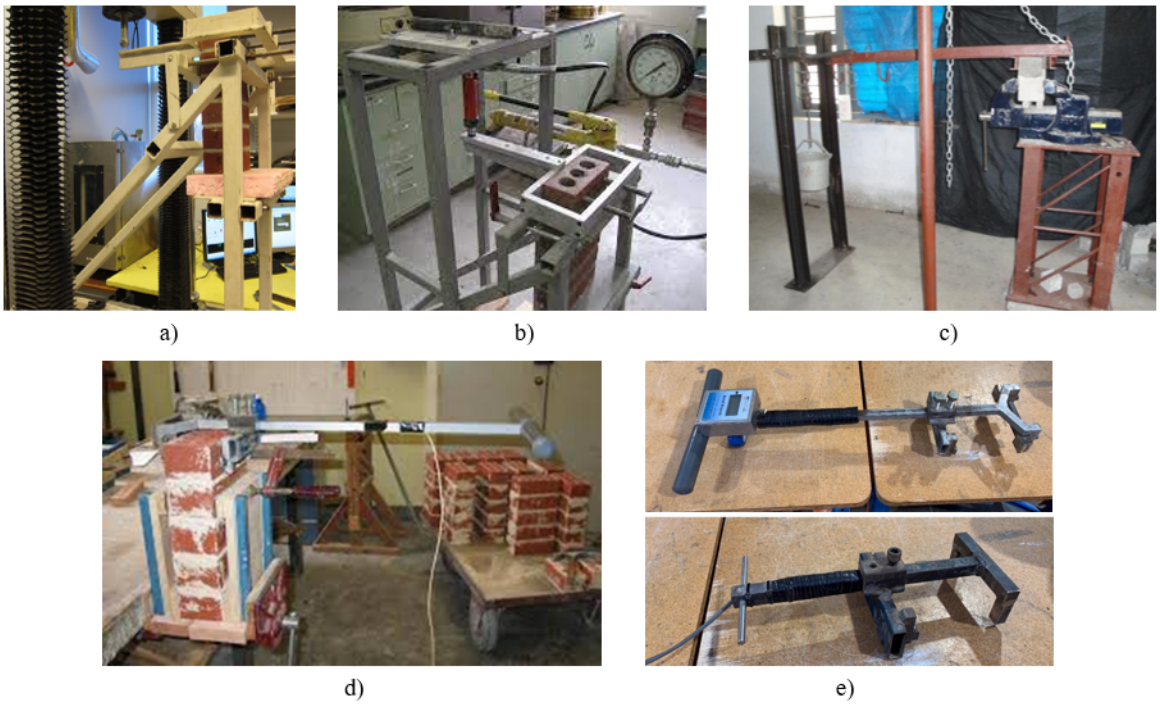

Figure 2.9: Practical implementations of the bond wrench test: a) American-inspired with displacement control [42], b) American-inspired using a manual jack [3], c) Long lever arm loaded with a hand-filled container [14], d-e) Australian-inspired with physical exertion [43, 44].

2.3 Evaluation

This section reviews evaluations of the bond wrench test. Here are summarized the main conclusions:

- The bond wrench test can be a reliable, quick and easy, alternative to the test procedure recommended in Eurocode 6 [23] to determine the flexural strength of masonry.
- The distribution of strain may differ significantly from the linearly varying distribution that is assumed in the calculation of the flexural bond strength.
- The utilization of diverse equipment and/or procedures in bond wrench tests might introduce a potential bias in the obtained flexural bond strength results.
- The significant variability (measured by the coefficient of variation)) observed in bond wrench test results is likely an inherent property of masonry materials and is not attributable to the test procedure or equipment.

2.3.1 Comparison with flexural strength test

In the Eurocode 6 [23], the experiment to evaluate the flexural strength of masonry is the wallette test. The referring norm is the EN 1052-2 [41]. It is a 4-point bending test on small wall executed parallel or perpendicular to the bed joints (Figure 2.10).

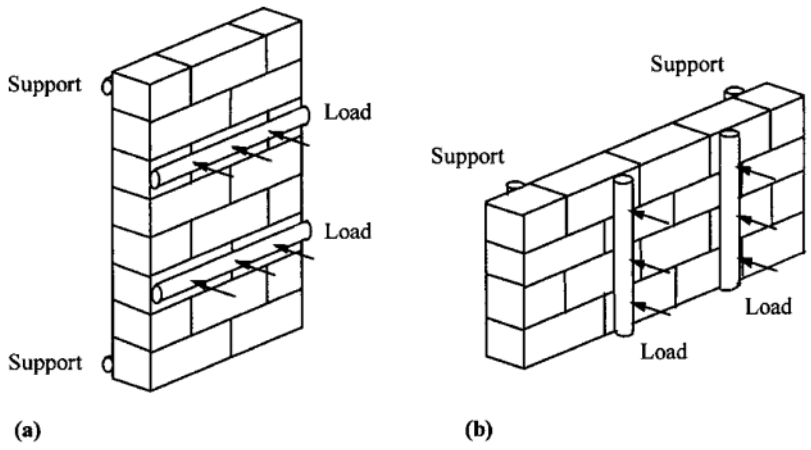

Figure 2.10: Flexural strength test on masonry wallette. a) Loading parallel to the bed joints. b) Loading perpendicular to the bed joints.[41]

In a study of the strength characteristics of hydraulic lime mortared brickwork, Zhou *et al.* (2008) observed that the bond wrench test can provides "a reliable, quick and easy, alternative

test procedure to determine flexural strength (with plane of failure) parallel to the bed joints" [45].

Indeed, the wallette test requires a large experimental set-up, particularly when compared with the bond wrench test. They executed the wallette and the bond wrench tests respectively according to the EN 1052-2 [41] and EN 1052-5 [33]. For eight different combinations of mortar and unit type, they executed each time 6 wallette test parallel to the bed joints and 12 bond wrench test (4 prisms of 4 units were used for the bond wrench test which gives a total of 12 results). Figure 2.11 reports a comparison of the results obtained with the 2 methods. As can be seen, there is generally a good correlation between the bond wrench test and the wallette test for both mean and characteristic strengths (5% fractile values) for each combination of mortar and unit type.

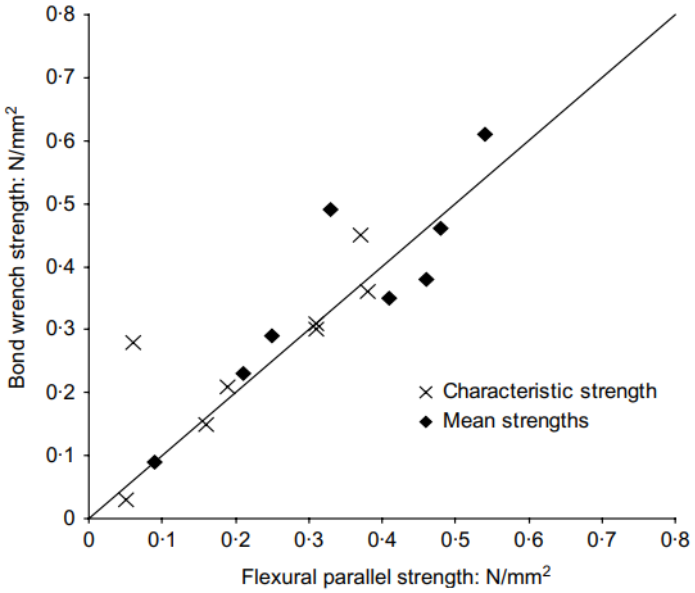

Figure 2.11: Relationship between bond wrench test and flexural parallel strength test [45]

.

In another study of brick/lime mortar masonry, Pavia *et al.* (2009) observed also this correlation: "The bond wrench test proved to be a relatively fast and accurate test. Results from which compare well with those obtained from the EN 1052-2:1999 flexural strength parallel to horizontal bed joints tests" [46].

In a comparative study, van der Pluijm used five different test methods, including the bond wrench and wallette test, in combination with two types of masonry to investigate the outcome of the bond wrench test. According to van der Pluijm, "Taking into account statistical considerations concerning the number of joints tested in flexure, the bond wrench is able to predict

the flexural strength parallel to the bed joint as reliable as the flexural test on wallettes"[12]. What is meant is that the two tests (bond wrench and wallette tests) differ in the number of joints that are under the same bending conditions. Since the flexural strength is a parameter with a significant coefficient of variation (typically 20-25% for laboratory tests [47]), the average test outcome of a wallette test with, for example, 4 joints in the constant maximum moment area does not equate to the average strength of the joint strength population (which is what is tested in the bond wrench test). In the wallette test, the measured strength is determined by the weakest of the four joints whereas in the bond wrench test, all joints are tested [12, 31]. Therefore, higher strength results can be expected with the bond wrench test than with the wallette test.

2.3.2 Influence of the apparatus on the stress distribution

McGinley conducted experiments to assess the validity of the bond wrench apparatus [4, 5]. More specifically, he evaluated the capacity of the apparatus and procedure described in ASTM C1072 to produce linear stress distributions on the specimens. He also determined the factors affecting this stress distribution.

To carry out these experiments, he used a calibration device designed to simulate a standard brick couplet specimen and equipped with linear strain gauges that were monitored and recorded during loading. This was done using a block-shaped device made of an epoxy material with a modulus of elasticity similar to that of masonry. The depth and width of the block were those of standard concrete brick unit, the height was about 280 mm. A total of sixteen strain gauges were mounted on the sides of the block. The block was placed in the bond wrench in such a way that the strain gauges were located in the same position as the upper mortar joint of a masonry unit (Figure 2.12).

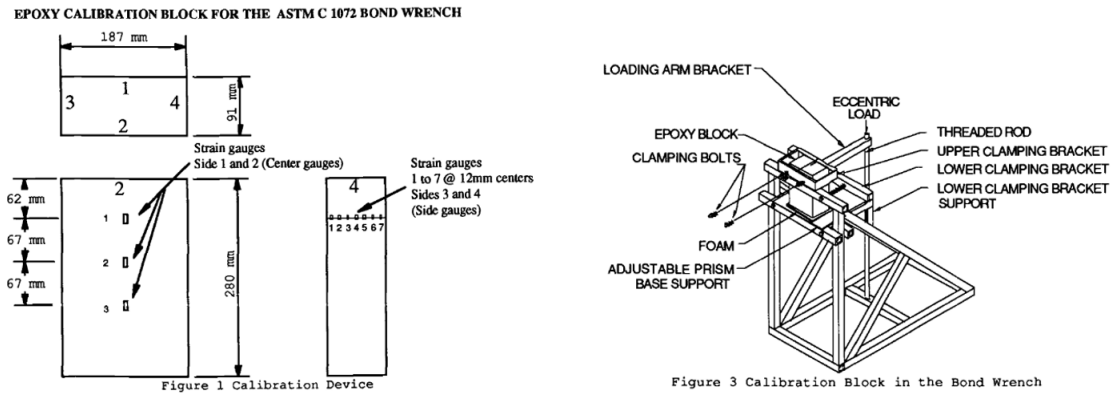

Figure 2.12: Calibration device.[4].

The main conclusions of the experiments were the following:

- The distribution of strain may differ significantly from the linearly varying distribution that is assumed. This was especially true for higher strain levels.
- The strain distribution in the specimen can be significantly impacted by the configuration of the clamping mechanism as the point of load application is very close to the layer under test. These local effects can be lessened by moving the point of load application as far away from the mortar joint being tested as possible. Furthermore, the clamping mechanisms should apply a uniform force over a consistent area on the brick face.
- Deviations from the linear strain distribution appear to increase as the ratio of axial to bending stress increases.
- A low and uniform loading rate may produce more consistent results (with a lower coefficient of variation).

One limitation of these studies is the utilisation of a solid replica without a joint to represent a bi-material couplet with a joint. This choice raises questions about the accuracy of this representation and its relevance to real masonry.

2.3.3 Bias between standards

This section presents the outcomes of a study that conducted bond wrench tests on masonry prisms using both the AS 3700 (Australian) and ASTM C1072 (American) standards, and subsequently compared the obtained results between the two standards [6]. The experimental procedures were undertaken by students who personally fabricated the wrenches. The visible differences between the applications of the two standards in the study referred to relate primarily to the design of the lever arm. The Australian device used four individual contact points for clamping on the top brick, while the American clamping mechanism provided full contact along the held brick. The experimental methodology outlined in Ref. [6] entails the following steps:

To start, a standardized clay masonry brick manufactured in Texas was used in conjunction with mortar adhering to a 1:1:6 volumetric ratio of Cement, Lime, and Sand. The experiments included both lime-based mortar and either Portland or Masonry Cement for conducting standard tests. Each set of prisms was crafted by a minimum of two masons, maintaining a 10mm mortar thickness between two masonry units. These prisms were composed of 5 joints.

The prisms underwent an open-air curing process for at least 7 days, during which the initial rate of absorption (IRA) for the bricks was measured. Subsequently, the prisms were randomly assigned to bond wrenches using a method analogous to a coin toss. In the comparative analysis of the AS 3700 and ASTM C1072 bond wrenches, each type was employed to test a total

of 25 prisms.

Upon completing the experiments, standard statistical procedures were used to estimate parameters such as mean and variance from the collected data.

Figure 2.13: On the left: the ASTM C1072 apparatus loaded with a bucket. On the rigth: The AS 3700 apparatus after the failure of a joint. [6]

No extensive information is given about the loading and measuring devices and procedures. It may be assumed that a bucket gradually filled with sand was used and then weighed after failure to assess the failure load, according to Figure 2.13.

The statistical results of the experiment are presented in table 2.2: As can be seen, there

Test method	**Mean [N/mm²]**	**Standard deviation [N/mm²]**	**Coefficient of variation [/]**
AS 3700	1.12	0.42	0.37
ASTM C1072	0.58	0.22	0.38

Table 2.2: Comparison of flexural bond strength results: Australian vs. American bond wrench test [6].

is a clear bias between the mean results of the AS 3700 and ASTM C1072 bond wrenches.This disparity is attributed to the variations in the apparatus employed according to these two standards. Additionally, Nichols offers a noteworthy observation about the ASTM C1072: "The American wrench at 16.6 kilograms and with a very short moment arm that requires significant loads to cause failure, up to 75 kg, is difficult to place and tends to fly about at the time of failure. A longer moment arm and lower mass would reduce the danger inherent in this testing." [48]. This issue with the ASTM C1072 setup could therefore contribute to the observed bias.

Other explanations not addressed by the author for this significant bias may lie within the loading and measurement procedure. The study does not delve into the precision of measurements or the consistency and uniformity of the loading rate. As such, the adequacy of the stipulated requirements for these parameters remains uncertain.

2.3.4 Influence of the test set-up and the specimen type

Gaggero and Esposito conducted experiments with the bond wrench test using various set up and specimens type to study their influence on the results [9].

The experimental program conducted tests on masonry specimens with poor bonding, which exhibited a high coefficient of variation in bond wrench tests. Two types of masonry were used: calcium silicate (CS) brick masonry with a cement-based mortar and clay brick masonry with a cement-lime mortar. Several mortar batches were utilised to construct the masonry specimens. Three standardized set-ups were used on "stack-bonded couplets" (see Figure 2.14):

1. A force-controlled set-up where a user manually operated a jack by turning a crank to apply the load.
2. A computer-controlled system that operated by controlling the crack mouth opening displacement (CMOD) on the tensile side of the specimen.
3. A simplified and portable force-controlled bond-wrench apparatus, designed for in-situ applications, where the user applies the load by hand using a torque wrench.

In all three configurations, the identical bottom and top clamps were utilized, with the only difference being the length of the lever arm. For the firsts two set-ups described above, a 100 kN jack was used to exert the vertical load on the lever arm's free end, while a load cell accurate to ± 1 N was used for precise measurement. For the third set-up, a digital display was used to indicate the applied failure load with a reading accuracy of $\pm 2\%$.

Besides "stack-bonded couplets" (Figure 2.15a), the simplified and portable setup has been employed on two additional types of masonry specimens: "running-bonded couplets" (Figure 2.15b) and "running-bonded wallets" (Figure 2.15c).This was done to examine how the specimen's type affects the assessment of flexural bond strength.

The main results of the study are presented in Figures 2.16 and 2.17. As can be seen, regardless of the test configuration, similar coefficients of variation are reported. These coefficients are approximately 7% to 16% for CS (Figure 2.16a) and 34% to 39% for clay (Figure 2.16b) units. Irrespective of the type of masonry depicted in Figure 2.16, the variability is slightly reduced for specimens tested at later stages, where complete bond development is expected to occur.

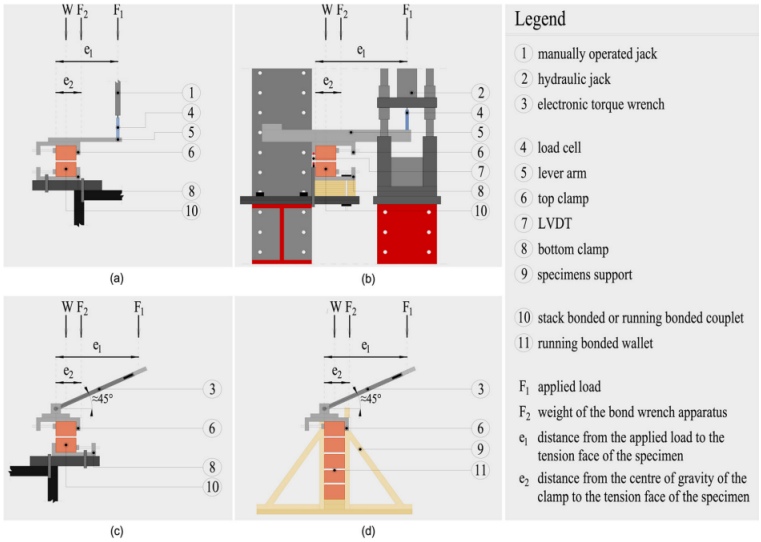

Figure 2.14: a) Force-controlled and b) CMOD-controlled set-up for laboratory tests on couplets. Set-up for in-situ tests on c) couplets and d) wallets[9]

.

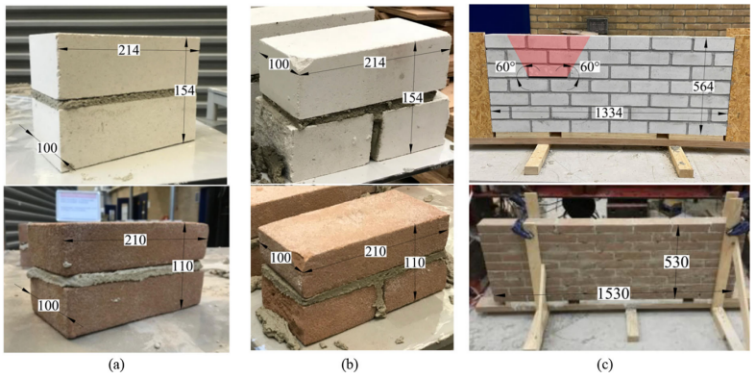

Figure 2.15: a) stack-bonded couplets, b) running-bonded couplets and c) running-bonded wallets [9].

.

Consequently, the significant variability observed in bond wrench test results is likely an inherent property of masonry materials.

The study suggests that the variation in average results can be attributed to the duration of hardening rather than the specific testing configuration used: The increase in long-term flexural strength for the clay samples is attributed to the presence of lime in the mortar and the decreasing trend over time in flexural bond strength for CS specimens is attributed to inherent shrinkage phenomena associated with the material itself.
While this hypothesis appears to be more applicable to clay masonry, its relevance to CS masonry seems less apparent. Overall, it remains challenging to discern the specific influence

of the test configuration and the duration of curing on the observed outcomes.

The study also highlights the influence of specimen type on masonry flexural bond strength assessment. Stack-bonded couplets show lower strength than running-bonded wallets. Interestingly, no consistent correlation emerged between joint position within the wall and bond strength. The difference in strength between stack-bonded couplets and running-bonded wallets could potentially be attributed to the presence of head joints in the latter, which may alter the drying process. The study's conclusion is limited by the restricted number of experiments performed.

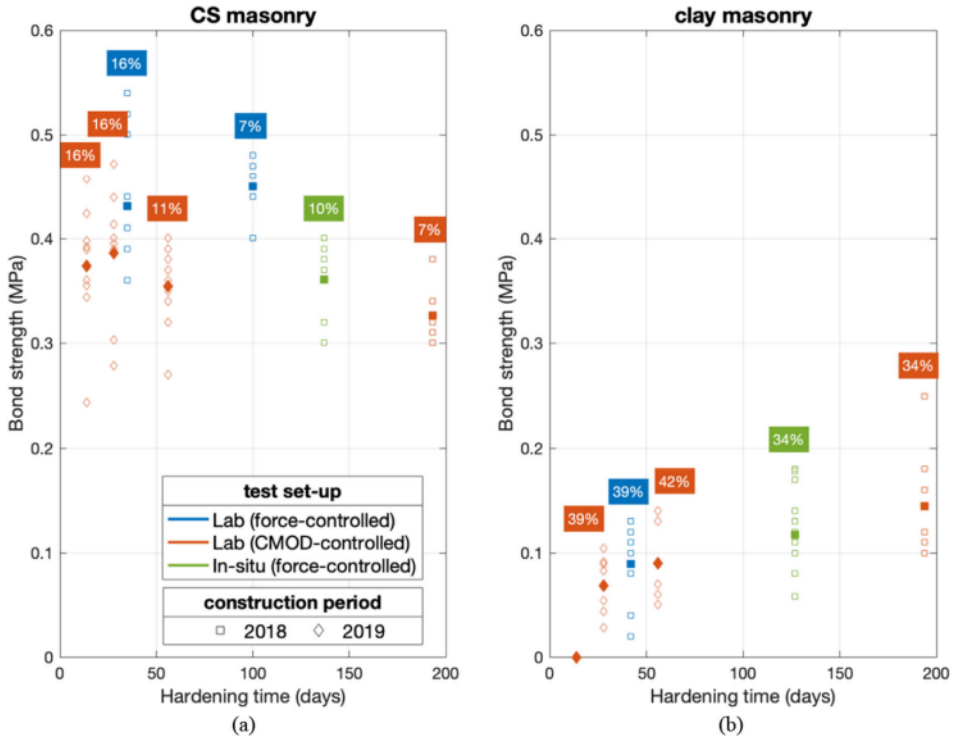

Figure 2.16: Variation of flexural bond strength of stack-bonded couplets with varying bond wrench test configurations in function of hardening time [9].

. .

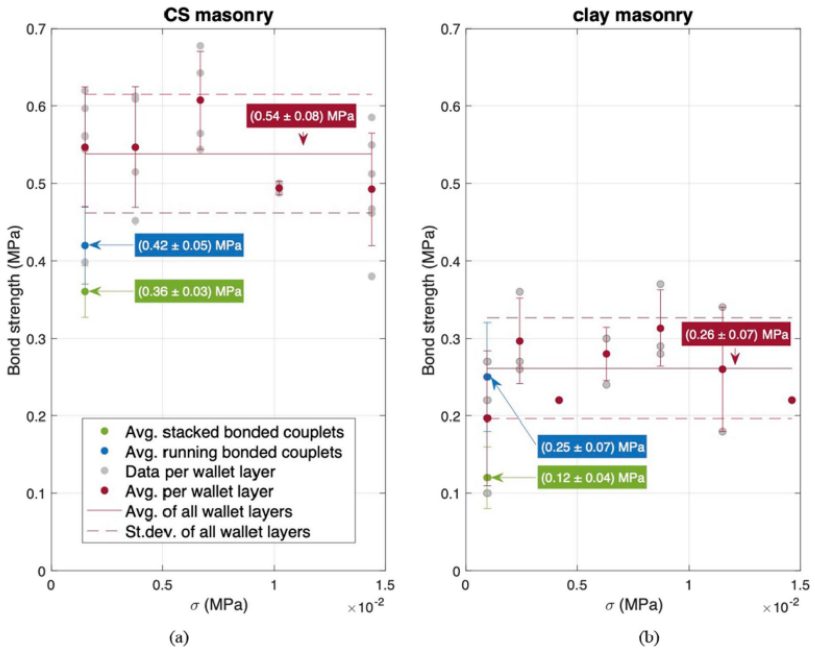

Figure 2.17: Relationship between flexural bond strength and pre-compression for: a) CS masonry, and b) clay masonry [9].

. .

2.4 Variants of the traditional bond wrench test

In research papers, significant variations of the traditional bond wrench test apparatus and procedure, such as described in Sections 2.1.2 and 2.2 can be found. Some of these modifications have been introduced to incorporate the findings of McGinley [4, 5]. They are presented in the following sections.

2.4.1 Modified bond wrench test

In a study of brick-mortar bond and masonry compressive strength, Sarangapani *et al.* (2005) used a "modified bond wrench test" to evaluate the flexural bond strength of masonry prisms composed of five bonded bricks [8].

The prism is supported on a rigid bottom, and the bottom brick is fully clamped (see Figure 2.18). The difference with the standard bond wrench test is that the load is applied horizontally on the top of the prism, through an arrangement of pulleys. This load creates a bending moment in the prism and is increased up to flexural failure of a joint of the prism. Generally, the lowest joint fails, as it is the one most subject to bending. The test is carried out only once for each masonry prism. The other joints in the prism (which have not failed) are not tested as they have already been subjected to bending.

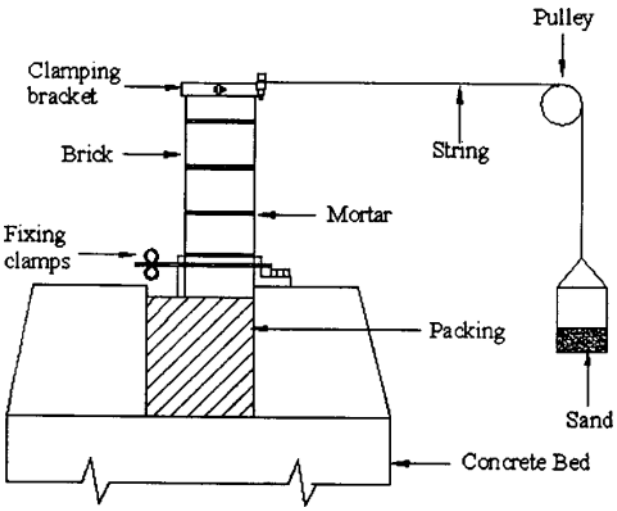

Figure 2.18: Modified bond wrench test [8].

The authors give the following justification for using this test rather than a standard bond wrench test: "This approach is used because with the specimen gripped at a few discrete points (as in the standard ASTM bond wrench test), joints close to the grip may not be stressed uniformly. Hence, a single joint failure at some distance away from the grips is preferred." No reference to a study is made in this statement but it can be assumed that it is based on McGinley's experiments described in Section 2.3.2.
There are two main drawbacks to this test:

- Firstly, the setup generates flexural stresses in the prism but also shear stresses which could impact the results.
- Secondly, only one joint of the prism is tested whereas in the standard bond wrench test, all the joints are tested.

2.4.2 Pure couple bond wrench test

In a study of highly cored extruded clay units, Radcliffe *et al.* (2004) used the method prescribed in the ASTM 1072 (American standard bond wrench test) to measure the masonry flexural bond strength [49]. However, they modified the apparatus of the standard bond wrench so that a (almost) pure couple could be applied to the tested joint. Indeed, as stated before (Section 2.1.2), the standard bond wrench imparts a combination of flexion and compression due to the eccentricity of the applied load.

As stated by Radcliffe and al., "The longer arm reduces the load required to produce the same flexural stress. Therefore, the longer the arm the smaller the influence the compressive load

has on the unbalanced stress distribution. McGinley [5] states that the discrepancy of actual strain distributions, compared to linear distributions assumed by theory, appears to be more pronounced as the percentage of axial stress, relative to the peak flexural stress, is increased."

Instead of using a long lever arm, Radcliffe *et al.* (2004) chose to incorporate two loading arms on opposite sides of the upper clamp bracket and load each with an equal but opposing force. The only remaining compressive load thus came from the weight of the upper clamp bracket, which was minimal compared to the loads required to produce the ultimate bending stress. In this configuration, the standard bond wrench test's issue of weak bonds potentially failing before the test is conducted is eliminated.

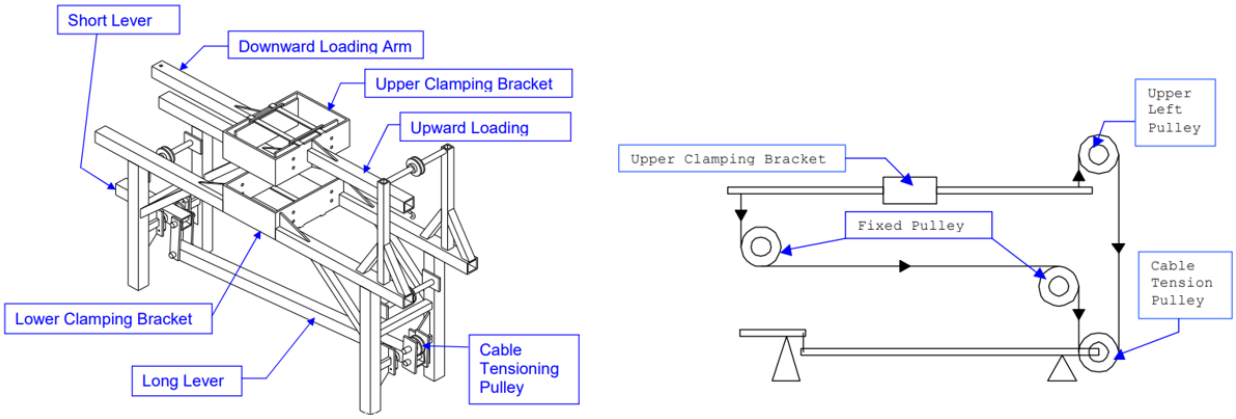

Figure 2.19: Pure couple bond wrench test apparatus [49].

The apparatus is composed of a lever system in conjunction with a system of near frictionless pulleys (see Figure 2.19). The loading on both lever arms is applied at a distance of 0.762 m from the centroid of the upper clamping bracket. The lever system has been designed to apply sufficient tension in the wire rope to ensure that equal and opposite loads are applied to the opposite lever arms. It is unknown if this apparatus has been already tested and compared with a standard bond wrench. Photos of the apparatus described here are provided in Appendix 4.7.

2.4.3 In-situ bond wrench test

Several research papers provide examples of in-situ applications of the bond wrench test, including works by Gaggero [9], Heffler et al. [50], and Schuller et al. [51]. The apparatus is adapted to facilitate the testing of masonry wall joints. In such applications, two common designs for in-situ bond wrench tests are typically employed.

The first design features a crossbar handle mounted on a load cell. Load is manually applied by exerting body weight onto the crossbar handle (refer to Figure 2.20.a). The load can be indicated using a LCD (liquid crystal display) type screen, which displays the maximum reading until reset. The second design involves the use of a torque meter to measure the applied bending moment (refer to Figure 2.20.b).

a) b)

Figure 2.20: In-situ bond wrench testing [50, 51].

2.4.4 CMOD controlled bond wrench test

Gaggero [9] designed a controlled setup that operated by controlling the crack mouth opening displacement (CMOD) at the tensile side of the tested specimen. The CMOD-controlled procedure allowed the capturing of the material's post-peak behavior and the evaluation of the flexural bond fracture energy. The CMOD-controlled setup utilized a hydraulic jack operated in a displacement-controlled manner. In this setup, the control variable was the average displacement measured by two LVDTs (Linear Variable Differential Transformer). These LVDTs were attached to the upper clamp to record relative vertical displacements with respect to the bottom clamp. This approach enabled the assessment of post-peak behavior and the amount of energy dissipated due to joint cracking. Figure 2.21 illustrates an example of the measured data in terms of clamp opening and vertical displacement of the jack.

Characterising the tensile softening behavior of masonry is important for the numerical assessment of existing masonry structures. However, direct tensile tests are often challenging and not available in laboratories, leading to assumptions about this factor [9]. Therefore, investigating the use of flexural type tests, which are easier to perform, to indirectly estimate the tensile bond fracture energy is relevant.

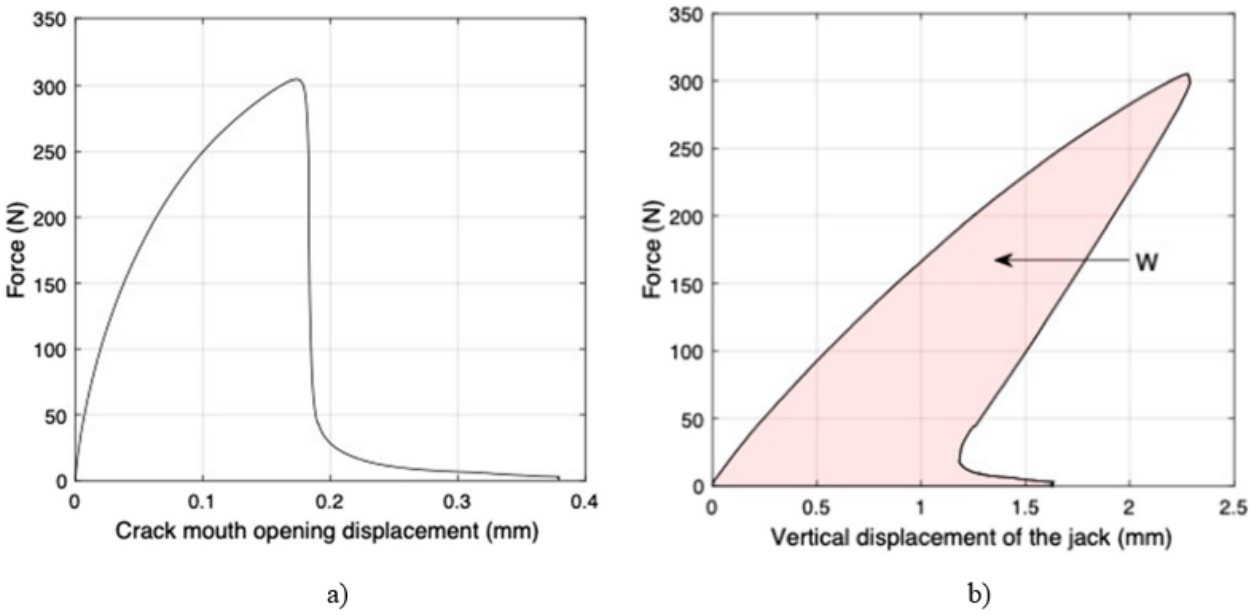

Figure 2.21: Illustration of recorded data using the CMOD-controlled bond wrench test setup: a) Applied force plotted against CMOD, and b) Vertical displacement of the hydraulic jack [9].

2.5 Summary of the chapter

This Chapter initiated with a general presentation of the two existing methods to determine the flexural bond strength of masonry: the beam test and the bond wrench test. Through this examination, it becomes apparent that the bond wrench test is often favored due to its simplicity and cost-effectiveness. The implementation of the test in American, Australian, and European standards was then presented. It has been observed that while the fundamental principles of the test remain uniform across these international standards, distinct criteria exist for diverse parameters (the lever arm's length, the characteristics of the clamping mechanisms of the lever arm, and the rate at which load is applied). Furthermore, it was observed that these standards are not always strictly followed in practice. While they serve as references, their specific requirements are not consistently met. As a result, there is a wide variety of implementations of the bond wrench test in practice. Next, the chapter involved a review of the existing evaluations of the bond wrench test. Here are summarized the main conclusions of this investigation:

- The bond wrench test may be a reliable, quick and easy alternative to the test procedure recommended in Eurocode 6 [23] for determining the flexural strength of masonry.

- The distribution of strain may differ significantly from the linearly varying distribution that is assumed in the calculation of the flexural bond strength.

- The utilization of diverse equipment and/or procedures in bond wrench tests might introduce a potential bias in the obtained flexural bond strength results.
- The significant variability (expressed by the coefficient of variation) observed in bond wrench tests is likely an inherent property of masonry materials and is not attributable to the test procedure or equipment.

Finally, variations of the bond wrench test setup were presented. Notably, a significant one involves a bond wrench test conducted by controlling the crack mouth opening displacement (CMOD) at the tensile side of the tested specimen. This CMOD-controlled approach captures the material's post-peak behavior and evaluates the flexural bond fracture energy, which could be of interest for the numerical assessment of masonry structures.

Chapter 3

Experimental setup and methodology

3.1 Initial objectives of the experimental phase

As discussed in Chapter 2, the bond wrench test is implemented in different standards, each with varying requirements concerning several parameters. The present study aims to conduct an assessment of the bond wrench test's sensitivity to these various parameters, which include the length of the lever arm, clamping mechanisms, distance between the gripping points of the clamping mechanisms and the joint, and the rate of load application.

In the American standard, comprehensive drawings enable precise apparatus construction, specifying the lever arm length, clamping mechanism characteristics, and all necessary dimensions. The clamping mechanism ensures complete contact along the held brick without specific requirements regarding the distance between the clamping devices and the joint. Additionally, the American standard sets requirements for the time within which the tested specimen should break.

Conversely, the Australian standard provides a schematic diagram with force-controlled loading and fewer specific details about the lever arm length or clamping mechanisms are given. The Australian bond wrench uses four punctual contacts for the clamping mechanism's contact points with the brick.

In the European standard, only minimal design specifications are provided, including a lever arm length greater than 1 meter and a minimum distance of 10 millimeters between the clamping mechanisms and the joint. Time requirements for specimen failure are also included in the European standard.

In practical applications, researchers often deviate from strict adherence to these standards, modifying the apparatus to accommodate available resources and encountered limitations.

Furthermore, precise control of parameters such as the loading rate/time to failure can be challenging in experiments.

Nichols [6] conducted bond wrench tests on masonry prisms using AS 3700 and ASTM C1072 standards, revealing significant mean strength differences between them. Variations in clamping mechanisms, lever arm length, and applied loading rates may contribute to these discrepancies. Nichols observed challenges when utilizing the American wrench due to its high mass and short lever arm. This could potentially account for the notable discrepancy between the two standards. Nonetheless, other factors, like the accuracy of loading and measurement equipment, might also introduce biases that influence results significantly. Unfortunately, the lack of detailed information in the published papers about these aspects does not allow for a conclusive statement.

McGinley's studies [4, 5] focused on the discrepancy between actual and assumed strain distributions in the bond wrench test. Utilising a calibration device with sixteen linear strain gauges to simulate masonry, he investigates the impact of lever arm length and clamping mechanism on strain distributions. Higher axial stress relative to peak flexural stress leads to significant deviations from the assumed strain distribution, and non-linear strain distributions are observed at higher strain levels. However, a limitation of McGinley's research lies in the use of a solid replica without a joint, which may not fully represent the complexities of real masonry.

In light of the aforementioned comments, the primary objectives of the experimental phase of the present work are to assess the sensitivity of the bond wrench test to different parameters, including:

1. The length of the lever arm.

2. The type of clamping mechanisms.

3. The distance between the gripping points of the clamping mechanisms and the joint.

4. The rate of application of the load.

Furthermore, the research aims to study crack openings along the joint during the bond wrench test.

By addressing these objectives, the present study aims to evaluate the significance of adhering to specific standards requirements and enhance the test's accuracy and reliability.

3.2 Masonry material and construction

To fulfill the objectives defined in Section 3.1, the decision was made to design a test battery based on 10 prisms, each comprising 5 joints, resulting in a total of 60 joints for examination. To address potential uncertainties and challenges, an additional 5 prisms were constructed. This precautionary measure was taken due to the first-time implementation of this test in the LEMSC (Laboratoire essais mécaniques, structures et Génie civil) and taking into account reports of joint failure during the setup process in the literature. Consequently, the testing phase encompassed a total of 75 joints to ensure a comprehensive evaluation of the results.

Initially, various individuals, companies, and institutions were contacted to determine an interesting brick and mortar combination and source the materials. It was deemed valuable to include the study of Belgian traditional masonry and its bond strength as a secondary objective. Also efforts were made to find a skilled mason to handle the construction of the prisms. The list of the contacted individuals, companies, and institutions is provided below:

- Fédération Belge de la Brique, which supports 12 member bricklaying companies in Belgium,, recommended a book that could assist in the research of brick/mortar combinations. Additionally, they advised reaching out to a demolition firm to provide the required materials for the study.
- WS Demolition was contacted to inquire if they had bricks from any of their construction sites that they could provide. While an initial contact was established, it did not lead to further progress or response.
- IFAPME of Wavre and ITN (Namur), both technical schools, were contacted to explore the possibility of involving either a last-year student or a teacher in the construction of the prisms. However, they were unable to participate in the project.
- JMD Construction, a construction company based in Gembloux, generously provided the bricks and mortar. One of their masons handled the prism construction. Ultimately, the decision to collaborate with JMD Construction for the masonry work was driven by convenience and timing considerations. Moreover, utilising bricks from demolition sites would introduce potential variability, which could compromise the ability to isolate the influence of bond wrench test parameters on the test results.

3.2.1 Bricks

The bricks used are clay hand-made frogged bricks (see Figure 3.1). The term "frogged" indicates that these bricks possess a central cavity. The dry mass of the bricks was 2139 g (calculated from the mean value of 5 units). The dimensions of the brick were 214 mm x 101 mm x 65 mm The technical data sheet of the bricks is provided in the Appendix 4.7.

Figure 3.1: Bricks utilized for the present study.

Initial rate of absorption (IRA)

As discussed in Section 1.3, evaluating the Initial Rate of Absorption (IRA) of bricks is relevant when studying masonry bond strength due to its direct impact on the bonding process between bricks and mortar. Bricks with higher IRA values tend to absorb water rapidly, leading to excessive water uptake from the mortar during bonding. This can result in premature drying and weaker bonds. Conversely, bricks with with low IRA values may repel water, hindering effective bonding between the brick and mortar.

In this thesis, the IRA of the bricks was determined according to EN 772-11 [52]. Five specimens (bricks) were dried to constant mass $m_{\mathrm{dry,s}}$ in a ventilated oven at 105°C. After cooling, the specimens were immersed in water to a depth of 5 mm for 1 minute.
Subsequently, the specimens were weighed ($m_{\mathrm{so,s}}$), and the initial rate of water absorption was calculated using the formula:

$$\mathrm{IRA} = \frac{(m_{\mathrm{so,s}} - m_{\mathrm{dry,s}})}{A \cdot t} \ \left[\mathrm{kg\,m^{-2}\,min^{-1}}\right] \tag{3.1}$$

where A is the gross area and t is the immersion time (1 minute) for clay masonry units. The mean of the initial rates of water absorption of the bricks was calculated.

The mean IRA of $0.9\,\mathrm{kg\,m^{-2}\,min^{-1}}$ calculated falls within the typical range of values for clay bricks, which spans from 0.35 to $3.6\,\mathrm{kg\,m^{-2}\,min^{-1}}$ [1]. Referring to the technical data

Sample	IRA [kg/(m²min)]
1	0.9
2	0.8
3	1
4	0,7
5	1
Mean	**0.9**

Table 3.1: Initial Rate of Absorption (IRA) of the bricks used in the present study.

sheet of the material (Appendix 4.7), it falls within the range of coated bricks. Coating is commonly applied to bricks to impart water-repellent properties, primarily for aesthetic reasons and to enhance freeze resistance. As indicated in the technical data sheet, the bricks are classified as IW2, which corresponds to moderately absorbent bricks with an IRA (Initial Rate of Absorption) ranging from 0.5 to 1.5 $\mathrm{kg\,m^{-2}\,min^{-1}}$. This classification indicates that the bricks exhibit a moderate level of suction, potentially contributing positively to the bond strength.

3.2.2 Mortar

The mortar was composed of Portland cement and yellow sand, with no lime in the mix. An air-entraining agent was added to the mortar to improve its workability. The technical data sheets of the cement is provided in the Appendix 4.7. This mortar was prepared by a mason at the JMD Construction warehouse in Gembloux and subsequently transferred to the LEMSC lab.

As noted by the mason, the mortar exhibited important dryness, which could be attributed to the prevailing hot and windy weather conditions of the day. The mason therefore re-tempered the mortar several times before applying it to the bricks in order to enhance its workability. As discussed in Section 1.3, these particular conditions are recognized to have a potential negative impact on the effective cement hydration process, which in turn has a negative effect on bond strength.

Flow table test

The flow table test is a technique used to evaluate the workability and consistency of freshly prepared mortar. This examination gauges the mortar's ability to flow and distribute itself under its inherent weight. This method is detailed in EN 1015-3 [38].

The testing equipment consists of a conical mold positioned on a small vibrating table. The cone is then filled with mortar in two distinct layers. After an interval of around 15 seconds, the mold is gradually lifted upwards, prompting the mortar to disperse onto the surface below through a series of 15 controlled vibrations at a consistent frequency of roughly one per second. Following this procedure, the diameter of the mortar is measured in two mutually perpendicular directions, and the mean value of these two measurements is calculated. A larger spread diameter indicates a more workable and fluid mortar, while a smaller diameter suggests a stiffer consistency.

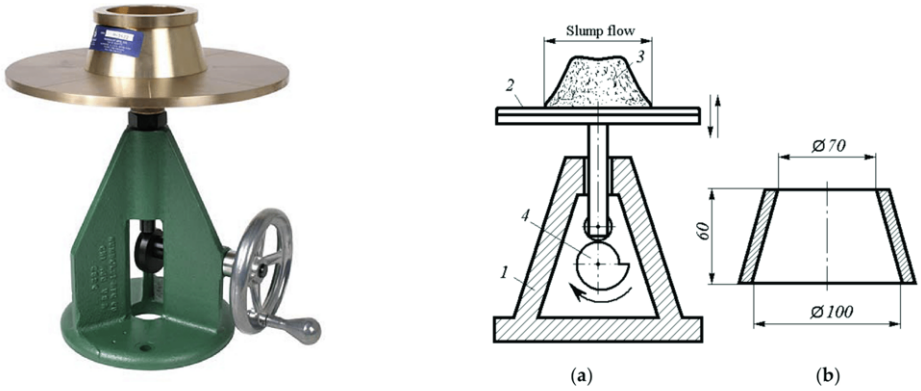

Figure 3.2: Flow Table Test Apparatus: (a) Flow Table, (b) Conical Mold. Components: 1. Base, 2. Flow Table, 3. Mortar Cone, 4. Tappet [53, 54].

Individual results on the mortar of the present study gave 125 mm and 129 mm which give a mean of 127 mm. In accordance with EN 1015-6 [55], this result classifies the mortar as "stiff mortar" (refer to Table 3.2). This finding aligns with the mason's observation that the mortar displayed dryness. This raised questions about the strength of the joints intended for testing, a concern supported by literature indicating a notable reduction in bond strength observed in dry mixtures [1]

Consistence in use	**Flow value [mm]**
Stiff mortar	<140
Plastic mortar	140 to 200
Soft mortar	>200

Table 3.2: Mortar classification based on flow value [55].

Flexural and compressive strength of mortar

The flexural and compressive strength of the mortar were assessed following the guidelines outlined in EN 1015-11 [40]. The flexural strength is initially determined through a three-point bending test until failure. Subsequently, the compressive strength of the mortar is ascertained for both components resulting from the flexural strength test. The testing principle is illustrated in Figure 3.3.

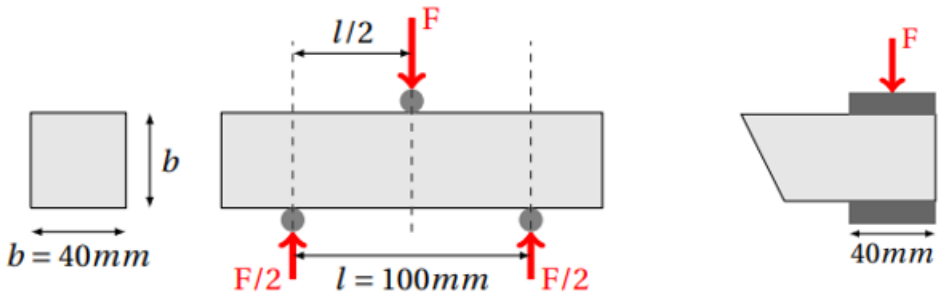

Figure 3.3: Illustration of the mortar flexural and compressive testing [15].

To conduct the tests, three prismatic specimens with dimensions of 160 mm x 40 mm x 40 mm were prepared. This resulted in three outcomes for the flexural test and six outcomes for the compression test. The specimens were initially stored in sealed plastic bags for seven days, followed by an open-air curing period of 35 days. These specimens were then tested concurrently with the flexural bond strength testing of the prisms.

The prisms are placed on support rollers and subjected to a load applied at a rate of $10\,\mathrm{N\,s^{-1}}$. The obtained half-prisms are subjected to a compression test. A load is applied at a rate of $50\,\mathrm{N\,s^{-1}}$.

The flexural strength f_{mt} is calculated using the following formula:

$$f_{mt} = 1.5\,\frac{F \cdot l}{b \cdot d^2} \tag{3.2}$$

Where b is the width, d is the thickness, F is the maximum load applied in flexion, and l is the distance between support roller axes.

The compressive strength f_{mc} is calculated using to the following formula:

$$f_{mc} = \frac{F_c}{A} \tag{3.3}$$

Where F_c is the maximum load applied in compression, and A is the cross-sectional area.

Results from the tests are presented in Table 3.3. A compressive strength of 2 MPa could be considered low for cement mortar when comparing with findings in existing literature [8, 9, 16]. Such a lower compressive strength is unfavorable for bond strength, as higher mortar compressive strength is typically associated with stronger bonds [22].

Sample	**Flexural strength [MPa]**	**Compressive strength [MPa]**
1	0.680	2.339
2	0.630	1.250
3	0.881	1.631
4	\	1.741
5	\	2.714
6	\	2.464
Mean	**0.730**	**2.023**

Table 3.3: Flexural and compressive strength of the mortar of the present study.

Figure 3.4 is a photograph of one of the sample. It is observed that the surface is not smooth, a result attributed to the dryness of the mortar, which prevented its even spread within the molds.

Figure 3.4: Mortar sample of the present study.

3.2.3 Construction and curing conditions

The set of 15 prisms was built by a professional mason on the same day within a duration of 1 hour and 30 minutes. The mortar was prepared by the mason in his workshop and subsequently transported to the LEMSC lab. Consequently, the entire process, from mortar preparation to the construction of the 15 prisms, was completed within 2 hours. These prisms were fabricated with the frogged face oriented downwards, and the joints were maintained at a thickness of 13±2 mm.

In accordance with the EN 1052-5 [33] recommendations, the prisms were assembled within plastic sealed bags that were subsequently closed upon completion (refer to Figure 3.5). Also, two additional bricks were positioned atop the prisms to achieve a precompression of 2 kPa.

In the initial stage, the prisms were sealed in bags for a comprehensive 27-day curing process. Indeed, enclosing the prisms in moisture-proof bags optimizes the hydration process [2]. Furthermore, this controlled environment also minimises the influence of external factors like wind and temperature, ensuring, normally, more predictable and desirable curing results. Subsequently, the prisms were exposed to open air for an additional period of 1 day for a first set of tests and 12 to 16 days for a second set of tests. The time gap between these two sets of tests was due to the unavailability of a jack required to perform the tests.

Figure 3.5: Masonry prisms of the present study prepared for the curing process.

3.3 Construction of a bond wrench test apparatus

Due to the absence of a bond wrench apparatus at UCLouvain, it was necessary to construct one. This section details the design undertaken to create the required bond wrench. Appendix 4.7 provides technical drawings utilised in its construction. The bond wrench apparatus consists of two main components: a restraining frame and a lever arm. First, an explanation of the working principle of the frame is provided.

Following discussions with the LEMSC lab, it was determined that a bond wrench frame inspired by the American standard ASTM C1072 [32] would be built. It is noteworthy that the dimensions were enlarged to cater to the testing of diverse masonry prism sizes, extending beyond those employed solely in this experiment. A graphical representation of the frame restraining a prism is displayed in Figure 3.6. The frame primarily consists of an assembly of rectangular hollow profiles measuring 40 mm × 40 mm with a thickness of 2 mm.

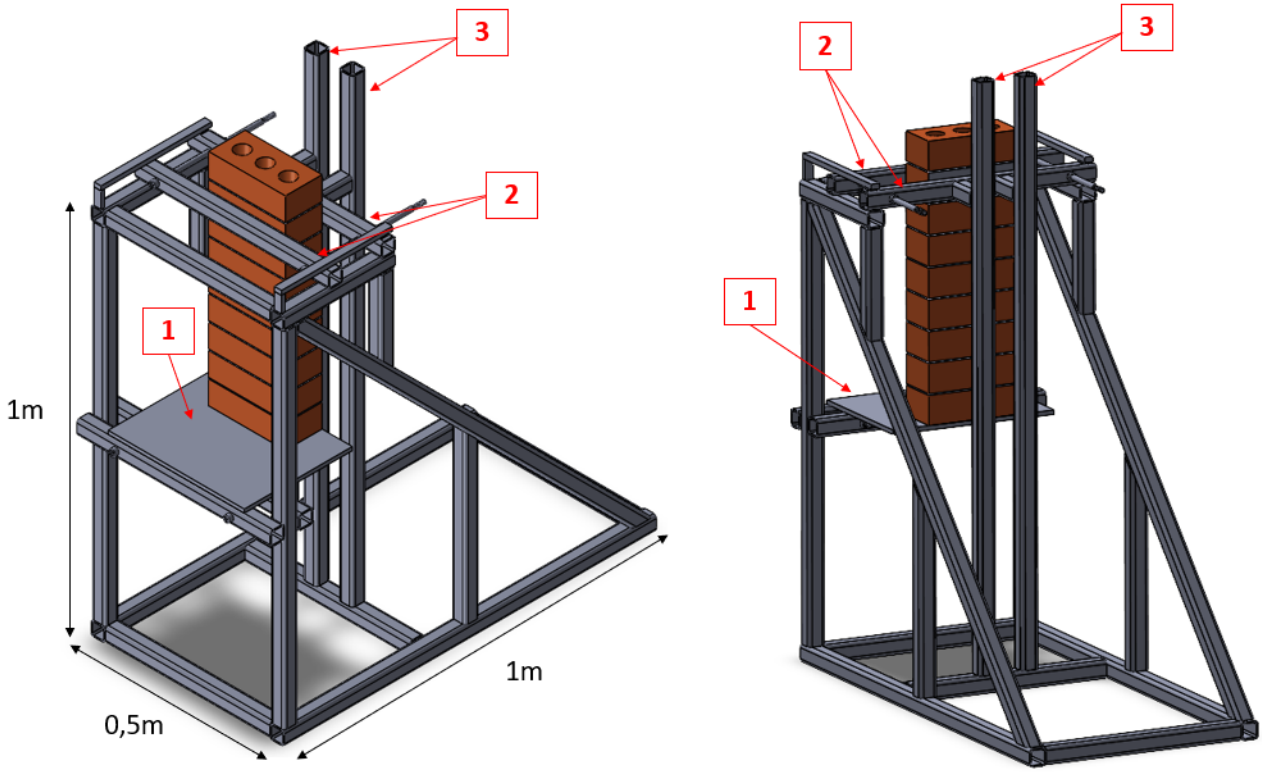

Figure 3.6: Bond wrench frame holding a prism. Components: 1. Adjustable support, 2. Clamping mechanism for prism restraint, 3. Profiles guiding and preventing torsional movement of the lever arm.

Referring to Figure 3.6, the prism is placed upon an adjustable support that enables vertical

positioning of the prism. A closer view of this component is illustrated in Figure 3.7. This adjustable support consists of a plate welded to one of the horizontal profiles as indicated in Figure 3.7.b. The two horizontal profiles supporting the plate can be either tightened or loosened against the vertical profiles of the frame using a system of screws and nuts. Properly loosening them allows for vertical adjustment of the support to the desired position. Once adjusted, the screw and nut mechanism is employed to bring the two horizontal profiles closer together, establishing contact with the two vertical profiles. The resulting friction between these profiles effectively secures the support in its designated position.

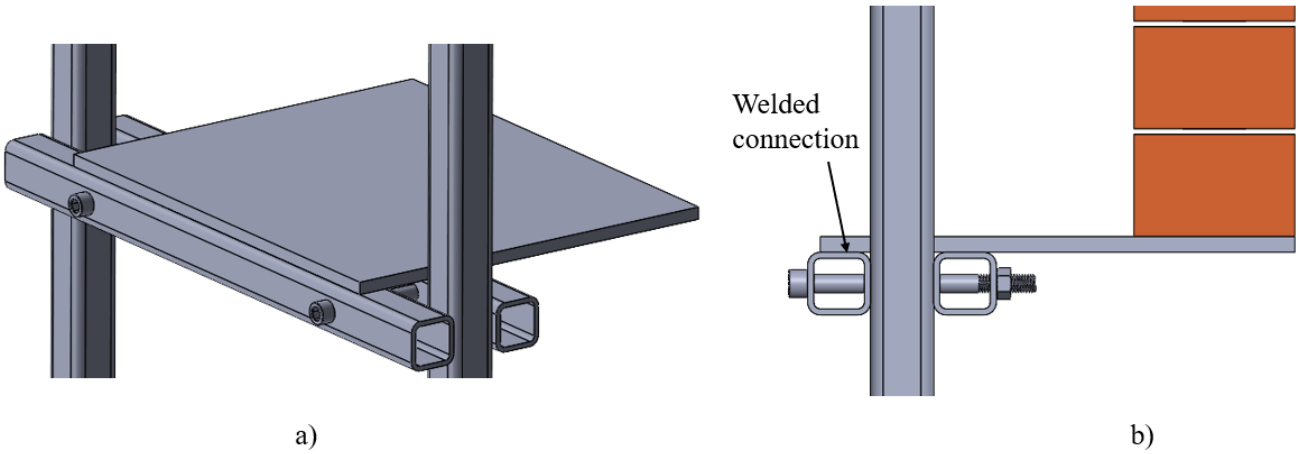

Figure 3.7: Adjustable support: a) General view. b) Side view.

Once the prism is positioned at the desired location using the adjustable support, it is secured in place by clamping it to the frame. The localisation of the clamping mechanism is highlighted in Figure 3.6. A detailed view of this mechanism is presented in Figure 3.8. In the same Figure, all profiles are permanently joined through welding except a sliding tube that can move within a groove. This sliding tube is equipped with a screw and nut system, that enables it to be tightened against the masonry prism.

Upon completing the aforementioned steps, the lever arm is positioned atop the prism such as seen in Figure 3.9. Its placement is constrained by the two tall vertical metal profiles, preventing excessive torsional movement of the lever arm (see components 3 in Figure 3.6). The lever arm consists of a 1.4 m long rectangular hollow profile welded to a U-shaped profile. To counteract the bending moment due to the lever arm's self-weight, it is partially extended on the opposite side. This helps mitigate the induced bending moment without adding excessive length and weight to the lever arm.

Following that, the lever arm is firmly attached to the prism using a screw-nut mechanism that enables lateral movement of a metal plate. This clamping arrangement guarantees full

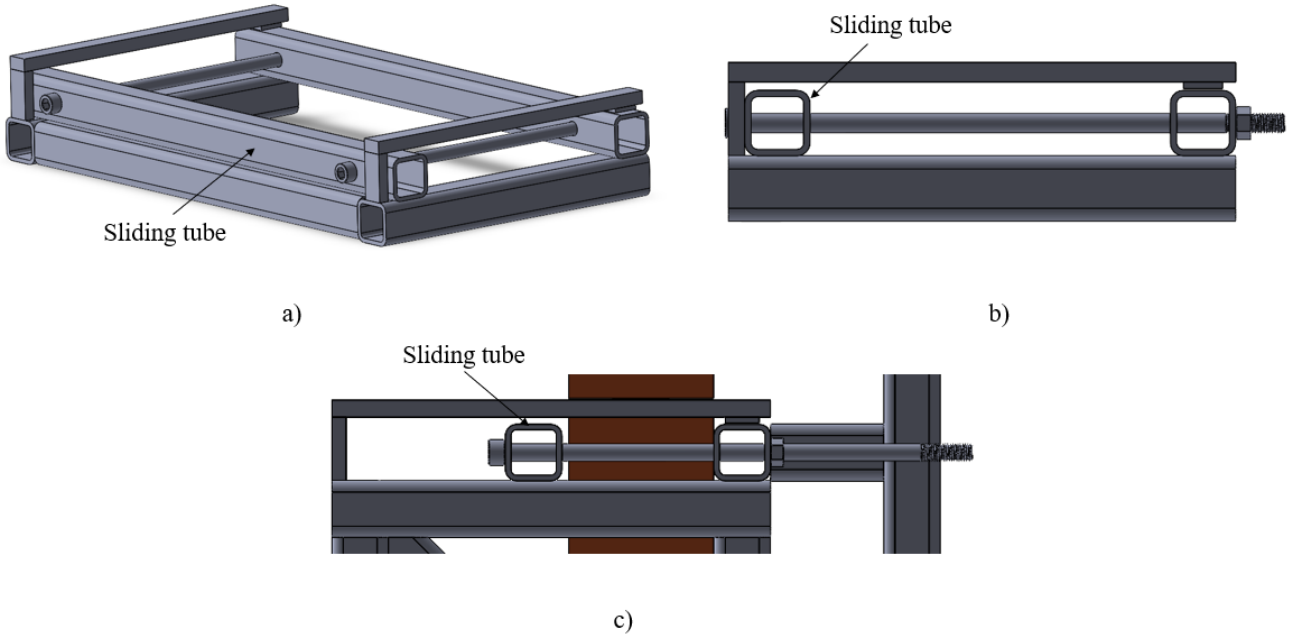

Figure 3.8: Clamping mechanism for prism restraint: a) General view, b) and c) Side views.

contact along the surface of the secured brick. An illustration of the lever arm can be observed in Figure 3.10.

Originally, for a portion of the tests, two additional plates measuring 15 mm × 30 mm were meant to be affixed onto the two surfaces of the lever arm that come into contact with the brick. This alteration was inspired by the lever arm design outlined in the Australian standard (refer to Figure 2.6). The objective was to investigate whether the clamping mechanism could potentially exert an influence on the outcomes. However, due to the reasons explained in Section 3.5, this modification was ultimately not carried out.

After the completion of the apparatus design, the subsequent phase encompassed the manufacturing of the apparatus. The initial step in constructing the apparatus involved cutting the various profiles to their correct dimensions. Subsequently, each element was assigned a numerical identifier corresponding to a drawing, facilitating the accurate assembly of different components during the welding process. This plan is available in the Appendix 4.7. All the manufacturing was executed by the LEMSC lab.

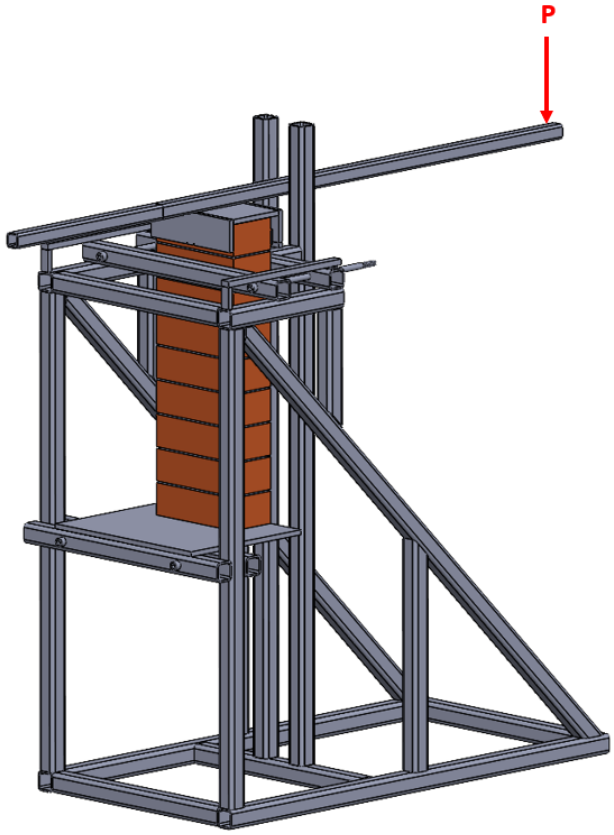

Figure 3.9: Prism secured within the frame and lever arm affixed to its upper brick. P is the applied load.

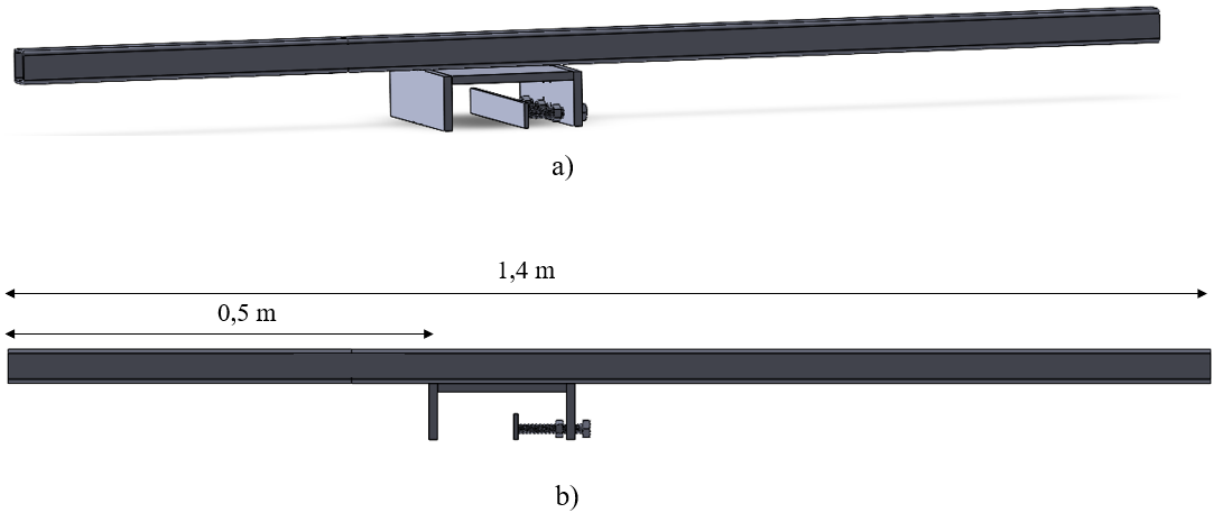

Figure 3.10: Lever arm: a) General view, b) Side view.

3.4 Instrumentation

3.4.1 Loading devices

The force was applied to the lever arm through a hydraulic jack, with control based on displacement. The decision to employ displacement control was a deliberate measure taken to reduce the risk of material fracture, particularly considering the lever arm's potential to fly after joint rupture.

The applied load was measured using a 100 kN load cell which offers an overall precision of approximately 1% within the range of forces utilized during the test. This load cell was connected to a ball joint, which was welded to a metallic profile measuring 10 cm in length. This profile had a larger cross-section than the lever arm, allowing the position of the load to be adjusted along it.

These elements are shown in Figure 3.11.

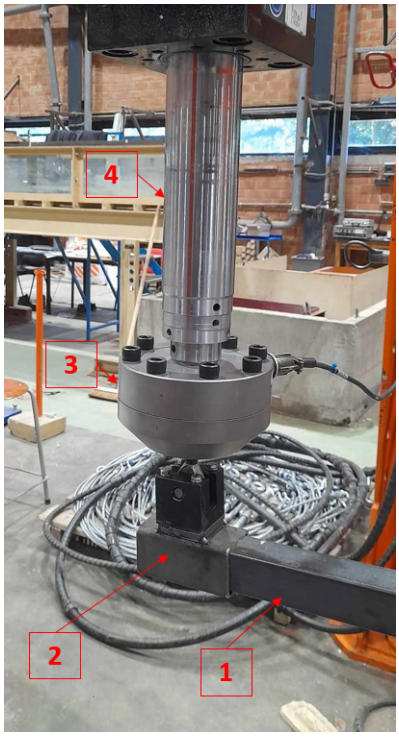

Figure 3.11: Loading equipment. Components: 1. Lever arm, 2. Ball joint, 3. Load cell, 4. Hydraulic jack.

3.4.2 Deformation measurement

As outlined in Section 3.1, one of the established objectives was to investigate deformations occurring along the joints during the bond wrench testing. With this objective in mind, the initial approach aimed to employ strain gauges, esteemed for their adeptness in providing measurements of localized deformation. A strain gauge essentially operates as a resistor, whose value fluctuates in response to the strain experienced by the affixed material. However, due to unforeseen challenges in the laboratory both prior to and during the testing phase, the laboratory was unable to supply these strain gauges.

Consequently, an alternative solution was adopted, which consists in the use of LVDTs (Linear Variable Differential Transformers). These devices, while less optimal for capturing local deformations, offer simple setup procedures. LVDT sensors, facilitate precise measurement of displacement at a micrometer scale

Figure 3.12: Placement of LVDT, targeting the area of maximum tensile strain.

After several trials, it was observed that the most effective technique for positioning the LVDT was to attach it onto small metallic plates using a hot glue gun. However, a drawback of this method is that the adhesive hardens within a few seconds, necessitating rapid placement of the device. As a result, achieving precise LVDT placement can prove to be quite challenging. Figure 3.12 visually presents the device's placement. Considering the time required for LVDT placement and in consultation with the laboratory's planning, a decision was made to place only one LVDT on the most extreme tensile fiber for a dozen joints. The objective was to investigate the relationship between stress and crack opening during the bond wrench test.

3.5 Test procedure

The testing methodology is represented in Figure 3.13.

Figure 3.13: Test procedure: a) Clamping the second uppermost brick of the prism to the apparatus, b) Clamping the lever arm to the top brick of the prism, c) Running the test, d) Bond failure.

Initially, the adjustable platform is lowered onto support jacks to enable the placement of the prism within the apparatus. Subsequently, the jacks are employed to adjust the prism's position, enabling the clamping of its second uppermost brick to the apparatus. The horizontal alignment is maintained using a spirit level. The distance between the apparatus's clamping mechanism and the joint is held within the range of 10 to 15 mm.

Subsequently, the lever arm is positioned onto the prism, and its horizontal alignment is adjusted using the hydraulic jack before being clamped to the uppermost prism brick.

The test is then conducted until the joint fails, and the detached brick is subsequently weighed along with any adhering mortar. Also, the failure mode is reported (refer to Figure 2.8). Assuming a linear stress distribution, the flexural tensile bond strength f_m is calculated thanks to the following formula (refer to Figure 3.14):

$$f_m = \frac{P_1.L_1 + P_2.L_2}{Z} - \frac{P_2 + P_1 + W}{A} \tag{3.4}$$

With Z the section modulus of the cross-section of the specimen, P_1 the weight of the loading arm, P_2 the maximal applied load, L_1 the distance from the centre of gravity of the lever arm to the centre of the prism, L_2 the length of the cantilever arm, A the area of the cross-section of the specimen and W the weight of the detached unit and any adherent mortar.

For all tests, the weight of the lever arm $P_1 = 95$ $[N]$, and the distance from the center of gravity of the lever arm to the center of the prism $L_1 = 75$ $[mm]$.

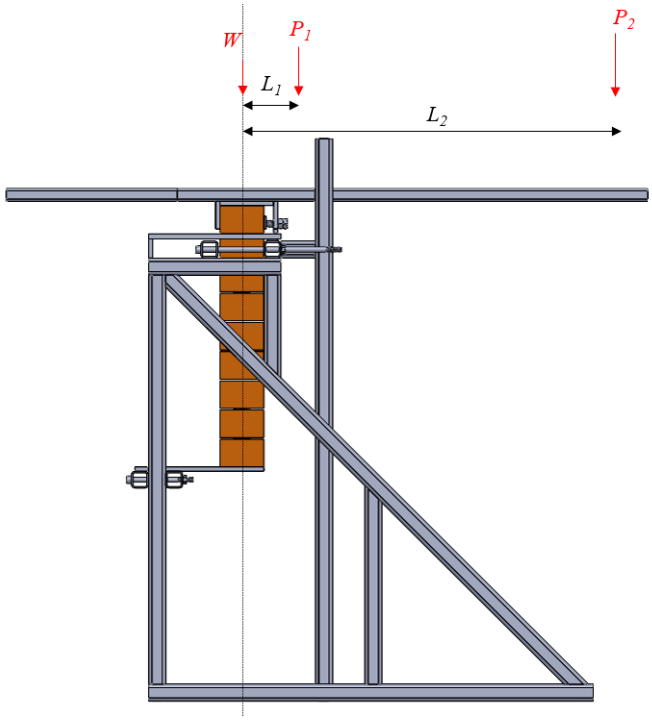

Figure 3.14: Schematic diagram of the bond wrench test.

3.6 First set of test

After 28 days of curing, an initial set of 15 joints, that is to say 3 prisms, underwent testing. This test set aimed to yield preliminary results, gather experience with the testing process, and identify and address any potential shortcomings.

Out of the 15 joints subjected to testing, 6 experienced failure during the setup when positioning the prism in the apparatus or clamping the lever arm to the top brick, accounting for 40% of the total. While literature acknowledges the possibility of failures occurring during setup, the amount of joint breakage observed during this process was particularly noteworthy. The concerns raised in Section 3.2 have therefore been verified. Consequently, obtaining consistent initial results was unfeasible due to the insufficient sample size.

The failures can be attributed to two potential sources:

1. The inherent weakness of the masonry bond.
2. Improper handling of the setup and testing procedure.

In order to mitigate failures from the latter cause, corrective measures were implemented before carrying on with next experiments:

- Neoprene bands were fixed to both the clamping surface of the apparatus frame and the lever arm. This adjustment was undertaken to facilitate a more uniform grip.
- On multiple occasions, the lever arm detached from the upper brick adjacent to the joint during testing, occurring prior to the joint's actual failure. This necessitated the re-tightening of the lever arm to the prism and the subsequent rerun of the test, causing disruption. Hence, it is imperative to securely tighten the lever arm against the brick to prevent any motion or detachment.
- The lever arm consists of a long rectangular hollow profile welded to a U-shaped profile (see Figure 3.10). Initially, the dimensions of the U-shaped profile were slightly oversized. As a result, there were occasions when it made contact with the apparatus during testing, obstructing the test's progression. This scenario is depicted in Figure 3.15. Consequently, adjustments were made to the dimensions of the profile to rectify this issue.

Figure 3.15: Lever arm in contact with the apparatus frame during testing.

3.7 Final objectives of the experimental phase

Based on the observations presented in Section 3.6, which highlighted a significant occurrence of failures during the setup phase, the investigation into the influence of the clamping mechanism's type and position was intentionally omitted. Instead, the study concentrated on exploring the impact of the following variables:

1. The length of the lever arm.
2. The rate of application of the load.

Moreover, a LVDT was positioned at the location of the most extreme tensile fiber for several tests, enabling the examination of the stress/crack opening curve during the bond wrench test.

3.8 Summary of the chapter

This Chapter started by outlining the initial objectives of the experimental phase of the present thesis, derived from the findings of Chapter 2. These stated objectives aimed to assess the sensitivity of the bond wrench test to various parameters, namely the lever arm's length, the characteristics of the clamping mechanisms of the lever arm, and the rate of application of the load. Additionally, another objective was to investigate crack opening along the joint during the bond wrench test by utilizing strain gauges.

Subsequently, the manufacturing of a bond wrench apparatus and the construction of fifteen stack-bonded prisms, each consisting of five joints, were presented. These prisms were fabricated using clay bricks and cement mortar. An observation was made that the mortar employed in construction displayed noticeable dryness, possibly due to hot weather conditions and the time gap between mixing the mortar and its application. This dryness raised concerns regarding bond strength, which were confirmed by initial test results: nearly half of the joints broke during the test installation process.

As a result of this, along with practical challenges faced in the laboratory, the focus of the study shifted to investigating the impact of lever arm length and the rate of load application on the bond wrench test. Moreover, the study of crack opening was limited to analyzing the crack opening at the level of the most extreme tensile fiber for part of the tests, using a Linear Variable Differential Transformer (LVDT).

Chapter 4

Experimental results and discussion

4.1 Test battery description

The test battery consisted of four distinct tests, these are detailed below:

- Test 1: This test involved a long lever arm (800 mm) and a moderate applied bending rate, resulting in failure generally occurring within the time frame required by European or American standards (i.e, between 1 to 5 minutes) [32, 33].
- Test 2: In this test, a short lever arm (275 mm) was combined with a rapid applied bending rate, leading to a failure time generally shorter than the ones required by standards.
- Test 3: Similar to Test 2, this test included a short lever arm (275 mm) but maintained a moderate applied bending rate equivalent to that of Test 1.
- Test 4: This test utilized a long lever arm (800 mm) with a slow applied bending rate, resulting in an average failure time longer than the ones required by standards.

The study incorporated these diverse test configurations to assess the flexural bond strength using the bond wrench test under different set-up conditions, specifically varying the lever arm length and applied bending rate.
Test 1 served as the baseline measurement, providing a reference point for comparison. In contrast, Test 2 was deliberately designed to accentuate the combined influence of both parameters by employing a short lever arm and a rapid applied bending rate (in comparison with Test 1). On the other hand, Tests 3 and 4 were specifically intended to isolate and examine the individual impact of the two parameters.

Due to the relatively low bond strength, the number of tests giving valid results was lower than anticipated. From the initial testing of the first 16 joints, it was observed that 3 joints failed during the installation phase, resulting in a validity rate of 81.25%. With the assumption that

the ratio of valid results would remain constant, a series of 4 tests was designed to provide a total of 48 valid results (12 for each test). However, upon completion, only 42 joints gave valid results. As a result, the 4th test was concluded with only 6 valid results.

4.2 Influence of lever arm length and loading rate

The results from the 4 different tests are summarized in Table 4.1 and depicted in Figure 4.1. Upon comparing the mean flexural bond strength and coefficient of variation (COV) across the test setups, no significant and consistent differences are observed, except for Test 3. Indeed, Test 3 stands out with mean strength results approximately 30% higher compared to the average strength of the other three tests. This specific test configuration combines a shorter lever arm with a moderate rate of the applied bending moment, resulting in failures occurring, on average, within the expected time frame required by European and American standards.

Test	Lever arm length [mm]	Loading rate at the end of the lever arm [mm/min]	Angular loading rate [mrad/min]	Mean flexural bond strength [MPa]	Standard deviation [MPa]	COV [%]	Number of valid tests
1	800	10	13	0.105	0.047	45	12
2	275	10	36	0.099	0.037	38	12
3	275	3.5	13	0.134	0.046	34	12
4	800	2	2.5	0.102	0.034	33	6

Table 4.1: Experimental campaign overview.

Note 1: In the figures up to Section 4.4 (inclusive), individual results are represented by unfilled circle markers, mean values are indicated by filled square markers, and the COV is prominently displayed in percentage.

Note 2: Since the length of the lever arm and the rate of load application vary, it is important to consider the angular loading rate in order to properly compare the tests.

To evaluate the statistical significance of the variation in mean strength, an unpaired Student's t-test is utilised. The t-test calculates a t-value by comparing the means of two groups, considering the variability within each group as represented by the standard deviation. It takes into account the sample sizes of the groups and provides insights into whether the observed difference in means is statistically significant or simply due to chance.
Based on the calculated t-value, the t-test generates a p-value, which represents the probability of observing the observed difference (or a more extreme difference) if the null hypothesis

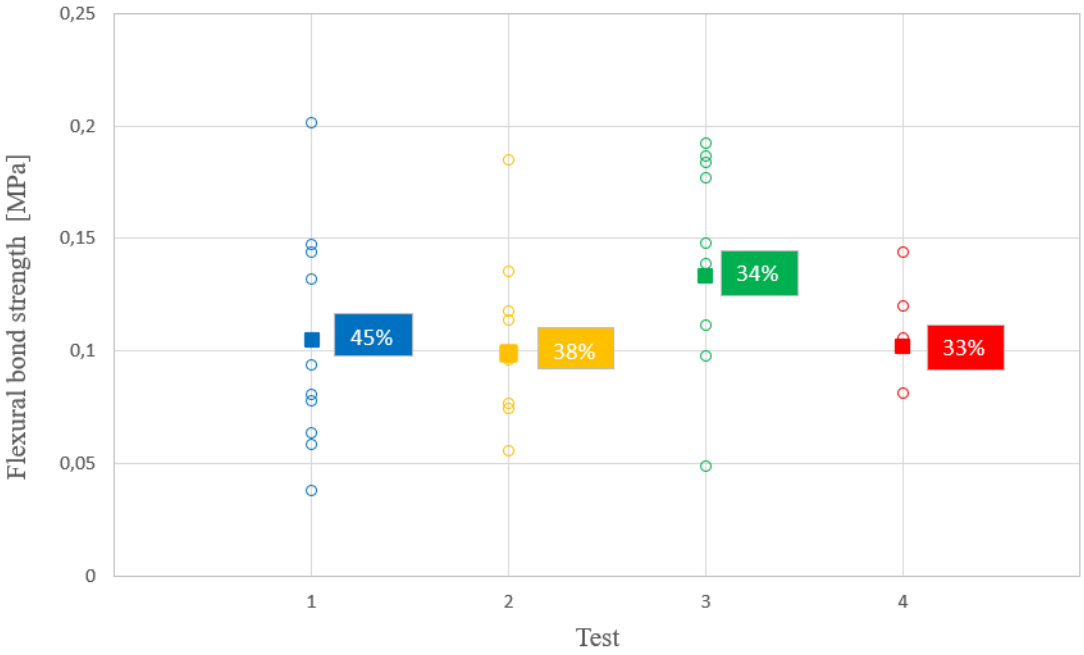

Figure 4.1: Flexural bond strength by test type.

is true (i.e., there is no real difference between the population means). If the p-value is below a predetermined significance level (such as 0.05), it suggests that the observed difference is statistically significant, leading to the rejection of the null hypothesis [56, 57] .

The summary of the t-tests comparing the mean of Test 3 with the means of the other three tests is provided in Table 4.2. The calculated p-values for all the tests surpass the predetermined significance level of 5%. Consequently, the null hypothesis cannot be rejected, suggesting no significant difference between the mean of Test 3 and the means of the other three tests.

T-test	p value	Level of significance	Null hypothesis
Test 1 vs Test 3	0.146	0.05	Accepted
Test 2 vs Test 3	0.057	0.05	Accepted
Test 4 vs Test 3	0.119	0.05	Accepted

Table 4.2: Student t-Test results.

By rearranging the data to analyse it in terms of the angular rate of displacement of the lever arm (see Table 4.3 and Figure 4.2) or in terms of lever arm length (see Table 4.4 and

Figure 4.3) it can be clearly seen that these parameters have no influence on the flexural bond strength. Regarding the COV, it is noteworthy that the slower angular loading rate at 2.5 mrad min^{-1} shows less variation in the results compared to the faster rates.
However, it is important to note that only 6 valid joints were tested with this slow loading rate. Additionally, there is no increase in the COV between the loading rates of 13 and 36 mrad min^{-1}. In fact, there is even a small decrease. Therefore, it can be concluded that there is no consistent trend indicating a reduction in result variations with a slower loading rate.

Angular loading rate [mrad/min]	**Mean flexural bond strength [MPa]**	**Standard deviation [MPa]**	**COV [%]**	**Number of valid tests**
2.5	0.102	0.034	33	6
13	0.119	0.048	40	24
36	0.099	0.037	38	12

Table 4.3: Results based on the angular loading rate. Considering only valid results.

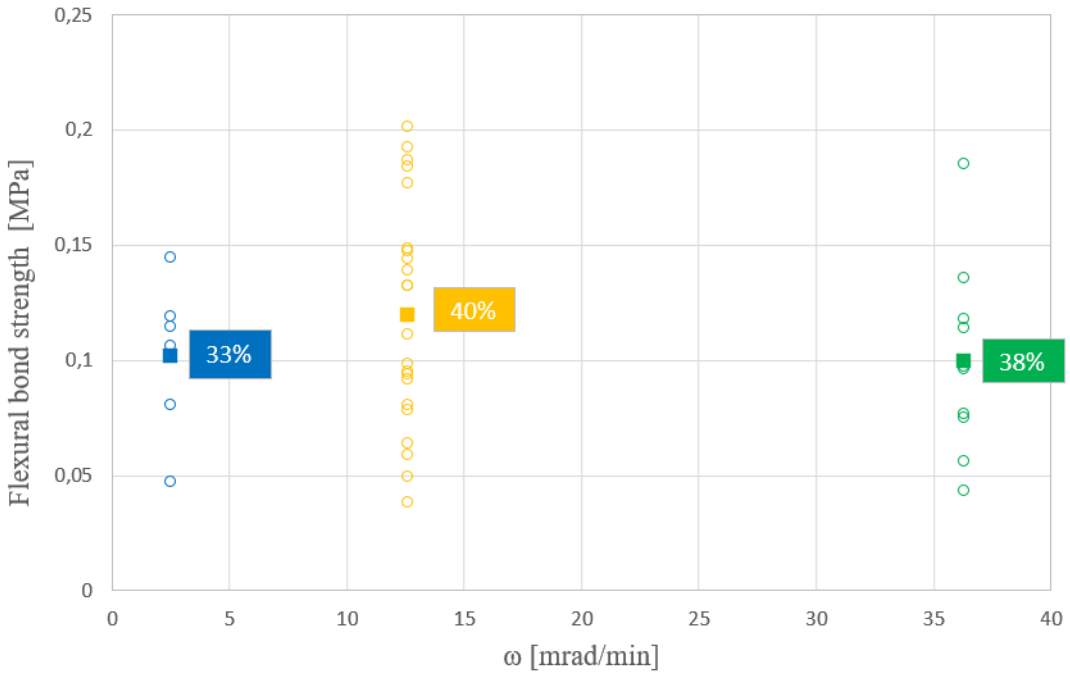

Figure 4.2: Flexural bond strength as a function of angular loading rate.

In Section 2.3.3, it was reported that Nichols [6] performed bond wrench tests on masonry prisms using both Australian and American standards, demonstrating notable differences in

Lever arm length [mm]	Mean flexural bond strength [MPa]	Standard deviation [MPa]	COV [%]	Number of valid tests
275	0.116	0.045	38	24
800	0.104	0.042	40	18

Table 4.4: Results based on the lever arm length. Considering only valid results.

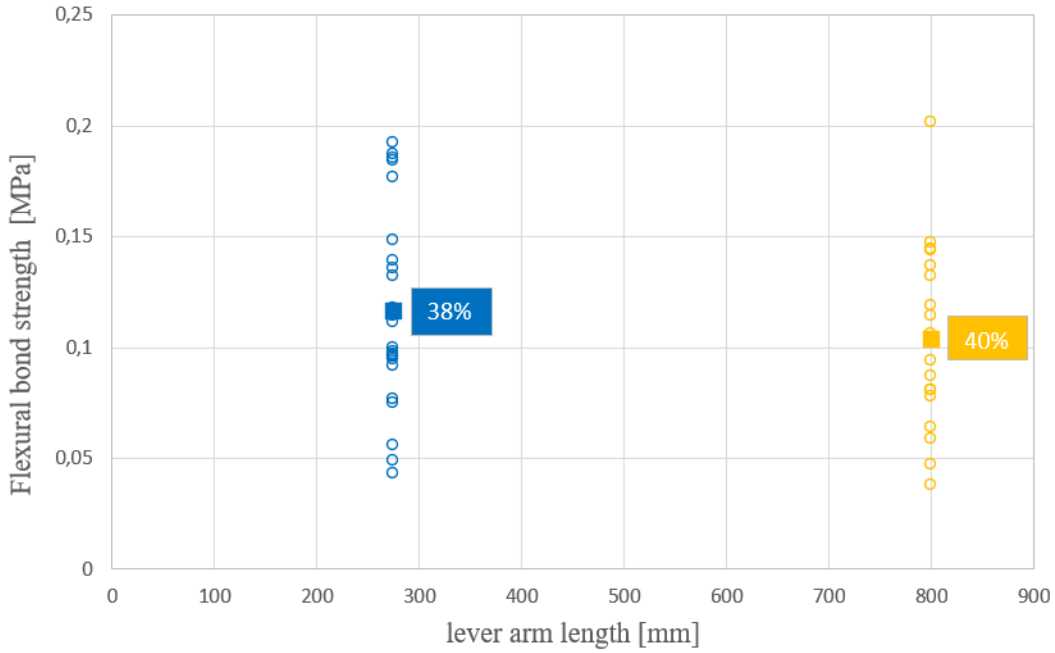

Figure 4.3: Flexural strength as a function of lever arm length.

mean strength between the two. The notable distinctions between the two apparatus of the norms are a different clamping mechanism, varying lever arm length, and certainly different loading rates (in terms of applied bending moment). However, the precision of the results was not provided, and Nichols reported that the American apparatus was particularly challenging to use.

Additionally, McGinley [4, 5] noted that the discrepancy between actual strain distributions and the linear distributions assumed by theory becomes more pronounced as the percentage of axial stress, relative to the peak flexural stress, increases. This discrepancy is directly related to the lever arm length. Furthermore, it was noticed that elevated load rates could lead to an increase in flexural strength, but this increment did not exhibit consistency concerning the loading rate. Additionally, the results demonstrated a higher coefficient of variation associated with higher loading rates .

In summary, the experimental findings of the present study demonstrate that there were no significant differences in the flexural bond strength of the tested joints when different lever arms length and loading rates were used. These results are in contrast to previous studies, which reported notable distinctions in mean strength between varying apparatus configurations.

The fact that the tested joints were particularly weak raises questions about how the joint's strength characteristics may have influenced the outcomes. Indeed, the mean flexural bond strength reported in Nichols' study [6] ranged between 0.58 MPa and 1.12 MPa, while the mean flexural bond strength of the joints in the present study was only 0.111 MPa. This considerable difference in strength could potentially have obscured any effects resulting from variations in lever arm or loading parameters.

4.3 Influence of joint precompression

Ultimately, the position of the tested joint within the prism, which reflects the precompression of the joints, was the sole parameter that influenced the flexural bond strength. As a reminder, each prism consisted of 5 joints. Position 1 represents the top joint and Position 5 represents the bottom joint. This parameter was initially not expected to be a subject of analysis.

When considering only the valid results (i.e., those that did not fail during the installation process), a notable trend of increasing mean strength can be observed (see Table 4.5 and Figure 4.4). Specifically, the mean strength of the joints between position 1 and position 5 demonstrates a substantial increase of 63%. Conducting a t-test between the valid results of position 1 and position 5 yields a p-value of 0.019, which falls below the common significance level of 0.05. Consequently, the null hypothesis is rejected, indicating that the difference in means is statistically significant and unlikely to be due to chance.

Position	Pre-compression [kPa]	Mean flexural bond strength [MPa]	Standard deviation [MPa]	COV [%]	Number of valid tests	Number of failed tests
1	3	0.085	0.024	29	5	7
2	4.3	0.083	0.023	28	7	5
3	5.5	0.107	0.046	43	10	2
4	6.9	0.119	0.047	39	10	2
5	8.2	0.139	0.042	30	10	2

Table 4.5: Results based on the joint position in the prism. Considering only valid results.

Considering the inclusion of failures during setup, the relevance of the findings becomes even

Figure 4.4: Flexural bond strength as a function of the position of the joint in the prism (excluding setup failures).

more apparent. Out of the 12 joints tested for each position, 7 and 5 joints failed during installation for Positions 1 and 2, respectively. Additionally, 2 joints failed during installation for Positions 3, 4, and 5. Taking these failures into account, assigned to a flexural bond strength of 0, the mean strength of the joints between Position 1 and Position 5 displayed a substantial increase of 231%. The results can be observed in Table 4.6 and Figure 4.5.
Repeating the t-test between the results of Position 1 and Position 5, considering failures during setup, gave a significantly low p-value of 0.002. This value falls well below the common significance level of 0.05 and even the stricter level of 0.01, reinforcing the statistical significance of the difference in means.

These last comments should be approached with particular caution, as the joints that broke during setup had an actual flexural bond strength that couldn't be precisely determined but was higher than zero. The provided numerical values serve as indications of a general trend. However, it is still evident that there is a decrease in the occurrence of failures with an increase in the position (i.e., precompression) of the joints during setup. Furthermore, even when considering only the valid results, there is a clear increase in strength corresponding to the position (i.e., precompression) of the joints.

Position	Pre-compression [kPa]	Mean flexural bond strength [MPa]	Standard deviation [MPa]	COV [%]	Number of valid tests	Number of failed tests
1	3	0.035	0.046	130	5	7
2	4.3	0.048	0.046	95	7	5
3	5.5	0.090	0.089	66	10	2
4	6.9	0.099	0.063	63	10	2
5	8.2	0.116	0.066	57	10	2

Table 4.6: Results based on joint position in the prism. Accounting for set-up failure with a value of 0.

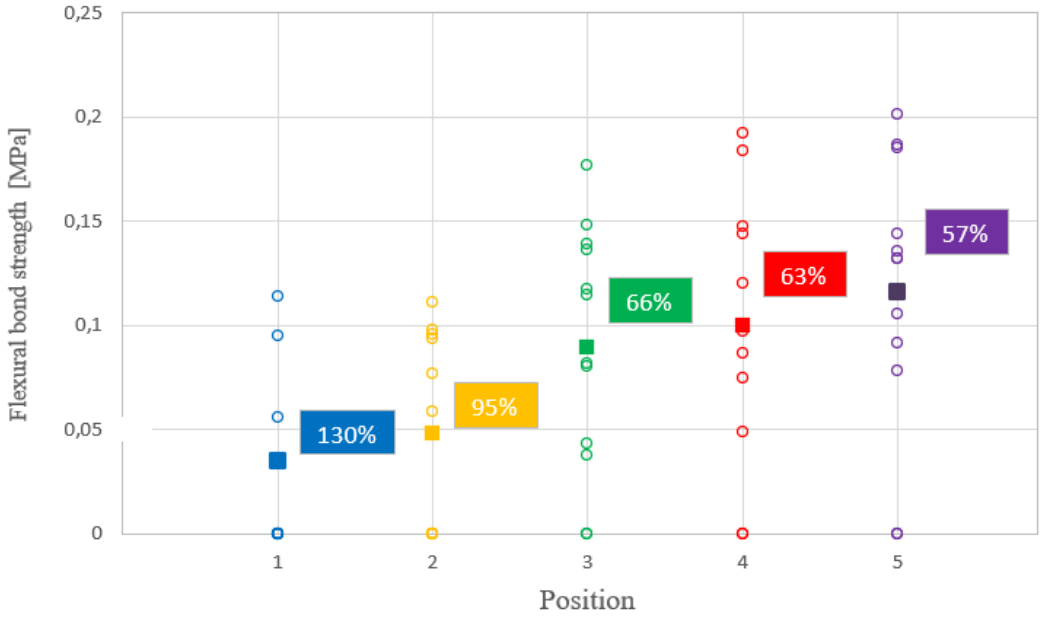

Figure 4.5: Flexural bond strength as a function of the position of the joint in the prism (including setup failures).

An observation of greater bond strength in the lower joints of a masonry prism compared to the upper joints has been reported in a previous study [48]. However, it was determined that this difference is generally not considered statistically significant. No additional information pertaining to this specific observation on bond strength in masonry prisms was found in the available literature.

Other studies have explored the correlation between flexural bond strength and pre-compression for masonry walls. Notably, Gaggero's study [9], observed that the tested joints' position within the wall had no significant impact. This study looked at two different types of masonry: calcium silicate brick masonry with a cement-based mortar, and clay brick masonry

with a cement-lime mortar. Additionally, in a study conducted by Correa *et al.* [58], six full-sized clay brick unreinforced masonry walls were built to mimic real-world conditions. The researchers used the bond wrench test to determine the flexural bond strength of each brick unit in the walls. The results indicated that there is minimal correlation observed between the units, both within individual courses and across different courses. Consequently, the study suggests that the flexural bond strengths between units can be considered statistically independent. This finding was further confirmed by Heffler *et al.* [50] in a similar research.

By contrast, the results of the present stsudy shows the influence of precompression and the potential significance of joint placement within the structure in determining its flexural bond strength.

One possible explanation for this discrepancy could be related to the fundamental differences between a masonry stack and a masonry wall. In a masonry stack, the joints may experience different stress distribution than masonry walls that typically have a more extensive and continuous layout, potentially leading to more uniform stress distribution across the joints. However, it's worth noting that in the current study, the mortar was adequately spread across the surface of the unit (see Figure 4.7), with only the corners most of the time remaining unfilled. This suggests that the variation in bond strength might be less influenced by mortar application.

Therefore, the explanation certainly lies more in other factors, such as the dryness of the mortar during prism construction and the weakness of the bonds, that are likely to have a crucial influence on the behavior of the joints. It is plausible that these factors introduce variations in the results when compared to findings from previous studies. However, it is important to acknowledge that this explanation remains a hypothesis, and further investigation is necessary to validate these claims.

4.4 Failure modes

Various failure modes of the joint can occur during the bond wrench test. These are depicted in Figure 2.8. The failure modes can be categorized as follows:

- Failure at the interface between the mortar and one or both brick surfaces.
- Failure within the mortar itself.
- Failure of a brick unit, occurring either next to the joint or at the clamping level.

In the present study, all ruptures occurred at the interface between the mortar and one of the two surfaces (failure modes 1 and 2, see Figure 4.6 and see Figure 4.7). Notably, no failures

occurred within the mortar. This suggests that the flexural bond within the mortar exhibits considerably superior strength compared to the flexural bond strength of the brick-to-mortar interface.
As depicted in Figure 4.6, the percentage of failure remains nearly unchanged, regardless of whether failure during set-up is considered or not.

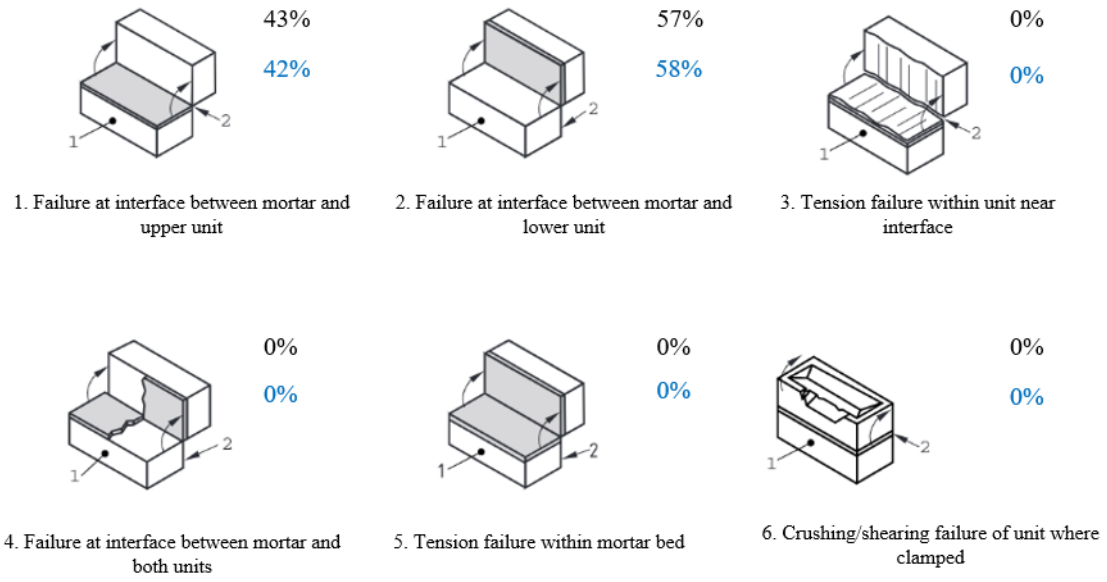

Figure 4.6: Percentage of occurrence of the various failure modes in the present study. Black percentage indicates valid results only. Blue percentage accounts for failure during set-up.

Figure 4.7: Failure modes observed during the study. Mode 1 on the left, mode 2 on the right.

The results from the two different failure modes are summarized in Table 4.7 and depicted in Figure 4.8. As observed, failures between the mortar and the upper unit surface (mode 2) lead to higher mean strength and reduced COV compared to failures between the mortar and

the lower unit (mode 1). It is worth noting, that there is a 31% ratio of failed joints during set-up for mode 2, indicating a significant occurrence of weak joints. This ratio is similar for mode 1 (28%).

No information in existing literature has been found to explain the discrepancy in strength and COV. An explanation might be found in the construction of the prisms and the materials used. Let's label the brick below a joint as the bottom brick and the brick above as the top brick. The prisms were constructed using frogged units facing downward. When an insufficient amount of mortar was initially applied to the bottom brick, a proper contact surface between the mortar and the top brick could not be established at the frog level. This led to a reduction in the overall surface contact compared to a plain surface. On the contrary, when an adequate amount of mortar was applied to the bottom brick, a contact surface between the mortar and the top brick at the frog level could be established, resulting in an increase in the overall surface contact compared to a plain surface.
It should be noted that this is merely a hypothesis and would necessitate further observations for confirmation.

Failure mode	**Mean flexural bond strength [MPa]**	**Standard deviation [MPa]**	**COV [%]**	**Number of valid tests**	**Number of failed tests**
1	0.085	0.038	45	18	7
2	0.130	0.037	28	24	11

Table 4.7: Summary of the results based on the failure mode considering only valid results.

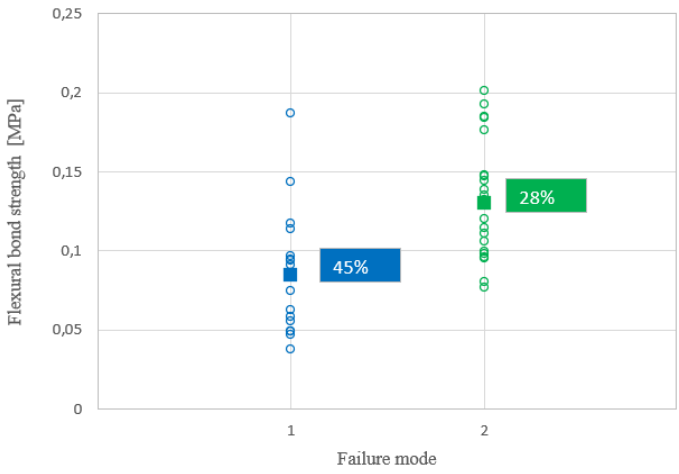

Figure 4.8: Flexural bond strength as a function of the failure mode, considering only valid results.

4.5 LVDt's measurement

This section presents the results of the LVDT placed at the location of the most extreme tensile fiber for a subset of bond wrench tests. The aim was to gain insights into the stress/crack opening behavior of the joints during the bond wrench test at this specific location.

The results presented are from 6 joints, which represent the only data obtained using the LVDT. Other results are not available due to joint failure before conducting the bond wrench test or due to irregular curves, likely caused by incorrect LVDT placement.

The results from the 6 joints are depicted in Figures 4.9, 4.10, and 4.11. Two distinct types of curves can be observed. The first type shows an approximately linear pattern with progressive deformations before failure. This behavior appears to correspond to the quasi-brittle nature of the masonry interface under bending, such as discussed in Section 1.2. These curves are observed in joints G3, K4, and K5.

Conversely, the second type is characterized by minimal deformation and sudden failure, indicating a brittle behavior. This pattern is observed in joints I3, K3, and L5.

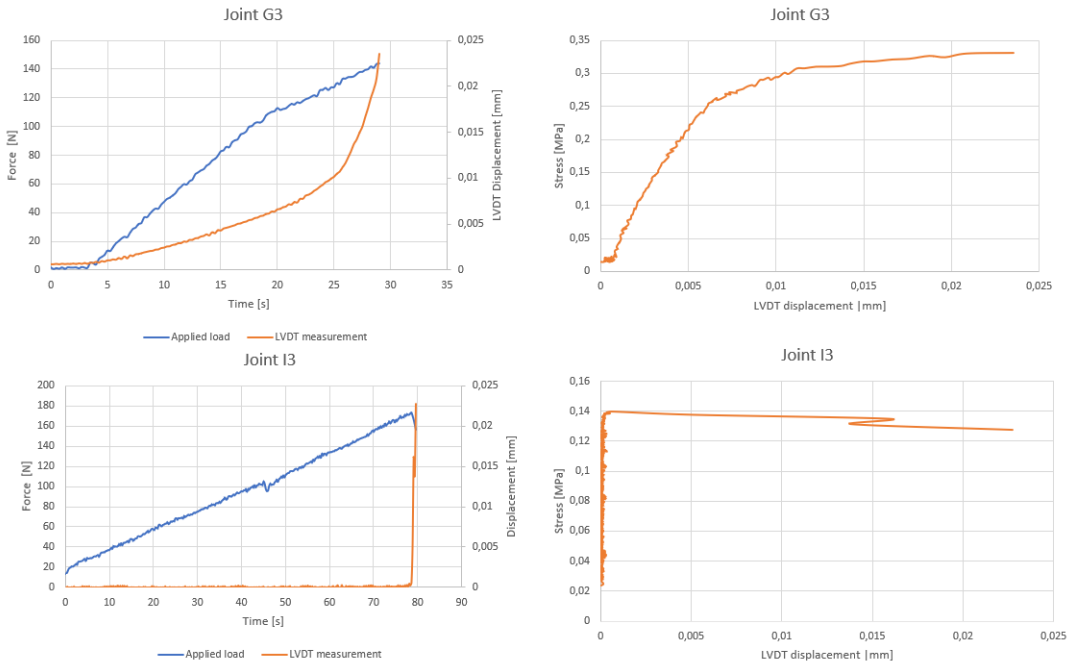

Figure 4.9: LVDT measurement: Joints G3 and I3.

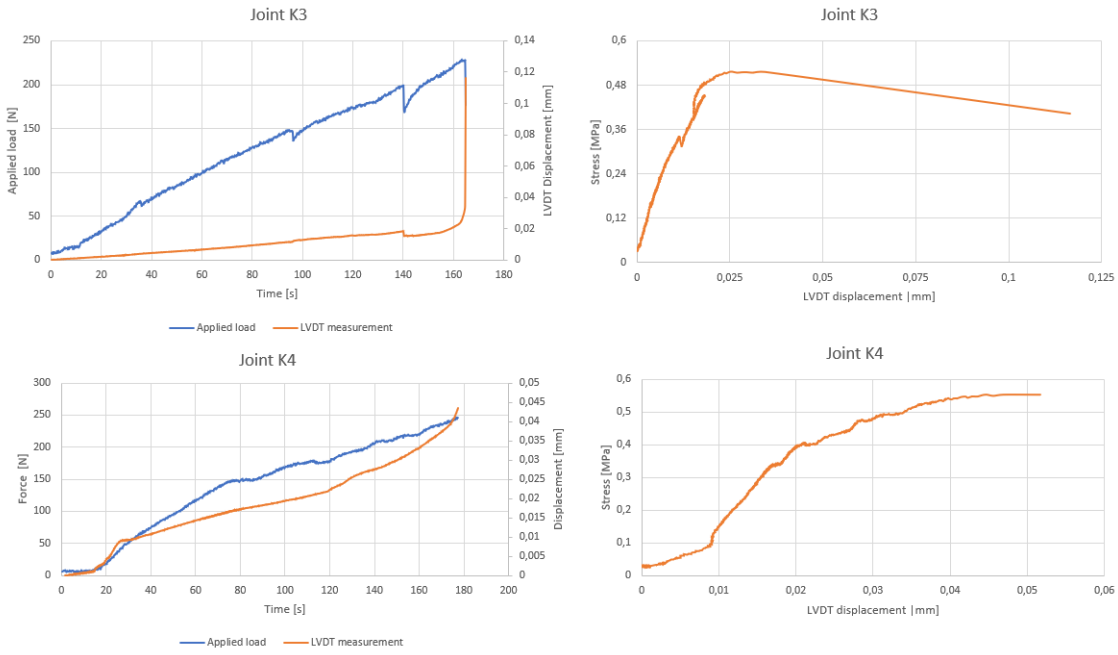

Figure 4.10: LVDT measurement: Joints K3 and K4.

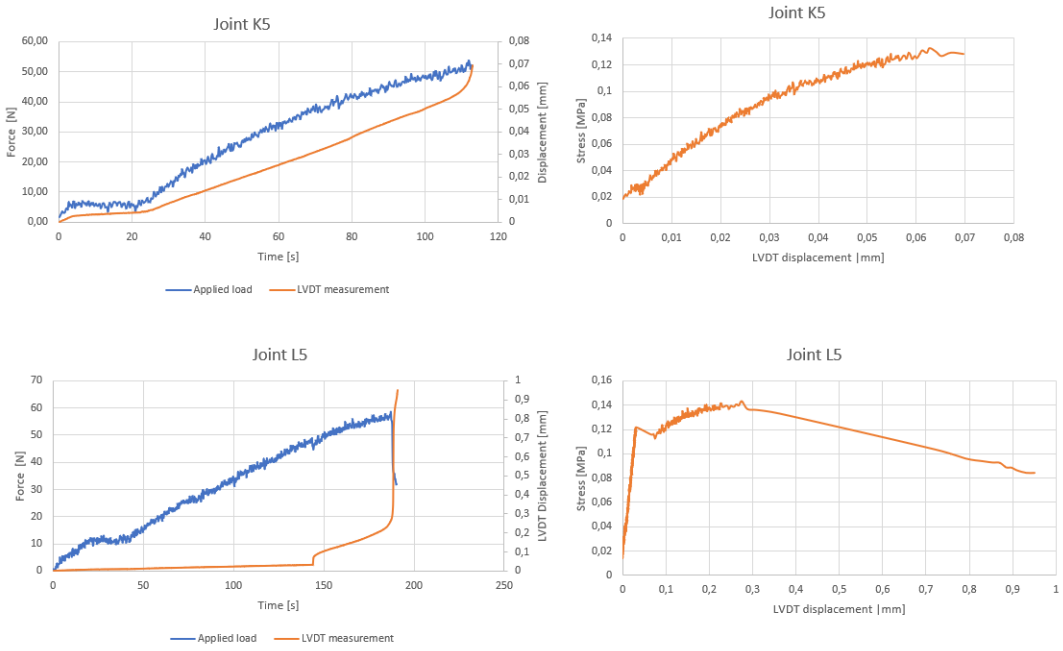

Figure 4.11: LVDT measurement: Joints K5 and L5.

4.6 General comments

The prisms employed to generate the results were tested over a duration of 5 days after a total curing time ranging from 39 to 43 days. As a general observation, the flexural bond strength of the tested masonry was very low. Firstly, a significant number of joints failed during the installation process, before any load could be applied to the lever arm. Of the 60 joints tested (equivalent to 12 prisms), 18 (30%) failed during installation, giving 42 valid results from which the flexural strength could be measured.
Looking at the results for the group of 42 valid joints, the mean strength was 0.111 MPa and the COV (ratio of standard deviation to mean expressed in %) was 39%. This COV is consistent with the variability previously reported in the literature when employing the bond wrench test [9].

The observed low results can be attributed to several factors discussed here. The mortar was initially prepared by a mason at a warehouse in Gembloux and later transported to the LEMSC lab. The mason's observation indicated that the mortar displayed significant dryness, potentially due to the prevalent hot and windy weather conditions during the roughly 20-minute transit from Gembloux to the lab. Additionally, the entire construction of the 15 prisms was accomplished in about 1.5 hours. Consequently, the entire process, spanning from mortar preparation to prism construction, was finalized within approximately 2 hours. Because of the mortar's dryness, the mason had to repeatedly re-temper it before application to the bricks to improve its workability. As discussed in Sections 3.2.3 and 1.3, these factors collectively may negatively impact the bond strength of masonry joints.

Refer to Appendix 4.7 for the detailed results of each joint.

4.7 Summary of the chapter

This chapter reported the results of a set of 60 bond wrench tests conducted to investigate the impact of lever arm length and load application rate on test outcomes. Additionally, a Linear Variable Differential Transformer (LVDT) was employed to measure crack opening at the most extreme tensile fiber level during a subset of tests.

The outcomes of the experiments were that the lever arm length and the rate of application of the load had no influence on the results when performing bond wrench tests. Interestingly, a factor not initially considered in the research objectives, the joint precompression, emerged as the sole element influencing the results. This observation stands in contrast to prior studies concerning masonry walls, where no discernible correlation between joint precompression and flexural bond strength was established through the utilisation of the bond wrench test.

However, it is important to underline the limitations of the experiments carried out and, consequently, the scope of the conclusions drawn. Firstly, as mentioned, the joints studied were relatively weak. Of the 60 joints tested, 18 (or 30%) failed during the test installation. The average flexural strength of the valid tests (those that did not fail during installation) was $0.111\,\mathrm{mega} - \mathrm{pascal}$. In addition, the experiments were conducted using a single combination of mortar and elements. Therefore, the conclusions drawn from this study may not be valid for stronger joints and for various combinations of mortar and elements.

Conclusion and future developments

After providing an overview of the masonry flexural bond strength in Chapter 1, the second Chapter of this work reviewed the existing literature on the bond wrench test. The analysis revealed that the primary advantage of the test is its simple setup and its possibility to evaluate each joint within a stack-bonded masonry prism. This is in contrast to its comparative counterpart, the beam test, which gives only a single result per prism. Furthermore, studies demonstrated that the bond wrench test offers a simple and rapid alternative for determining the general flexural strength of masonry as opposed to the conventional test prescribed by the Eurocode 6 [23], the EN 1052-2 [41]. Indeed, the EN 1052-2 demands a substantial experimental setup involving an entire masonry wall.

Then, the second chapter further encompassed a review and comparison of the bond wrench test within international standards, including European, American, and Australian norms. Furthermore, it investigated practical implementations of the test and the diverse variations encountered within existing researches. This analysis revealed that while the fundamental principles of the bond wrench test remain consistent across its various applications (both within standards and in practice), different characteristic and application of a set of parameters are used. These parameters include the lever arm's length, the characteristics of the clamping mechanisms associated with the lever arm, and the rate of application of the load. Studies highlighted that those parameters may significantly impact the test outcomes. As an example, a study performed bond wrench tests on masonry prisms using both the Australian and American standards, and compared the mean results according to these two standards [6]. The findings revealed a ratio of approximately 2:1 between the means of the two sets of results.

Subsequently, an experimental phase was initiated with the primary objective of evaluating the sensitivity of the bond wrench test to the parameters cited above. As described in Chapter 3, the preparatory steps for the experiment entailed the design and construction of a bond wrench apparatus, which could prove valuable for future research at UCLouvain. Additionally, fifteen stack-bonded masonry prisms, each consisting of five joints, were built, resulting in a collective total of 75 joints to be tested.

Due to a general weakness of the masonry joints used during the experiment, which led to

the failure of a significant number of joints (32% of the total number) before the initialisation of the test (during prism installation in the apparatus or lever arm clamping), a decision was made to focus the scope of the study on evaluating the sensitivity of the test to the lever arm length and loading rate.

Presented in Chapter 4, the outcomes of the experiments were that **variations in lever arm length and loading rates do not lead to noteworthy distinctions in the flexural bond strength of the assessed joints**. As an interesting and unexpected fact, it was observed that a factor not initially outlined in the research objectives, **the joint precompression, emerged as the sole parameter influencing the flexural bond strength**. This observation stands in contrast to prior studies concerning masonry walls, where no discernible correlation between joint precompression and flexural bond strength was established through the utilization of the bond wrench test.

However, it is important to underline the limitations inherent of this study, and consequently, the scope of the conclusions drawn. Firstly, as mentioned, the joints studied were relatively weak, with a mean flexural bond strength of the valid tests measuring 0.111 MPa. Moreover, the experiments were conducted using only one combination of mortar and unit. Consequently, the conclusions derived from this study may not hold true for joints of higher strength and for various combinations of mortar and unit.

Moreover, the experiments aimed to examine the stress/crack opening behavior of the joints during the bond wrench test. As detailed in Section 3.4.2, LVDTs (Linear Variable Differential Transformers) were placed on the most extreme tensile fibers for a subset of joints. However, the insights obtained were restricted, and it is recommended to employ more suitable measurement devices.

Finally, the present study could serve as a basis for further researches:

- **Various combinations of mortar and units**: Replicating the experiments using diverse combinations of mortar and units. Specifically, conducting experiments involving a combination of concrete-silicate units with cement-based mortar, and another combination comprising clay bricks with lime based mortar, as it is historically practiced, could offer valuable insights. This divergence in combinations holds interest since cement based mortars often exhibit higher strength but can also manifest a more brittle behavior, while lime-based mortars have a more plastic behavior. Consequently, the response to variations in the parameters of the bond wrench test might not be uniform across these two combinations. Furthermore, considering the weak nature of the bonds studied in the present work, performing tests on strong masonry bonds could serve as a valuable complement.

- **Advanced Instrumentation**: Employing advanced instrumentation, when performing the bond wrench test, such as Digital Image Correlation (DIC) or optical fibers to better understand and characterize the behavior of the brick-mortar interface. DIC enables precise tracking of surface deformation and displacement patterns in real-time, aiding the capture of subtle variations during testing. Optical fibers embedded within the mortar offer a means to directly measure strain changes along the joint during loading, providing localized deformation insights. Furthermore, the use of these advanced instrumentation with direct tensile tests could offer insights into the stress distribution along the joint during the bond wrench test.

- **CMOD-controlled bond wrench test and comparison with direct tensile tests**: The use of a crack mouth opening displacement (CMOD)-controlled bond wrench test, as performed by Gaggero [9], particularly if coupled with direct tensile tests is worth exploring. The tensile post-peak behavior is an important element for numerically assessing masonry structures. However, direct tensile tests are often complicated to perform and not available in laboratory, contrary to flexural tests. Therefore investigating if a relation could be found between the flexural bond fracture energy of masonry and tensile bond fracture energy is of interest.

- **Numerical Simulation**: Alongside with these experimental projects, engaging in numerical simulations could offers a complementary approach. For example, comparing the results of numerical simulations calibrated with the outcomes of the bond wrench test and with the outcomes direct tensile test could prove insightful.

Bibliography

1. Pavia, S. *et al.* Flexural bond strength of natural hydraulic lime mortar and clay brick. *Materials and Structures* **43,** 913–922 (2009).
2. Sarhosis, V. *et al. Computational Modeling of Masonry Structures Using the Discrete Element Method* (Engineering Science Reference, 2016).
3. Laboratory website, M. *Bond Wrench Test Setup* `https://masonrysociety.org/Masonry%20Lab/Lab%203/Lab-3-pics.html`. (Latest access: 06.08.2023).
4. McGinley, W. Flexural bond strength testing: An evaluation of the bond wrench testing procedures. *Masonry: design and construction, problems and repair* **1180,** 213–227 (1993).
5. McGinley, W. An Evaluation of Bond Wrench Testing Apparatuses. *Masonry: Esthetics, Engineering. and Economy* **1246,** 100–115 (1996).
6. Nichols, J. *et al.* A Precision and Bias Study for the Measurement of Flexural Strength of Masonry Prisms. *Journal of the International Masonry Society* **30,** 71–80 (2018).
7. Lourenço, P. B. Experimental and numerical issues in the modelling of the mechanical behaviour of masonry (1998).
8. Sarangapani, G. *et al.* Brick-Mortar Bond and Masonry Compressive Strength. *Journal of materials in civil engineering* **17,** 229–237 (2005).
9. Gaggero, M. Experimental characterisation of flexural bond behaviour in brick masonry. *Materials and Structures* **56** (2023).
10. McNeilly, T. *et al.* A site survey of masonry bond strength. *Aust Civ/Struct Eng Trans,* 103–109 (Jan. 1996).
11. Almesfer, N. *et al.* Material properties of existing unreinforced clay brick masonry buildings in New Zealand. *Bulletin of the New Zealand Society for Earthquake Engineering* **47,** 75–96 (2014).
12. van der Pluijm R. Measuring Of Bond: A Comparative Experimental Research. *The Proceedings of the 7th North American Masonry Conference* **1,** 267–281 (1996).

13. Barr, S. *et al.* Bond-strength performance of hydraulic lime and natural cement mortared sandstone masonry. *Construction and Building Materials* **84,** 128–135. ISSN: 0950-0618. https://www.sciencedirect.com/science/article/pii/S0950061815002639 (2015).

14. Radhakrishnan, R. *et al.* A Modified Bond Wrench Test for Evaluating Bond Strength of Concrete Repairs. *International journal of engineering research and technology* **2.** https://api.semanticscholar.org/CorpusID:135560874 (2013).

15. Bisoffi-Sauve, M. *Etude des ouvrages maçonnés en pierre par la méthode des éléments discrets: Caractérisation et modélisation du comportement cohésif des joints* PhD thesis (Université de Bordeaux, 2016).

16. van der Pluijm R. *Out-of-plane bending of masonry behavior and strength* PhD thesis (Eindhoven University of Technology, 1999).

17. Jukes, P. *et al.* Review of masonry tensile bond strength test methods. *Masonry International* **12,** 51–57 (1998).

18. Van Geel, E. *et al.* The variability of tensile and flexural bond strength. *Proceedings of the 10th International Brick and Block Masonry Conference* **2,** 959–968 (1994).

19. Hillerborg, A. *et al.* Analysis of crack formation and crack growth in concrete by means of fracture mechanics and finite elements. *Cement and Concrete Research* **6,** 773–781. ISSN: 0008-8846. https://www.sciencedirect.com/science/article/pii/0008884676900077 (1976).

20. Lourenço, P. Computational strategies for masonry structures [Ph. D. thesis]. *Delft University of Technology* (1996).

21. The Brick Industry Association. *Mortars for brickwork. Technical notes on Brick Construction* (2020).

22. Venu Madhava Rao, K. *et al.* Flexural bond strength of masonry using various blocks and mortars. *Materials and structures* **29,** 119–124 (1996).

23. EN, C. 1-1 Eurocode 6–Design of masonry structures–Part 1-1: general rules for reinforced and unreinforced masonry structures. *European Committee for Standardization, Brussels* (2005).

24. Heffler, L. *Variability of unit flexural bond strength and its effect on strength in clay brick unreinforced masonry walls subject to vertical bending* (University of Newcastle, 2009).

25. ASTM International. *ASTM C270* (2010).

26. The Brick Industry Association. *Hot and cold weather construction. Technical notes on Brick Construction* (2020).

27. Ritchie, T. *et al. Factors affecting bond strength and resistance to moisture penetration of brick masonry* in *Symposium on Masonry Testing, ASTM STP* **320** (1963), 16–30.

28. Melander, J. *et al. Effect of fabrication and curing on bond strength of masonry* in *Symposium on Masonry Testing, ASTM STP* **320** (1995), 16–30.
29. ASTM International. *ASTM E518* (2010).
30. Standards Australia. *AS 3700* (2017).
31. Grimm, C. T. *et al.* Flexural strength of masonry prisms versus wall panels. *Journal of Structural Engineering* **111,** 2021–2032 (1985).
32. ASTM International. *ASTM C1072* (2013).
33. Comité européen de normalisation. *EN 1052-5* (2005).
34. ASTM International. *ASTM C780* (2020).
35. ASTM International. *ASTM C67* (2017).
36. Comité européen de normalisation. *EN 772-10* (1999).
37. Comité européen de normalisation. *EN 772-1* (2011).
38. Comité européen de normalisation. *EN 1015-3* (1999).
39. Comité européen de normalisation. *EN 1015-7* (1998).
40. Comité européen de normalisation. *EN 1015-11* (2019).
41. Comité européen de normalisation. *EN 1052-2* (2016).
42. Park, M. S. *Reusing brick: Properties of brick to mortar bond strength* PhD thesis (Columbia University, 2013).
43. Vaculik, J. *Unreinforced masonry walls subjected to out-of-plane seismic actions.* PhD thesis (2012).
44. Burton, C. *et al.* Field testing of vintage masonry: Mechanical properties and anchorage strengths. *Structures* **28,** 1900–1914. ISSN: 2352-0124. `https://www.sciencedirect.com/science/article/pii/S2352012420305804` (2020).
45. Z. Zhou, P. *et al.* Strength characteristics of hydraulic lime mortared brickwork. *Proceedings of the Institution of Civil Engineers - Construction Materials* **161,** 139–146 (2008).
46. Pavia, S. *et al.* Compressive, flexural and bond strength of brick masonry. *Proceedings of PROHITEC 09* **1,** 1609–1615 (2009).
47. Vekey, R. D. *et al.* The Variability of Bond Wrench Measurements in UK, Australia and USA. *Masonry International* **8,** 21–25 (1994).
48. Nichols, J. A comparative study of four bond wrenches with recommendations on changes to ASTM C1072. *12th Canadian Masonry Symposium At Vancouver* (2013).
49. Radcliffe, M. R. *et al.* Highly Cored Extruded Clay Units: Testing and Design Procedures. *Structures 2004: Building on the Past, Securing the Future* **1,** 1–8 (2004).

50. Heffler, L. M. *et al.* Statistical analysis and spatial correlation of flexural bond strength for masonry walls. *Masonry International* **21,** 59–70 (2008).

51. Schuller, M. P. Nondestructive testing and damage assessment of masonry structures. *Progress in Structural Engineering and Materials* **5,** 239–251 (2003).

52. Comité européen de normalisation. *EN 772-11* (2011).

53. Kondraivendhan, B. *et al.* Flow behavior and strength for fly ash blended cement paste and mortar. *International Journal of Sustainable Built Environment* **4,** 270–277 (2015).

54. Barabanshchikov, Y. *et al.* Influence of Microfibrillated Cellulose Additive on Strength, Elastic Modulus, Heat Release, and Shrinkage of Mortar and Concrete. *Materials* **14,** 6933 (2021).

55. Comité européen de normalisation. *EN 1015-6* (1998).

56. Gregersen, E. *Student's t-test* `https://www.britannica.com/science/Students-t-test`. (Latest access: 06.08.2023).

57. Université de Liège. *Test t de student : Deux échantillons indépendants* `http://www.biostat.ulg.ac.be/pages/Site_r/t.html`. (Latest access: 06.08.2023).

58. Corrêa, M. R. S. *et al.* An Experimental and Statistical Analysis of the Flexural Bond Strength of Masonry Walls. *Australian Journal of Structural Engineering* **13,** 139–148. `https://www.tandfonline.com/doi/abs/10.7158/13287982.2012.11465104` (2012).

Appendix

Extended results

Joints	Prism	Pulled out brick	Loading rate [mm/min]*	Test	L_1 [mm]	P_1 [N]	L_2 [mm]	P_2 [N]	Weight unit [N]	b [mm]	l [mm]	Z [mm3]	Failure mode	Days of curing	N [N]	M [Nmm]	fm [Mpa]
1	D	D1	10	N/A	75	95	800	N/A	\	100	214	356667	1	39	N/A	N/A	N/A
2	D	D2	10	N/A	75	95	800	N/A	\	100	214	356667	1	39	N/A	N/A	N/A
3	D	D3	10	1	75	95	800	52,37	32,7	98	211	337741	2	40	180	49021	0,136
4	D	D4	10	1	75	95	800	30,5	21,2	97	214	335588	1	40	147	31525	0,087
5	D	D5	10	1	75	95	800	28,36	32,6	99	214	349569	2	40	156	29813	0,078
6	E	E1	10	1	75	95	800	22,87	21,2	101	213	362136	1	40	139	25421	0,064
7	E	E2	10	1	75	95	800	21,5	27,3	102	215	372810	1	40	144	24325	0,059
8	E	E3	10	1	75	95	800	10,5	27,7	99	215	351203	1	40	133	15525	0,038
9	E	E4	10	1	75	95	800	60,6	33,1	100	214	356667	2	40	189	55605	0,147
10	E	E5	10	1	75	95	800	85,2	27,1	100	214	356667	2	40	207	75285	0,201
11	F	F1	10	2	75	95	275	112,1	27,4	100	214	356667	2	40	234	37950	0,095
12	F	F2	10	N/A	75	95	275	N/A	\	100	214	356667	2	40	N/A	N/A	N/A
13	F	F3	10	2	75	95	275	46,7	21,5	99	216	352836	1	40	163	19968	0,049
14	F	F4	10	2	75	95	275	112	26,9	99	215	351203	1	40	234	37925	0,097
15	F	F5	10	2	75	95	275	167,7	33,0	100	214	356667	2	40	296	53243	0,135
16	G	G1	10	2	75	95	275	138	21,6	100	215	358333	1	40	255	45075	0,114
17	G	G2	10	2	75	95	275	112,6	33,2	100	213	355000	2	41	241	38090	0,096
18	G	G3	10	2	75	95	275	144,1	23,4	100	216	360000	1	41	262	46747	0,118
19	G	G4	10	2	75	95	275	80,7	27,7	99	213	347936	1	41	203	29318	0,075
20	G	G5	10	2	75	95	275	236,1	33,0	100	214	356667	2	41	364	72053	0,185
21	H	H1	10	2	75	95	275	49,84	21,1	96	212	325632	1	41	166	20831	0,056
22	H	H2	10	2	75	95	275	86,48	33,3	100	214	356667	2	41	215	30907	0,077
23	H	H3	10	N/A	75	95	275	N/A	\	100	214	356667	2	41	N/A	N/A	N/A
24	H	H4	10	2	75	95	275	109,7	27,4	97	214	335588	2	41	232	37282	0,100
25	H	H5	3,5	3	75	95	275	100,9	22,0	98	214	342543	1	41	218	34867	0,091
26	I	I1	3,5	3	75	95	275	108,5	21,8	99	215	351203	1	41	225	36954	0,095
27	I	I2	3,5	3	75	95	275	136,4	32,3	100	217	361667	2	41	264	44624	0,111
28	I	I3	3,5	3	75	95	275	173,1	27,4	100	215	358333	2	41	295	54714	0,139
29	I	I4	3,5	3	75	95	275	234,5	27,5	100	214	356667	2	41	357	71613	0,184
30	I	I5	3,5	3	75	95	275	155,4	26,9	98	214	342543	2	41	277	49855	0,132

31	J	J1	3,5	N/A	75	95	275	N/A	\	100	214	356667	1	41	N/A	N/A	N/A
32	J	J2	3,5	N/A	75	95	275	N/A	\	100	214	356667	2	41	N/A	N/A	N/A
33	J	J3	3,5	3	75	95	275	176,3	26,8	98	214	342543	2	41	298	55602	0,148
34	J	J4	3,5	3	75	95	275	45,46	21,4	99	212	346302	1	42	162	19627	0,049
35	J	J5	3,5	3	75	95	275	226,2	21,7	98	213	340942	1	42	343	69319	0,187
36	K	K1	3,5	N/A	75	95	275	N/A	\	100	214	356667	1	42	N/A	N/A	N/A
37	K	K2	3,5	3	75	95	275	116,5	32,4	100	215	358333	2	42	244	39163	0,098
38	K	K3	3,5	3	75	95	275	228,8	26,9	100	218	363333	2	42	351	70056	0,177
39	K	K4	3,5	3	75	95	275	246	27,0	100	214	356667	2	42	368	74761	0,192
40	K	K5	10	1	75	95	800	53,86	27,3	100	215	358333	2	42	176	50213	0,132
41	L	L1	10	N/A	75	95	800	N/A	\	100	214	356667	1	43	N/A	N/A	N/A
42	L	L2	10	N/A	75	95	800	N/A	\	100	214	356667	2	43	N/A	N/A	N/A
43	L	L3	10	1	75	95	800	30,24	27,8	100	214	356667	2	43	153	31317	0,081
44	L	L4	10	N/A	75	95	800	N/A		100	214	356667	2	43	N/A	N/A	N/A
45	L	L5	10	1	75	95	800	58,58	21,7	100	213	355000	1	43	175	53989	0,144
46	M	M1	10	N/A	75	95	800	N/A	\	100	214	356667	2	43	N/A	N/A	N/A
47	M	M2	10	1	75	95	800	37,4	21,3	101	216	367236	1	43	154	37045	0,094
48	M	M3	10	N/A	75	95	800	N/A	\	100	214	356667	1	43	N/A	N/A	N/A
49	M	M4	2	N/A	75	95	800	N/A	\	100	214	356667	2	43	N/A	N/A	N/A
50	M	M5	2	N/A	75	95	800	N/A	\	100	214	356667	2	43	N/A	N/A	N/A
51	N	N1	2	N/A	75	95	800	N/A	\	100	214	356667	2	43	N/A	N/A	N/A
52	N	N2	2	4	75	95	800	14,46	21,7	99	214	349569	1	43	131	18693	0,047
53	N	N3	2	4	75	95	800	46,61	26,9	101	214	363836	2	43	168	44413	0,114
54	N	N4	2	4	75	95	800	59,46	26,6	100	215	358333	2	43	181	54693	0,144
55	N	N5	2	4	75	95	800	41	27,3	100	211	351667	2	43	163	39925	0,106
56	O	O1	2	N/A	75	95	800	N/A	\	100	214	356667	2	43	N/A	N/A	N/A
57	O	O2	2	N/A	75	95	800	N/A	\	100	214	356667	2	43	N/A	N/A	N/A
58	O	O3	2	4	75	95	800	21,23	21,6	99	213	347936	1	43	138	24109	0,063
59	O	O4	2	4	75	95	800	46,8	32,5	99	215	351203	2	43	174	44565	0,119
60	O	O5	2	N/A	75	95	800	N/A	\	95	213	320388	1	46	N/A	N/A	N/A

*Loading rate of the applied load

Bond wrench shop drawings

Vue de face

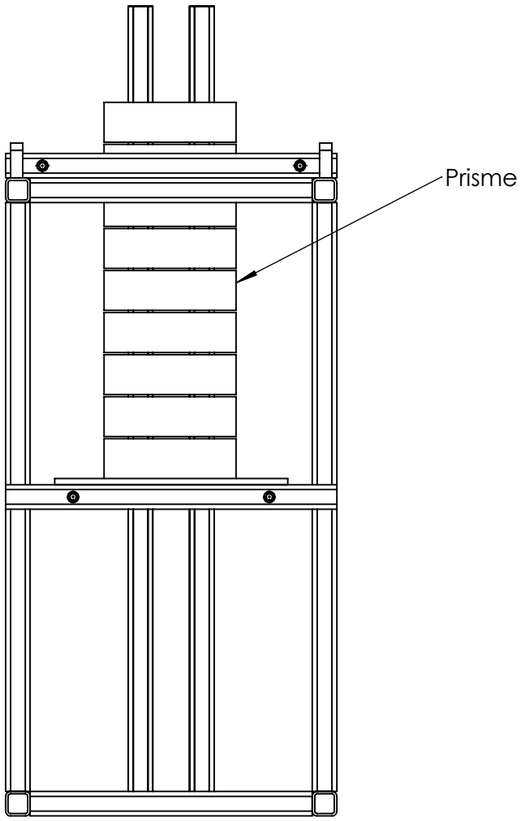

Vue de côté

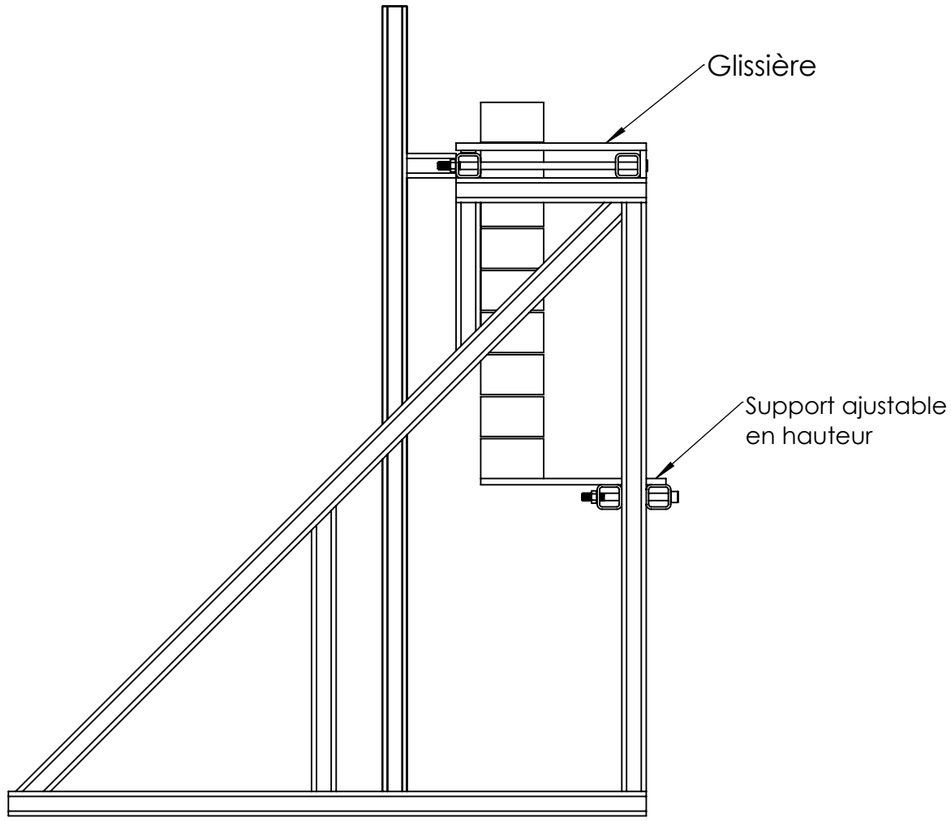

Vue trimétrique

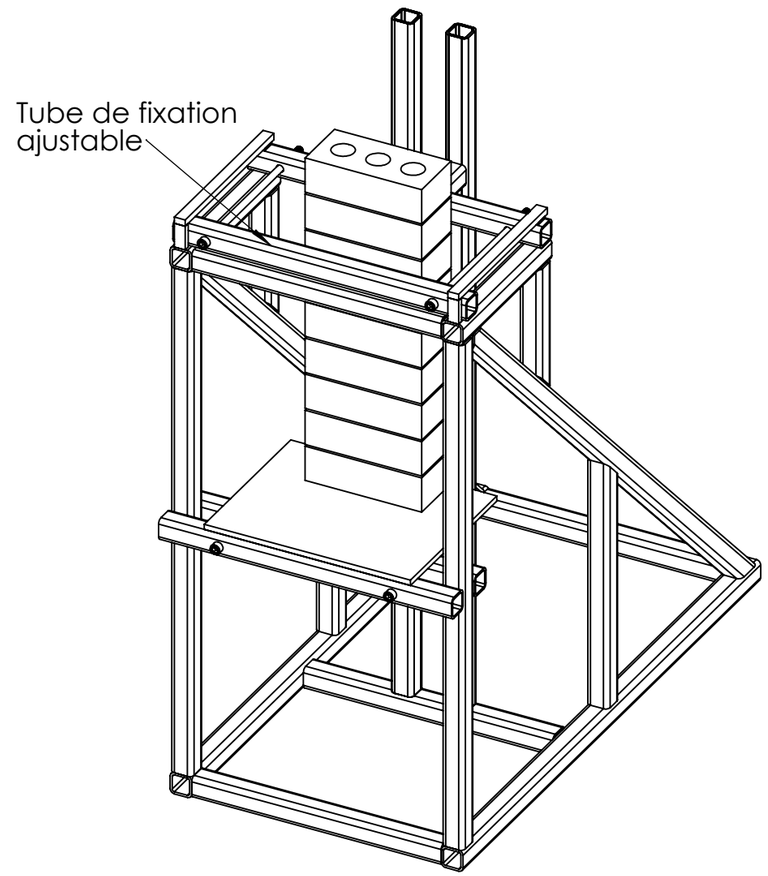

Vue du dessus

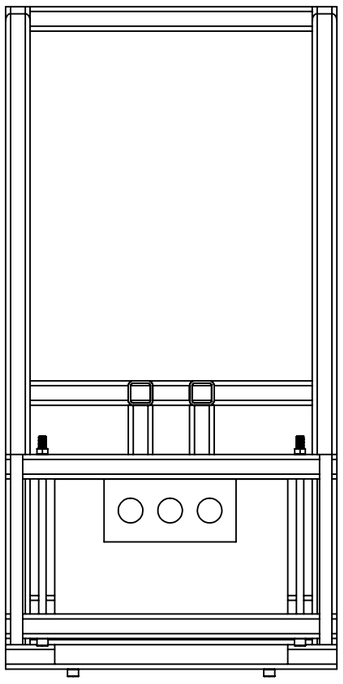

Vue du dessous

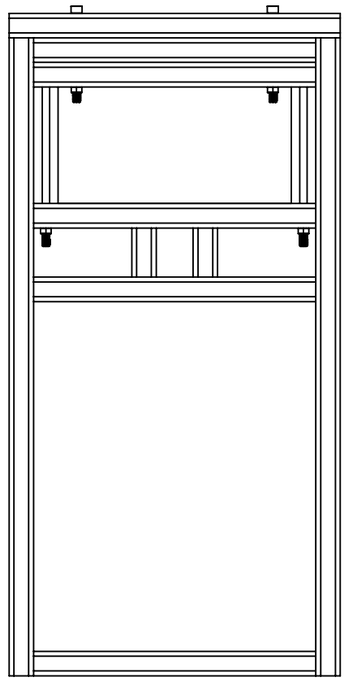

Auteur: Olivier Kestemont (UCLouvain)	
Vues générales avec prisme en maçonnerie	
Date: 16-05-23	Echelle: 1:10

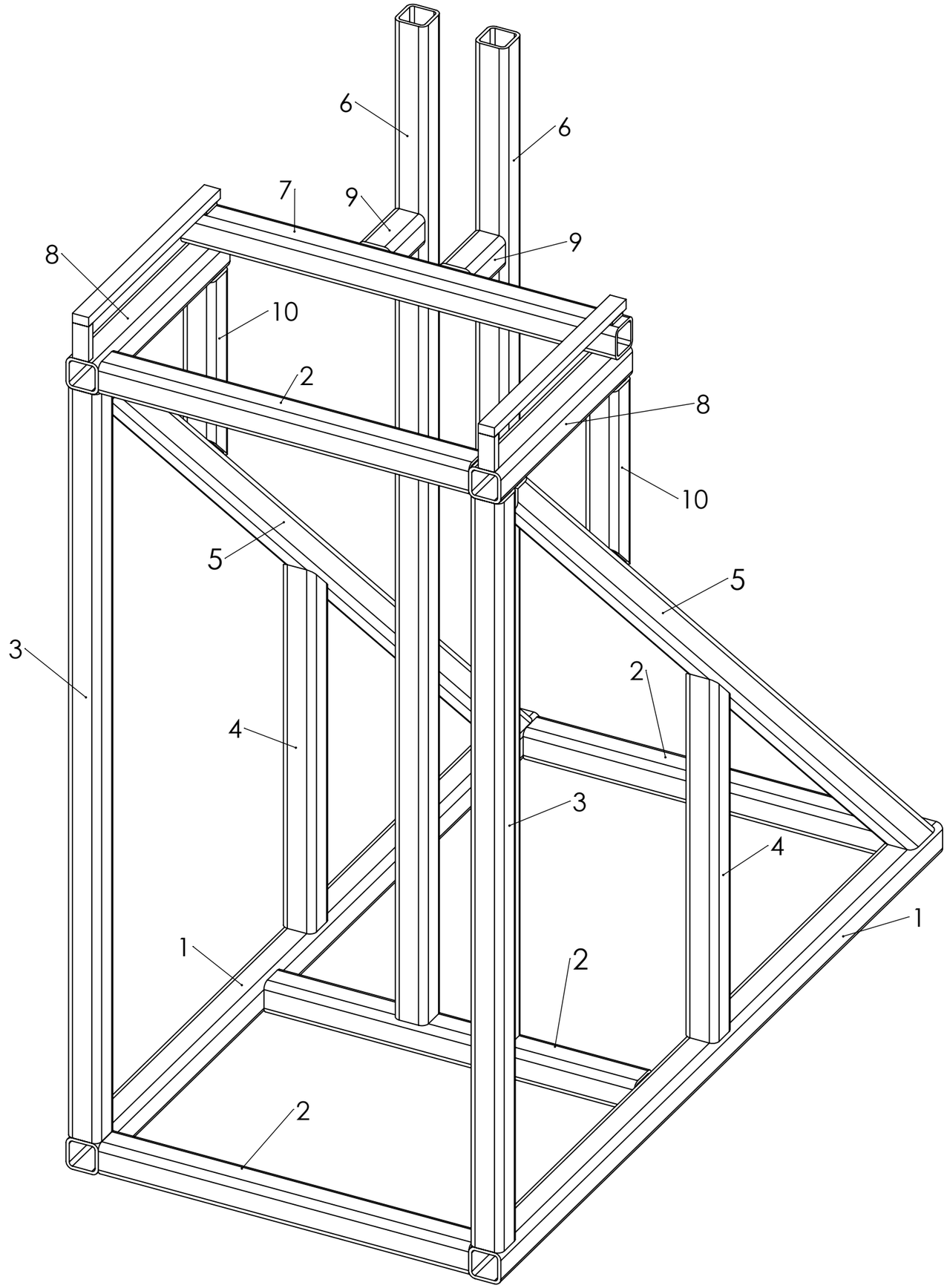

Element	Longueur en mm	Quantité
1	1040	2
2	460	4
3	960	2
4	466	2
5	1358	2
6	1280	2
7	580	1
8	330	2
9	80	2
10	242	2

Note: L'élément 7 n'est pas à l'échelle sur le plan. En réalité le tube dépasse plus de la glissière. (Sur plan: 540 mm; Découpe: 580 mm).

Auteur: Olivier Kestemont (UCLouvain)

Cadre principal: Identification des éléments à souder

Date: 16-05-23

Echelle: 1:5

Vue de côté

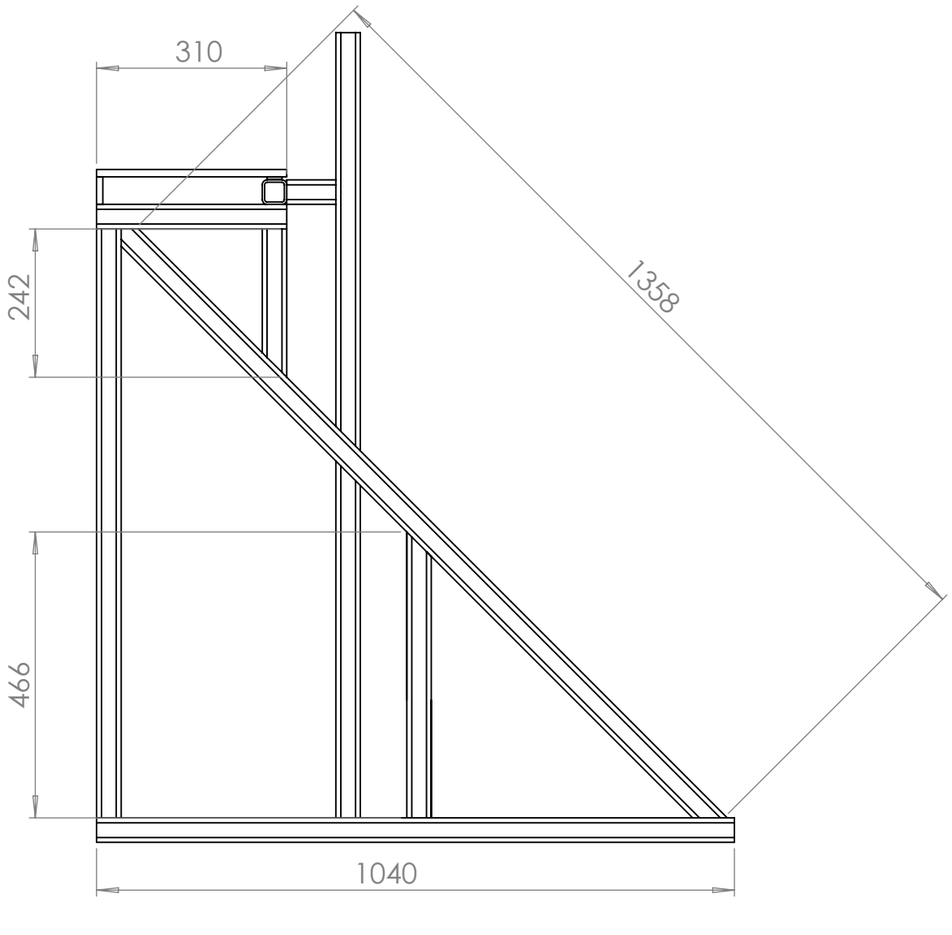

Vue de face

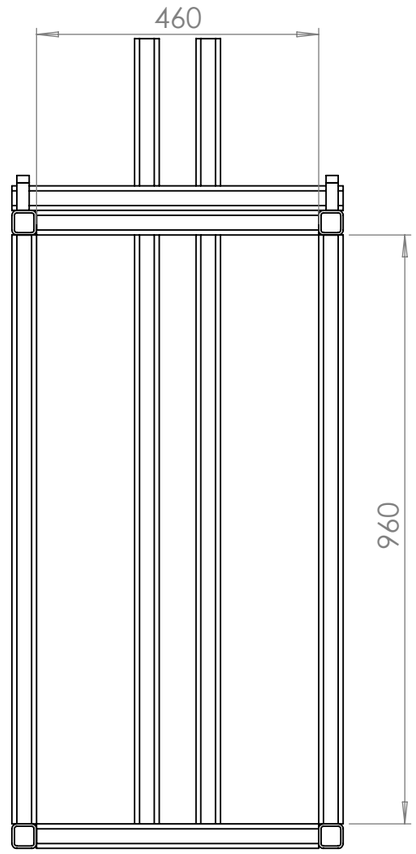

Vue de derrière

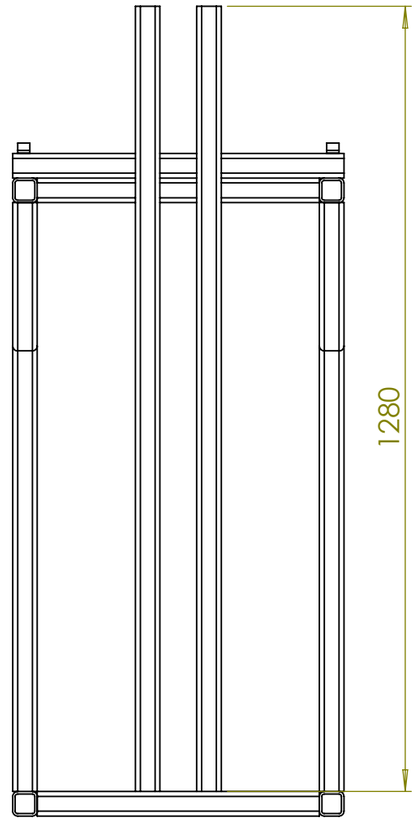

Vue du dessous

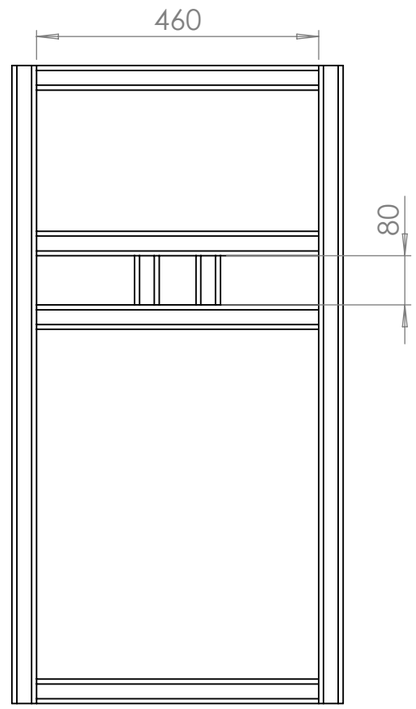

Auteur: Olivier Kestemont (UCLouvain)	
Cadre principal: Dimensions des éléments à souder	
Date: 16-05-23	Echelle: 1:10

Vue de côté

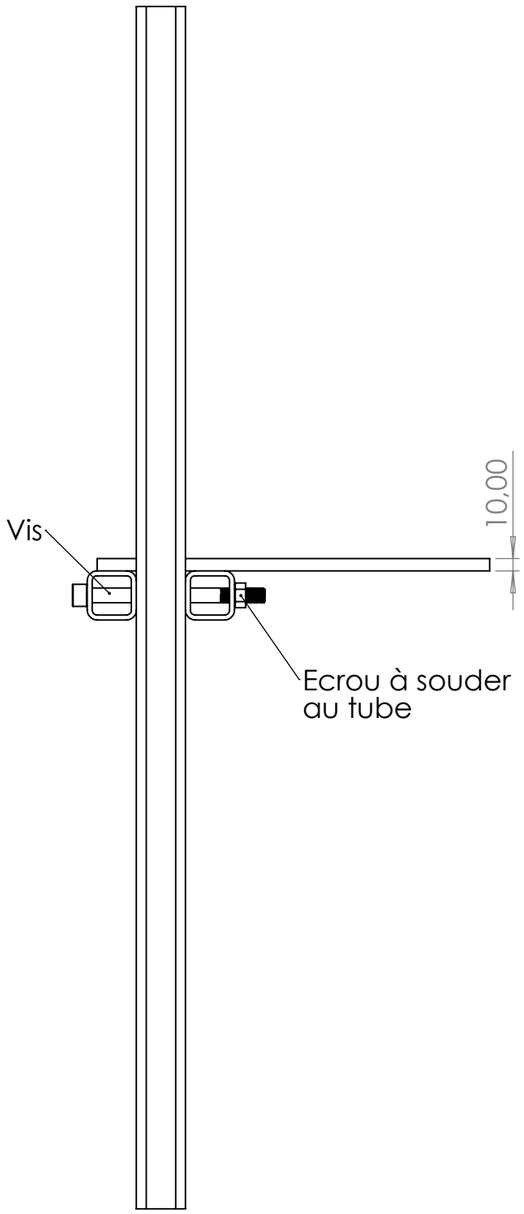

Vue du dessous

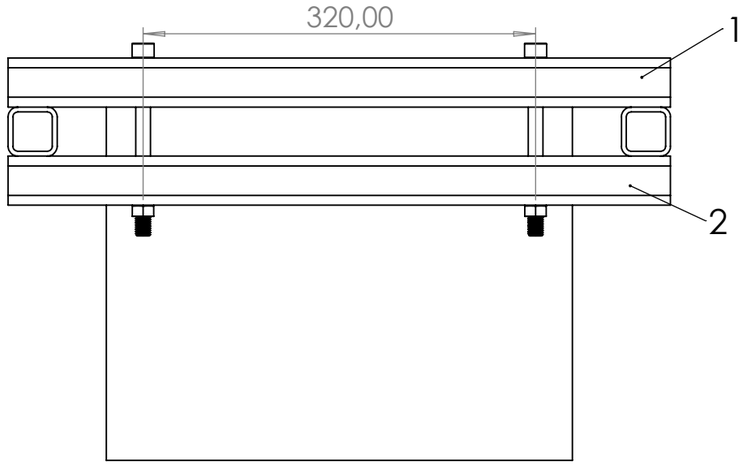

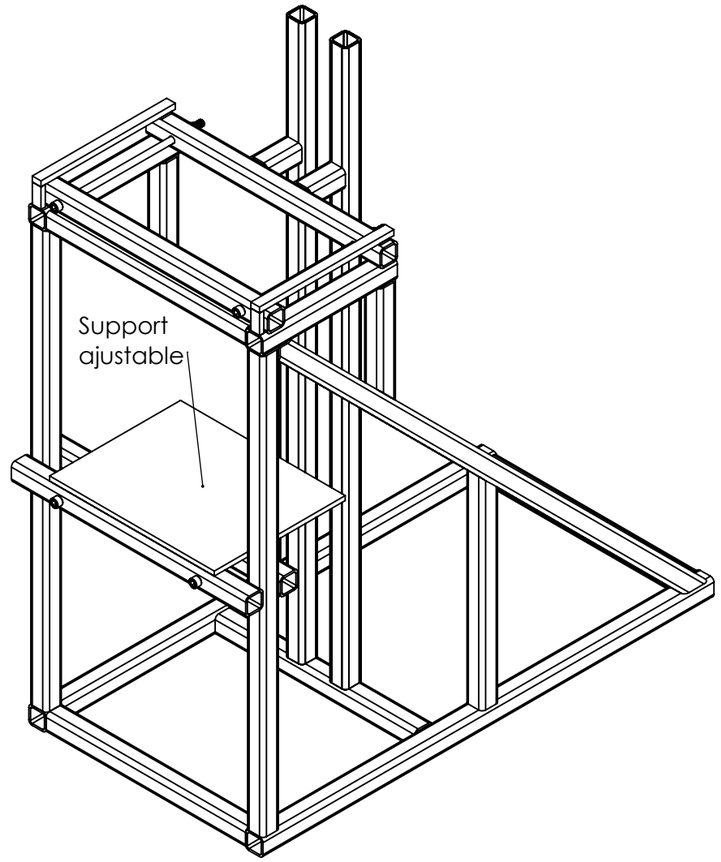

Vue du dessus

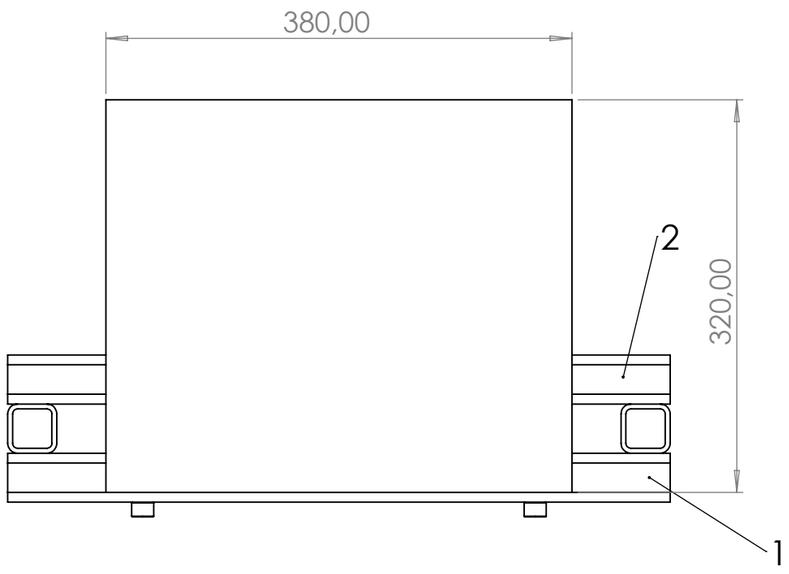

Note 1: Ne pas souder les tubes (1 et 2) au reste du cadre.
Note 2: Souder la plaque de support au tube 1.
Note 3: Les tubes 1 et 2 font 580 mm de long.

Auteur: Olivier Kestemont (UCLouvain)	
Support ajustable	
Date: 16-05-23	Echelle: 1:5

Vue du dessous

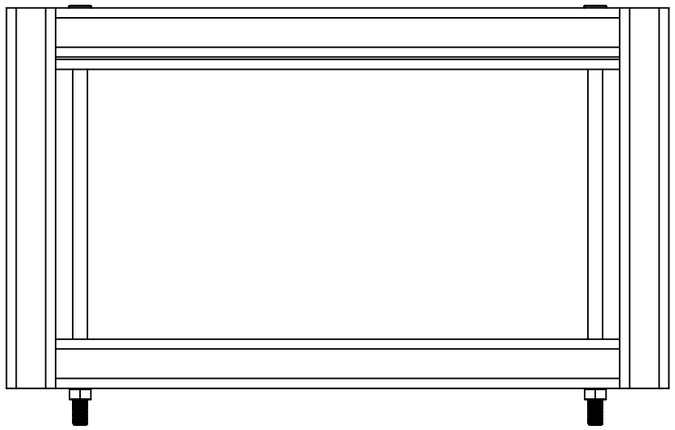

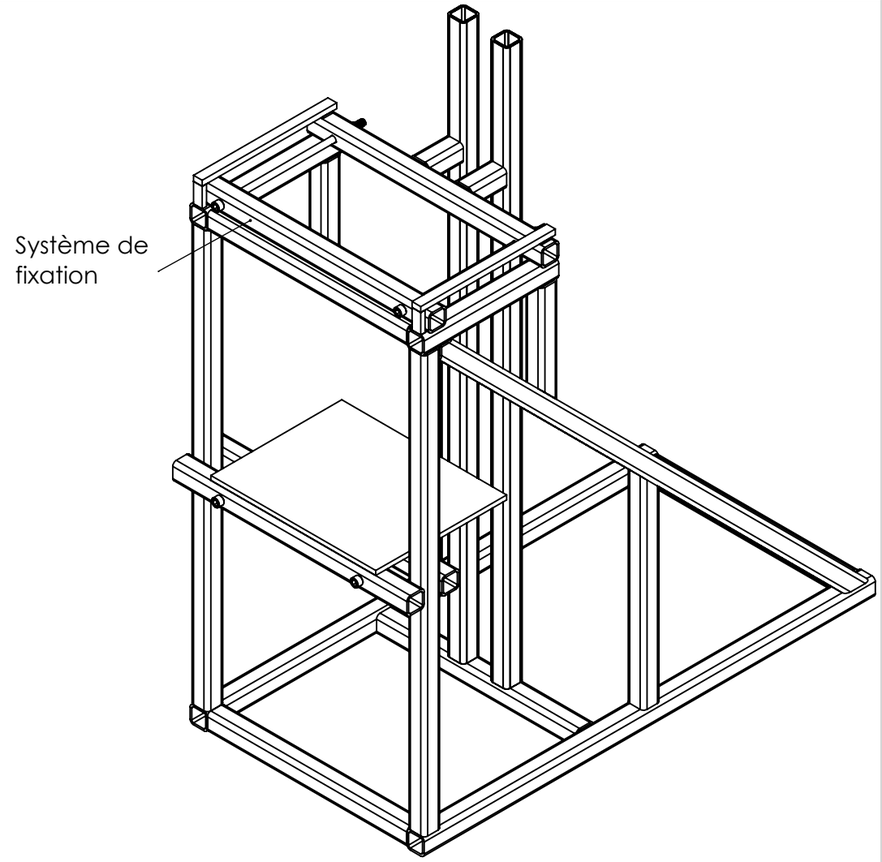

Vue de côté

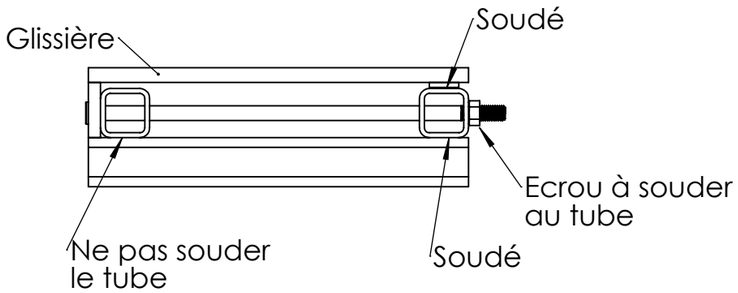

Vue de face

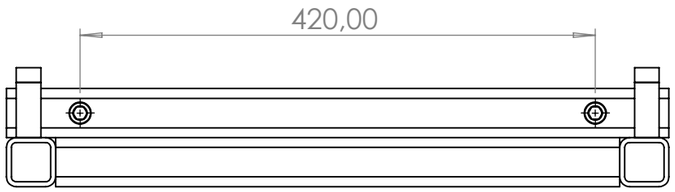

Vue du dessus

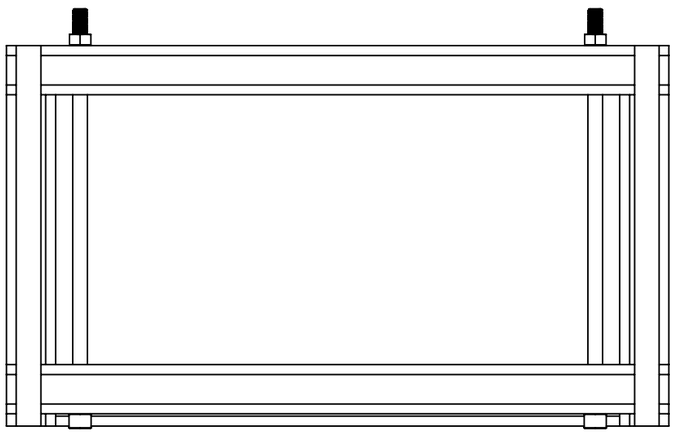

Auteur: Olivier Kestemont (UCLouvain)	
Système de fixation du prisme	
Date: 16-05-23	Echelle: 1:5

Vue trimétrique

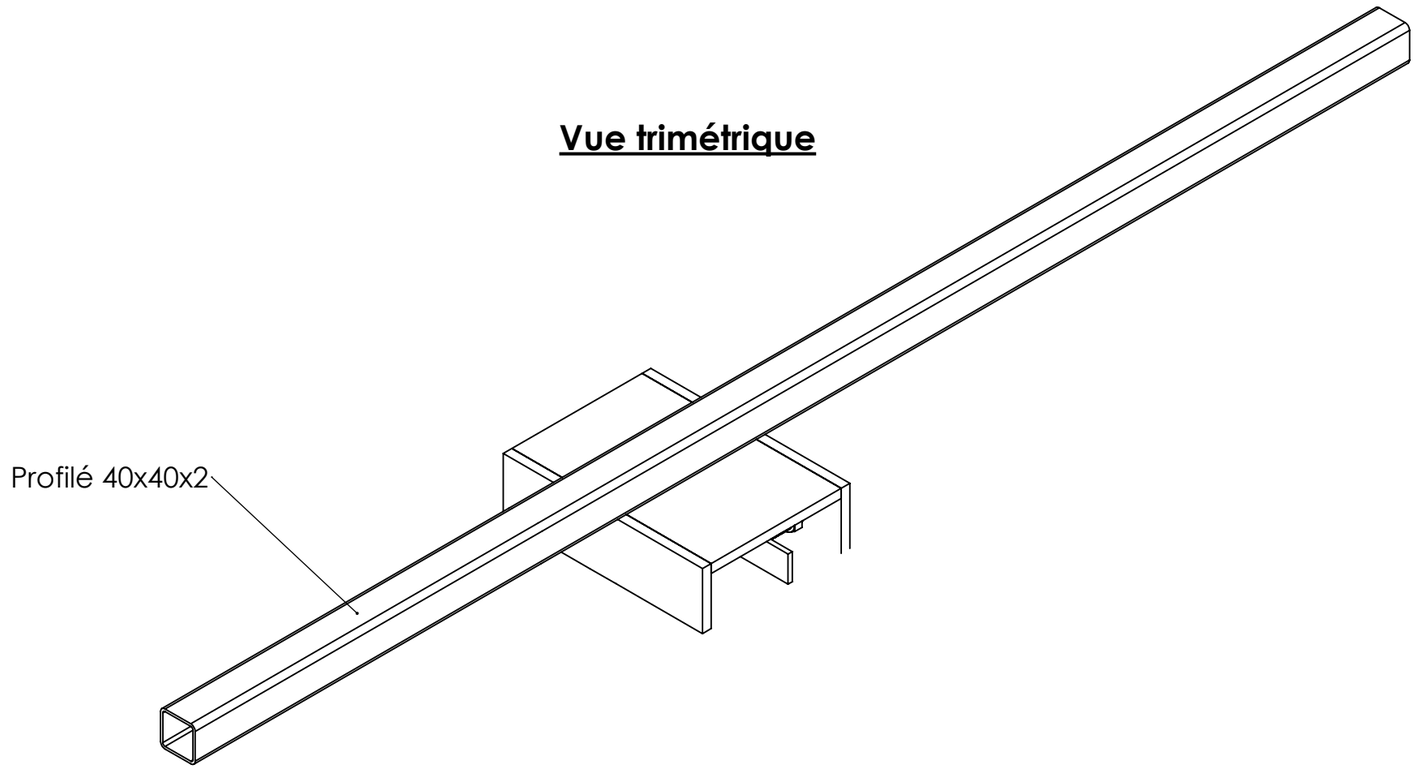

Vue de profil

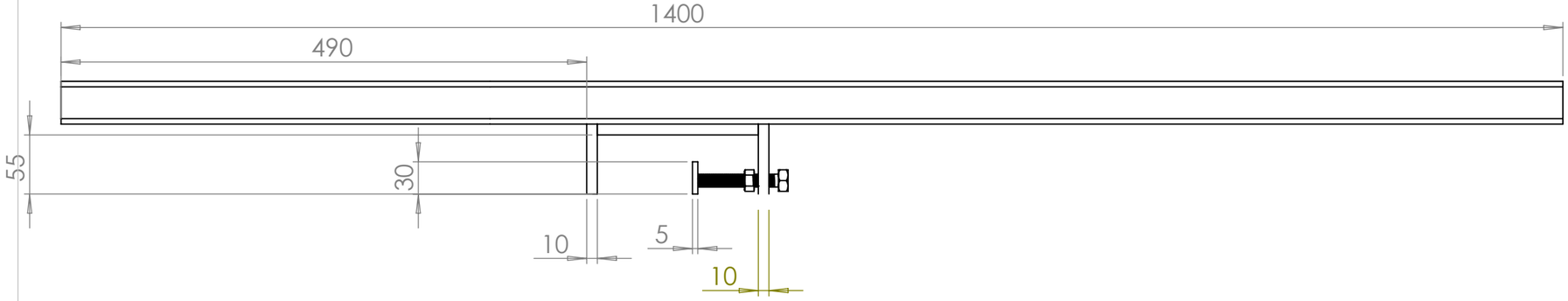

Vue du dessous

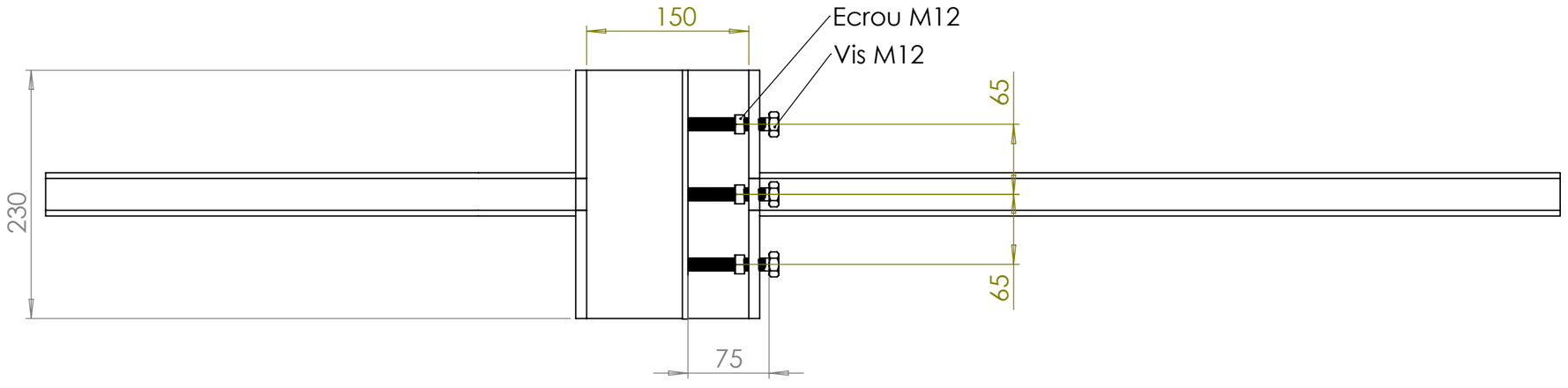

Note 1: Les écrous ne sont pas soudés.
Note 2: Il ne doit pas forcément avoir un angle vif à l'intérieur de la "boite". Un profilé en U peut-être utilisé. Ce qui est important c'est qu'il puisse y avoir un contact de 55 mm entre la plaque vertciale de la boite et la brique.

Auteur: Olivier Kestemont
Bras de levier EN 1052-5
Echelle: 1:5

Pure couple bond wrench apparatus

Figure 4.12: Pure couple bond wrench apparatus: Side view [49].

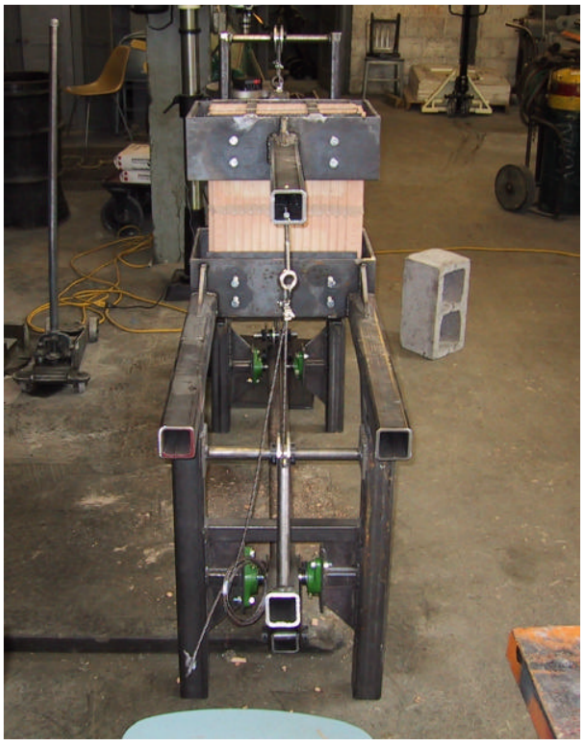

Figure 4.13: Pure couple bond wrench apparatus: Front view [49].

Figure 4.14: Pure couple bond wrench apparatus: General view [49].

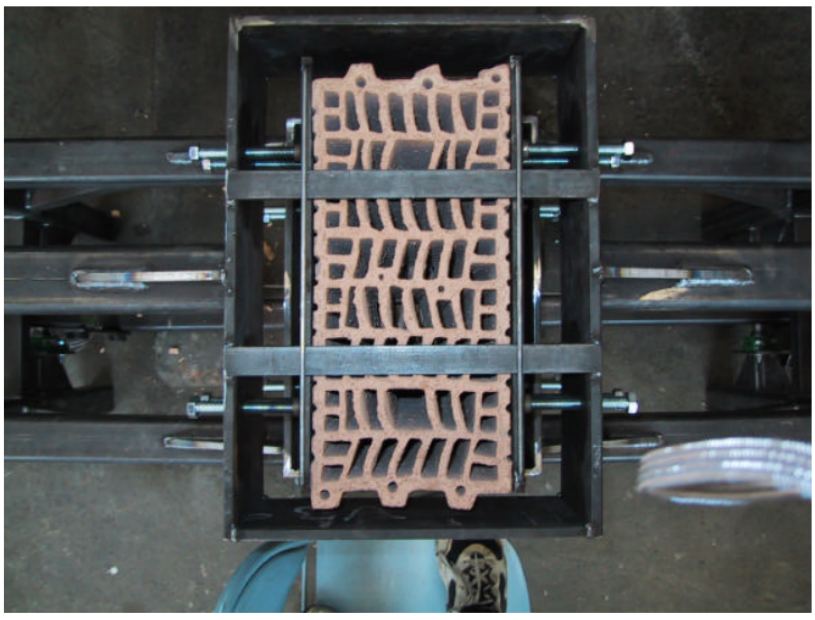

Figure 4.15: Pure couple bond wrench apparatus: Top view [49].

Figure 4.16: Pure couple bond wrench apparatus: Load cell [49].

Technical sheets of the materials

VANDERSANDEN

Product name	Product group	Production location
Salvia	L1	Lanklaar

The raw materials are excavated in Weichsel loam layers, the local loam of Aeolian origin dating from the Ice Age. This löss mainly consists of a silt-like fraction, suited ideally for the manufacturing of hand form bricks. By using specific sand types for surface covering, the desired colour is achieved.

Colour
unicoloured purple red

Format	
Moulding method	Hand form
DF: 214 x 101 x 65 mm	Between batches the average size and color may slightly differ.

Essential Characteristics - EN771-1			
CE EN 771-1 - CPR-97884 NOBO 0063 (ex 0620)		UKCA EN 771 - 1855-CPR-24914	
2+		2+	
Dimensional tolerances	T2		
Range	R1		
Active Soluble Salts	S2		
Mean Compressive strength	>= 20 N/mm²	Tested to the bed face	
Normalized Compressive strength	>= 20 N/mm²	Tested to the bed face	
Dimensional stability	NPD		
Bond Strength general	0,15 N/mm²		
Bond Strength thin layer	0,30 N/mm²		
Reaction to fire	A1	Category	
Water absorption	<= 14% m/md		
Water vapour permeability	5/10		
Net dry density	1740 kg/m³ (D1)		
Gross dry density	1630 kg/m³ (D1)		
Thermal conductivity Lambda 50/50	<=0,60 W/m.K		
Durability against freeze thaw	F2		
Dangerous substances	NL-BSB	According to Annex ZA 3	

Other Characteristics		
Initial rate of water absorption - Non-coated Bricks	1,5 - 4.0 kg/m².min (IW3)	Value according EN771-1:2011 - 5.3.8
Initial rate of water absorption - Coated bricks	0,5 - 1,5 kg/m².min (IW2)	Value according EN771-1:2011 - 5.3.8
Freeze/thaw resistance - PTV 23-002	NPD	NBN 27-009
Thermal conductivity Lambda 90/90	0,65 W/m.K	
Thermal conductivity Lambda Ui	0,697 W/m.K	
Thermal conductivity Lambda Ue	1,376 W/m.K	

Storage & handling	Cutting
- Store packs on a clean surface and cover them - Process from multiple packs at the same time - Follow the Vandersanden processing guidelines	Cutting with power tools may generate dust. This dust may contain silica or quartz particulate which may constitute a hazard. Persons undertaking work of this nature are advised to wear dust masks (FFP3).

*All our Coated bricks are only coated on the facing sides. Coated products are specially labeled and recognisable with a "C" logo on the top left-hand side of the packaging. Always check if using coated or non-coated bricks. Match the mortar to the specified initial water absorption.

CEM II/B-M 32,5 N

Ciment multi-usage (sacs)

Holcim (Belgique) S.A. / Usine d'Obourg

Holcim (Belgique) S.A.
Avenue Robert Schuman 71 - B-1401 Nivelles
T +32 67 87 66 01
Technical helpdesk:
bel-tsc@lafargeholcim.com
www.holcim.be

A member of LafargeHolcim

CEM II/B-M 32,5 N
Ciment multi-usage (sacs)

SAC

Le produit

Le ciment CEM II/B-M 32,5 N est un ciment portland composé suivant la EN 197-1 dont les constituants principaux sont le clinker portland (K), le calcaire (LL), le laitier granulé de haut fourneau (S) et les cendres volantes siliceuses (V). La teneur en clinker est comprise entre 65 % et 79 %.

Domaine d'application

Domaines d'application préférentiels (Holcim)

- Mortiers de maçonnerie et de pose, enduits et chapes
- Béton de résistance moyenne pour petits travaux, pouvant durcir lentement et exposé à des milieux non agressifs

Contre-indications (Holcim)

- Béton sur résistance
- Travaux en période hivernale
- Béton en milieu agressif (classes d'environnement EA2 et EA3)
- Béton exposé aux sels de déverglaçage (classe d'environ-nement EE4)
- Rejointoiement (mur et sol)

Précautions à l'usage (Holcim)

- Bien protéger le béton et le mortier contre la dessiccation afin d'éviter la pulvérulence de la surface
- Prendre des mesures pour le durcissement lent
- L'emballage Magic peut être ajouté au malaxeur avec le ciment. En fonction de l'application, un temps de malaxage plus long peut être nécessaire afin d'obtenir la désintégration (par friction interne) de l'emballage. Il n'est pas impossible de trouver encore quelques petites traces de l'emballage (zones multicouches).

Avantages du CEM II/B-M 32,5 N

- Excellente ouvrabilité et facilité de mise en oeuvre des mortiers
- Bonne résistance à longue échéance.

Pays	Documents de référence	Dénomination	Marque
Belgique	TRA 600 PTV 603	CEM II/B-M (LL-S-V) 32,5 N V≤25% et perte de feu ≤ 7%	BENOR

Caractéristiques techniques

Caractéristiques mécaniques et physiques(1)

	Unités	Résultats	Spécifications Norme(s)
Besoin en eau Début de prise Fin de prise	% hh:mm hh:mm	26 5:25 6:15	- ≥ 1:15 ≤ 12:00
Stabilité	mm	< 1	≤ 10
Résistance à la compression 7 jours 28 jours	 N/mm² N/mm²	 34 46	 ≥ 16 ≥ 32,5 / ≤ 52,5
Surface spécifique Blaine	cm²/g	3610	-
Masse volumique absolue	kg/m³	3000	-
Refus au tamis de 200 µm	%	< 1,0	≤ 3,0

Composition chimique(1)

	Résultats (%)	Spécifications (%) Norme(s)
CaO	56,0	-
SiO_2	19,5	-
Al_2O_3	6,2	-
Fe_2O_3	4,1	-
MgO	2,7	-
Na_2O	0,36	-
K_2O	0,74	-
SO_3	2,7	≤ 3,5
Cl^-	0,07	≤ 0,10
Perte au feu	7,1	-
Résidu insoluble	4,2	-

(1) Remarque : les résultats repris dans les tableaux sont basés sur des valeurs moyennes et sont donnés à titre purement indicatif et n'ont en aucun cas un caractère contractuel. En conséquence, ils ne sauraient engager la responsabilité de Holcim (Belgique) s.a.

Le ciment CEM II/B-M 32,5 N est marqué CE en tant que CEM II/B-M (LL-S-V) 32,5 N. Par le marquage CE, le fabricant prend la responsabilité de la conformité du produit aux performances déclarées dans sa Déclaration des Performances (DoP). En outre, le ciment porte la marque volontaire de qualité BENOR qui garantit la conformité du produit aux spécifications techniques fixées dans les règlements de certification concernés (voir tableau en haut de page).

La Déclaration des performances (DoP) et la fiche de données de sécurité sont disponibles sur www.holcim.be

ISO9001 CERTIFIED VINÇOTTE ISO14001 CERTIFIED VINÇOTTE CE BENOR

Usine d'Obourg

UNIVERSITÉ CATHOLIQUE DE LOUVAIN
École polytechnique de Louvain
Rue Archimède, 1 bte L6.11.01, 1348 Louvain-la-Neuve, Belgique | **www.uclouvain.be/epl**